CRREL REPORT 96-13

Physical Processes and Natural Attenuation Alternatives for Remediation of White Phosphorus Contamination, Eagle River Flats, Fort Richardson, Alaska

Daniel E. Lawson, Lewis E. Hunter and Susan R. Bigl

December 1996

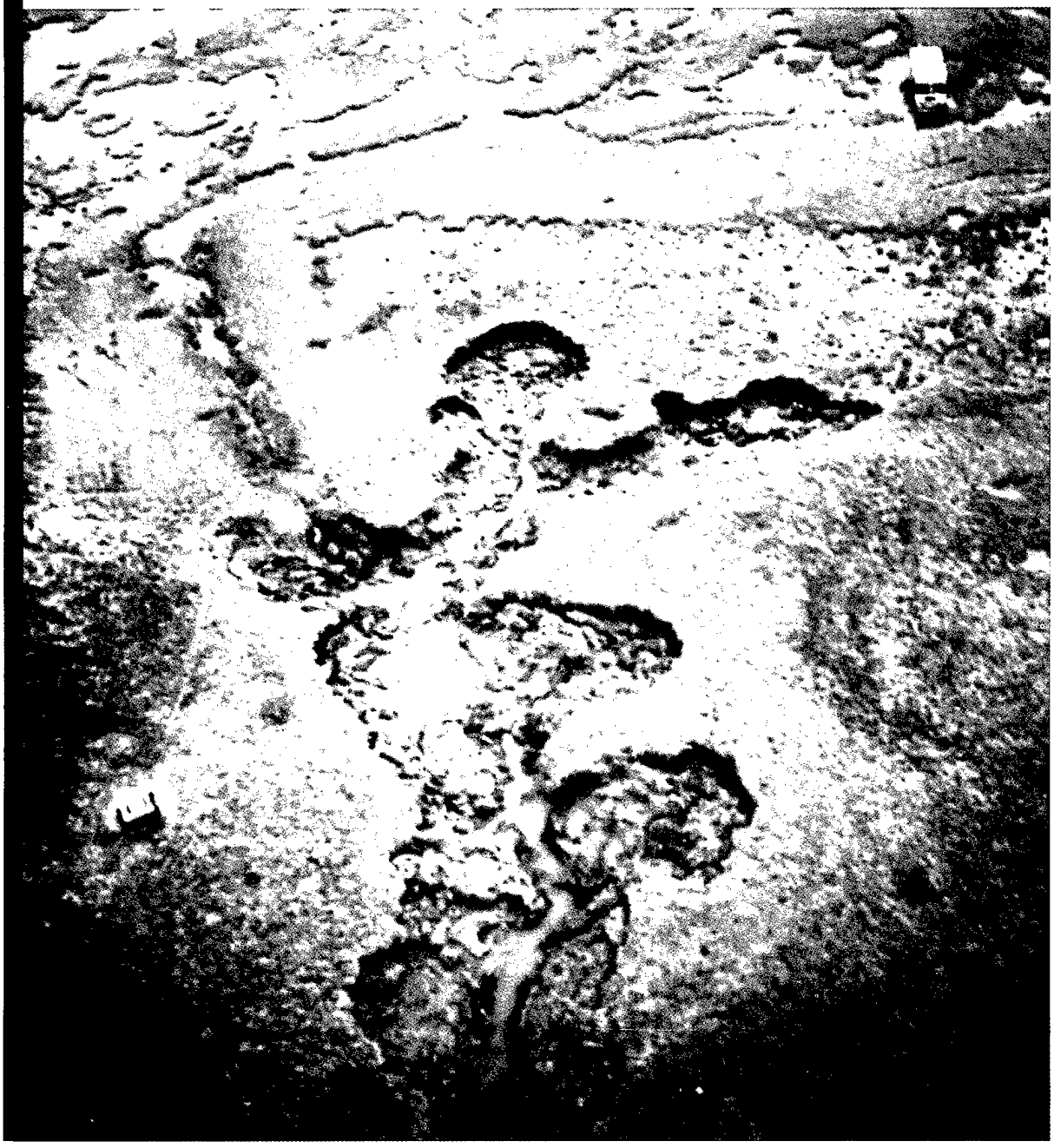

Abstract: This report describes the results of investigations into the role of tidal flat physical systems in the natural attenuation of white phosphorus (WP) contamination in Eagle River Flats (ERF) on Fort Richardson, Alaska. Waterfowl feeding in ponds and marshes here ingest the WP and die. These investigations found that natural attenuation and in-situ degradation of the WP could result from certain physical phenomena operating within the ERF ecosystem. Specifically, the on-going erosion and headward recession in the gullies will drain large areas of contaminated ponds in an estimated 1 to 10 years. Lowering of water levels should lead to in-situ WP degradation and natural attenuation as pond sediments dry. Annual sedimentation rates in some ponds and marshes are sufficient to bury WP in several years or more and thereby reduce the exposure to feeding waterfowl. Ice and water are also effective transporters of WP, moving it about ERF and into Eagle River and eventually into Knik Arm where its fate is unknown. Certain areas of ERF will require artificial drainage, but natural conditions can be restored following treatment. Recommendations are made for the use of natural attenuation and additional studies that are required to ensure the successful clean-up of ERF.

Cover: Oblique aerial photograph of the head of Bread Truck Gully. This gully is eroding headward at an average rate of 21.6 m annually, and will probably drain Bread Truck Pond (top of photo) within 1 to 2 years. A hydrostation platform (1.3 × 1.3 m) is located to the lower left.

How to get copies of CRREL technical publications:

Department of Defense personnel and contractors may order reports through the Defense Technical Information Center:

DTIC-BR SUITE 0944
8725 JOHN J KINGMAN RD
FT BELVOIR VA 22060-6218
Telephone 1 800 225 3842
E-mail help@dtic.mil
msorders@dtic.mil
WWW http://www.dtic.dla.mil/

All others may order reports through the National Technical Information Service:

NTIS
5285 PORT ROYAL RD
SPRINGFIELD VA 22161
Telephone 1 703 487 4650
1 703 487 4639 (TDD for the hearing-impaired)
E-mail orders@ntis.fedworld.gov
WWW http://www.fedworld.gov/ntis/ntishome.html

A complete list of all CRREL technical publications is available from:

USACRREL (CECRL-LP)
72 LYME RD
HANOVER NH 03755-1290
Telephone 1 603 646 4338
E-mail techpubs@crrel.usace.army.mil

For information on all aspects of the Cold Regions Research and Engineering Laboratory, visit our World Wide Web site:
http://www.crrel.usace.army.mil

CRREL Report 96-13

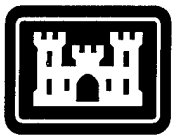

US Army Corps of Engineers®
Cold Regions Research & Engineering Laboratory

Physical Processes and Natural Attenuation Alternatives for Remediation of White Phosphorus Contamination, Eagle River Flats, Fort Richardson, Alaska

Daniel E. Lawson, Lewis E. Hunter and Susan R. Bigl

December 1996

Prepared for
U.S. ARMY ALASKA
ENVIRONMENTAL RESOURCES DEPARTMENT

PREFACE

This report was prepared by Dr. Daniel E. Lawson, Research Physical Scientist, Lewis E. Hunter, Research Physical Scientist, and Susan R. Bigl, Research Physical Scientist, Geological Sciences Division, Research and Engineering Directorate, U.S. Army Cold Regions Research and Engineering Laboratory.

Funding and support for this research was provided by the U.S. Army Alaska, Environmental Resources Department, Directorate of Public Works, Fort Richardson, Alaska, through the U.S. Army Engineer District, Anchorage. Technical review was provided by Dr. Steven Arcone and Dr. Jeffery Strasser, both of CRREL.

The authors thank William Gossweiler, Douglas Johnson, William Smith and Laurie Angell for helpful discussions, logistical support and assistance in the field, and their continuing support of our work, as well as Dr. Charles Racine, Charles Collins and Marianne Walsh for numerous scientific discussions and assistance in the field and laboratory on the Eagle River Flats project. They also thank Troy Arnold, Ron Bailey, Dennis Lambert, Beth Nadeau and Pat Weyrick for their assistance, Jodie Strasser and Audrey Krat for data analysis and plotting and Cora Farnsworth for her contribution to report preparation.

CONTENTS

	Page
Preface	ii
Executive summary	vi
Introduction	1
Environmental conditions	1
Results of previous physical system investigations	5
Study sites and methods	13
Sedimentation transects	13
Pond sedimentation measurements	16
Gully erosion and headwall recession	20
Historical aerial photographic analyses	21
Water quality parameters	21
Hydrostation configuration	24
WP transport and resuspension	24
Data acquisition record	26
Intrinsic remediation	28
External forcing	28
Gully erosion and discharge	28
Gully erosion and scarp recession rates	31
Historical analysis of the drainage system	44
Natural attenuation by pond drainage	46
Sedimentation and natural attenuation of WP by burial	47
Tidal inundation	47
Sediment transport and sediment sources	52
Landform sedimentation rates	53
Pond transects and stations	56
White phosphorus fate, transport and migration	59
Knik Arm and WP deposition	61
Conclusions and recommendations	62
Conclusions	62
Recommendations	63
Literature cited	64
Abstract	67

ILLUSTRATIONS

Figure

1. Location of ERF and other salt marshes in upper Cook Inlet 2
2. 1995 aerial photograph of ERF showing the dendritic drainage network 3
3. Drainage network in the C and D areas of ERF 4
4. Distribution of primary landform–vegetation units 4
5. Locations of gullies, ponds and areas 7
6. Aerial photograph of Racine Island taken 16 August 1995 showing remnant channel surrounded by overbank deposits 8
7. Aerial photographs of ERF 10
8. 1992 aerial photograph of northeastern ERF 13

Figure Page
9. Mudflat sedimentation transect locations 14
10. Sedimentation measurement techniques 15
11. Wedge-shaped sediment block used to measure vertical accretion 16
12. Pond sedimentation measurement locations 17
13. Locations of 1992–1994 pond sedimentation stations 19
14. Example of sedimentation station at an intermittent pond location showing layout of cup and plate sampler 19
15. Example of layout of hub and line stakes at River-North erosion site 20
16. Location of gully headwall and lateral wall erosion sites 21
17. 1995 locations of instrumentation recording water quality parameters and water depths 22
18. Extent of data collection at hydrostation sites from 1993–1995 23
19. Hydrostation layout at a gully location 25
20. Plankton net used for collecting WP in water transport 26
21. Sampling coverages for various types of field data 27
22. Relationship between peak velocity and maximum water elevation at selected sites 29
23. Summary of gully scarp recession 31
24. Measurements of bank erosion along Eagle River at the River-North site 34
25. Bank of Bread Truck Gully showing ice growth formation 35
26. Aerial view of Parachute Gully in October 1995 showing accelerated headward recession 36
27. Aerial view of gullies where recession and ebb flow have been modified by surface craters 36
28. Aerial view of Bread Truck Gully in October 1995 38
29. Eastward view of eroding cuspate embayments at B-Gully 39
30. Thick laminated peat layer at Coastal 6 39
31. Sediment flow at Bread Truck Gully 40
32. Historical gully recession 41
33. Spatial comparison of headward and lateral recession monitored at selected hub-line stake erosion sites 43
34. Aerial photographs depicting the morphologic changes in the Eagle River where it enters the ERF 45
35. Predictions for pond drainage by selected gullies in Areas C, Bread Truck and C/D 46
36. Ice rafting at ERF 47
37. Example of a flooding tide cycle 49
38. Water quality data from the Eagle River site showing the effect of water damming caused by a flooding tide 49
39. Water elevation record showing elevations required to flood selected landforms and tidal amplification at Parachute Gully above predicted high tide at Anchorage 50
40. Relationship between water rise time and peak water elevation at several gully sites 50
41. Tidal flooding time as a function of peak flood elevation at selected gullies 51

Figure Page
42. Runoff time vs. peak water elevation at Bread Truck Gully 52
43. Coastal vs. river TSS measurements 52
44. Maximum monthly TSS comparison at all sites 53
45. Typical TSS variation through a flooding tide 53
46. Net seasonal accumulation rates at sites spray-painted in the C and D areas 54
47. Variations in sedimentation rate as a function of landform type 55
48. Relationship between total sediment accumulation and vegetation cover at sites sprayed with paint in 1992 and measured in the fall of 1994 55
49. Sediment accumulation along mudflat lines sprayed with paint in early summer 1994 56
50. Pond sedimentation measured along transects from May to September 1995 57
51. Average sediment accumulation from May to September 1995 at pond sedimentation station transects, without data points suspected of disturbance 58
52. Fall 1995 measurements of accumulation at sedimentation stations established in 1992 59
53. Relationship between WP detected in plankton net samples and peak elevation of flooding event sampled 60
54. Bathymetry of Knik Arm near the mouth of the Eagle River and adjacent to the coast of ERF 61
55. Recommendations for site remediation 62

TABLES

Table
1. Controls on physical processes 5
2. Erosional processes 5
3. Transport processes 6
4. Depositional processes 6
5. Historical aerial photography of Eagle River Flats 21
6. Specifications of sensors used in water quality parameter measurements 22
7. Summary of gully velocity and discharge data 29
8. Summary of scarp recession 30
9. Summary of long-term gully erosion rates at selected sites 44
10. Gross sedimentation rates 54
11. Comparison of predicted and measured number of flooding events reaching critical heights during summer 1994 and summer 1995 55
12. May to September 1995 sediment accumulation along pond sedimentation transects 58
13. 1995 positive WP results from pond sedimentation station cup samples 60

EXECUTIVE SUMMARY

This report describes the results of the 1995 investigations of the physical ecosystem of Eagle River Flats (ERF) on Fort Richardson, Alaska. These investigations focused on the role of the physical system in the natural attenuation of white phosphorus (WP) contamination in this salt marsh area. Specifically, we evaluated 1) whether the processes of gully erosion, headward recession and drainage of contaminated ponds could result in a natural attenuation and in-situ degradation of WP contamination over a significant proportion of ERF, and 2) whether natural sedimentation would bury contaminated pond sediments sufficiently to form a barrier to feeding waterfowl. In addition, the erosion and potential for off-site transport of WP was examined.

Several important conclusions result from this and previous years' work:

1. Physical system processes can naturally attenuate and remediate a significant proportion of the WP in the ERF ecosystem.

2. Gully erosion and headwall recession towards contaminated ponds will begin to drain large areas in about 1 to 10 years. The resultant lowering of pond surfaces can lead to in-situ WP degradation and natural attenuation from drying of surface sediments. These processes are a cost-effective alternative to remediating the site by expensive removal methods such as dredging. Historical analyses and field measurements indicate that Bread Truck Pond will probably begin draining in 1 year, while C/D-Pond, Lawson's Pond and a large area of C-Pond will begin to drain in 10 to 15 years or less.

3. Annual sedimentation in certain ponds and marshes can bury WP in several years to a depth sufficient to reduce the exposure risk for feeding waterfowl. Artificial enhancement of sedimentation by introducing additives to increase flocculation may increase the effectiveness of the sediment barrier in some locations, while reducing the time required to build up an adequate thickness. Sedimentation (natural and enhanced) is a cost-effective alternative to the physical removal of WP from waterfowl feeding areas, particularly in areas of C/D-Pond, Lawson's Pond and A-Pond. Gully erosion and extension may subsequently drain and dry these areas, thereby permanently remediating them.

4. Ice is an effective erosion and transport medium for WP; large, sometimes thick slabs of WP-contaminated pond bottom sediments can be removed by ice plucking and transported to other locations in ERF during tidal flooding.

5. WP-bearing sediments are eroded from ponds and drainages by ice and water, and are subsequently transported by currents into the Eagle River and off-site into Knik Arm where their fate is unknown. Contaminated sediments are also transported to other locations within ERF.

6. Gully erosion, recession and pond sedimentation rates at Racine Island Pond are insufficient to naturally remediate the site in the short term. The pond floods frequently at low tidal heights and its sediments are rich in organics. It therefore appears that Racine Island Pond can be remediated most cost-effectively through artificial drainage and temporary berm containment to permit long-term drying and in-situ WP degradation.

On the basis of the investigations to date, the following recommendations are made:

1. Cost-effective remediation can be accomplished to a significant degree by allowing the physical system to remove or isolate WP contamination.

2. WP contamination of Bread Truck Pond and 50% or more of C-Pond, possibly including Lawson's Pond, should be treated by natural or enhanced drainage and subsequent in-situ WP degradation by drying.

3. Sedimentation and burial of WP will be effective in removing it from feeding waterfowl in several years; in a decade or less, burial will reduce waterfowl mortality in the C, Lawson's and C/D ponds.

4. Racine Island Pond may be effectively remediated by gully extension, artificial pond drainage and pumping, and long-term containment with a temporary berm, which will permit in-situ WP degradation by extended drying of pond bottom sediments. By removing the berm after WP has attenuated, the pond environment will be restored.

5. Erosion and recession rates, pond sedimentation, ground water, pond drainage and drying, and WP degradation and attenuation should be monitored to ensure that remediation is taking place. Continued analyses of the physical system will allow us to assess the rate and effectiveness of natural remediation and to evaluate if and where additional remedial actions are needed. Where artificial remediation techniques are applied, we suggest detailed site investigations to assess ecosystem impacts and how natural processes will influence the remediation measures.

6. WP migration and contamination in Knik Arm should be evaluated, focusing on areas of nearshore zones and mid-Arm bars where there is a potential for WP exposure to receptors.

7. The potential for natural WP attenuation by mechanical abrasion during transport by gully and tidal currents should also be evaluated.

Physical Processes and Natural Attenuation Alternatives for Remediation of White Phosphorus Contamination, Eagle River Flats, Fort Richardson, Alaska

DANIEL E. LAWSON, LEWIS E. HUNTER AND SUSAN R. BIGL

INTRODUCTION

Eagle River Flats (ERF) is a 865-ha salt marsh at the mouth of the Eagle River on the Knik Arm, northeast of Anchorage, Alaska (Fig. 1). The salt marsh has been used as an artillery range since the early 1940s. Previous work by CRREL has shown that an unusually high mortality of migratory waterfowl, particularly ducks, is attributable to the ingestion of elemental white phosphorus (WP) particles (Racine et al. 1992a,b). WP particles were introduced by smoke-producing compounds in devices detonated during military training (Racine et al. 1992a, 1993). WP is now present as particles and is also adsorbed to near-surface sediments at numerous locations in ERF, most notably in pond and marsh bottom sediments where dabbling ducks ingest it during feeding. In addition, WP-bearing sediment can be remobilized and transported to other locations within or external to ERF where it is redeposited (Lawson et al. 1996) and may pose a threat to unidentified receptors.

Our studies in 1993 and 1994 (Lawson et al. 1995, 1996) show that the physical system, and specifically the processes of erosion and recession of gullies draining the contaminated ponds and mudflats, can naturally attenuate WP contamination by increasing exposure and drying time of pond-bottom sediments. Until this takes place, natural sedimentation may reduce waterfowl exposure risks to WP ingestion by producing a thick sediment barrier between the surface and contaminated sediments.

Therefore, in 1995, we focused our efforts on understanding the rates at which these processes would alter the pond environments, removing or blocking the WP pathway to migrating waterfowl. We also examined WP erosion and transport to evaluate the potential for its off-site migration. These studies included analyses of the tidal and river hydrology and associated factors critical to evaluating proposed remedial technologies for WP contamination. This report describes the results of 1995 investigations of the physical ecosystem of Eagle River Flats and its role in the natural attenuation or intrinsic remediation of WP contamination.

ENVIRONMENTAL CONDITIONS

Eagle River Flats is one of several estuarine salt marshes in upper Cook Inlet, south-central Alaska (Fig. 1). Located at the mouth of the Eagle River, ERF is about 2.8 km wide at the coast and narrows inland. This subarctic region has a transitional maritime to continental climate, with moderate annual temperatures (daily mean 1.9°C; minimum mean –2.2°C) and precipitation (330–508 mm; Evans et al. 1972). Inundation results from both the semi-diurnal macrotidal fluctuations of 9 to 11 m in Knik Arm and the resultant overflow from the Eagle River as it meets the rising tide.

The Eagle River drains a 497-km^2 basin in the Chugach Mountains, 13% of which is covered by glaciers that significantly affect the runoff and sediment yield of the drainage basin (e.g., Lawson 1993). Glaciers modify peak discharges, the timing and volume of hourly, daily and seasonal discharges, the lag between precipitation and the

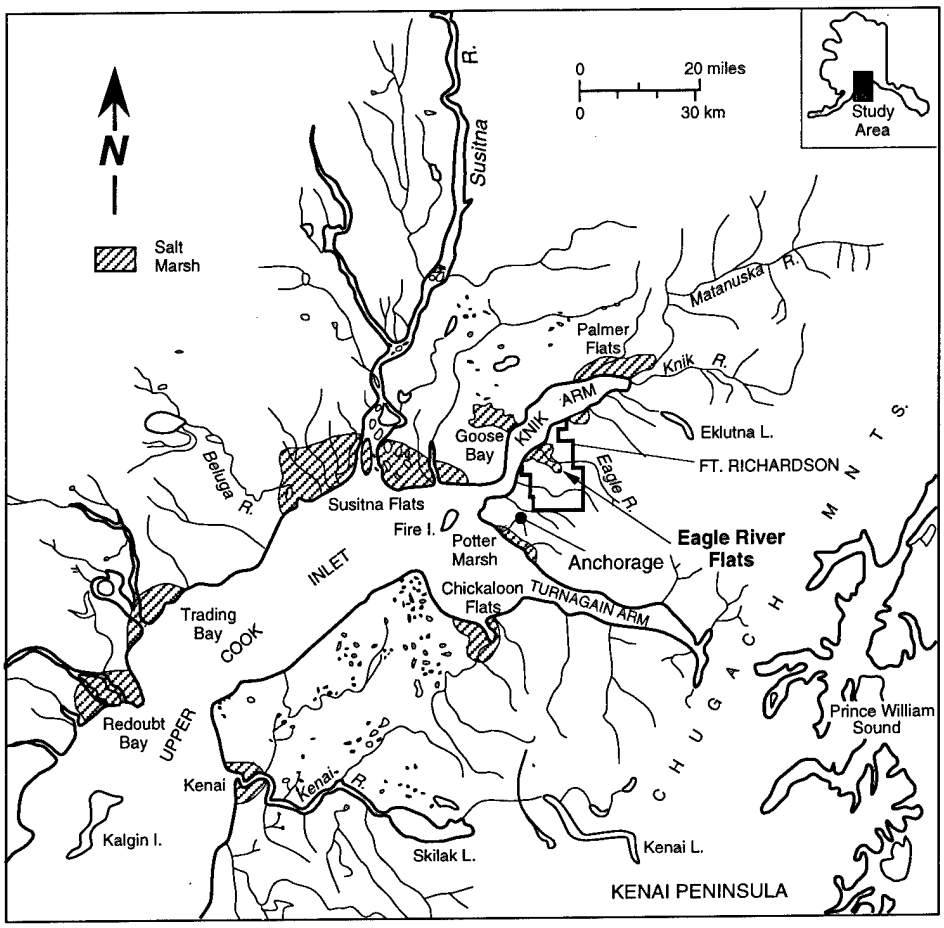

Figure 1. Location of ERF and other salt marshes in upper Cook Inlet.

resultant increase in runoff, and long-term trends in annual discharge of the basin (e.g., Gurnell and Clark 1987, Lawson 1993). Because of this glacial influence, maximum and peak discharges usually occur during the primary melt season of July and August. Sediment transport and sediment flux have diurnal, seasonal and annual variations caused primarily by glacial meltwater influx into the river basin (Lawson 1993). Similarly, massive quantities of silt- and clay-size particles are transported in suspension to Knik Arm by the large rivers draining into Cook Inlet from glacierized basins in the Alaska Range, Chugach Mountains and Kenai Peninsula (e.g., Susitna, Knik and Matanuska river basins, Fig. 1). These materials remain suspended for an extended time and are transported into the ERF salt marsh by tidal inundation (Lawson et al. 1996).

The Eagle River cuts approximately through the middle of ERF, with the ponds and marshes primarily draining through vegetated channels or drainageways and unvegetated tidal gullies that form a dendritic network (Fig. 2). Where gullies and drainageways do not follow a dendritic course, their location appears to be controlled by relict drainage networks abandoned during evolution of ERF (Fig. 3). The northern fifth of ERF along the coast is drained through gullies that discharge directly into Knik Arm. The east, west and southern boundaries of ERF are defined by uplands composed of glacial deposits covered by spruce and birch forests.

As with other estuarine salt marshes in Cook Inlet (e.g., Hanson 1951, Vince and Snow 1984, Rosenberg 1986), vegetation grows in bands or zones that approximately parallel the river and

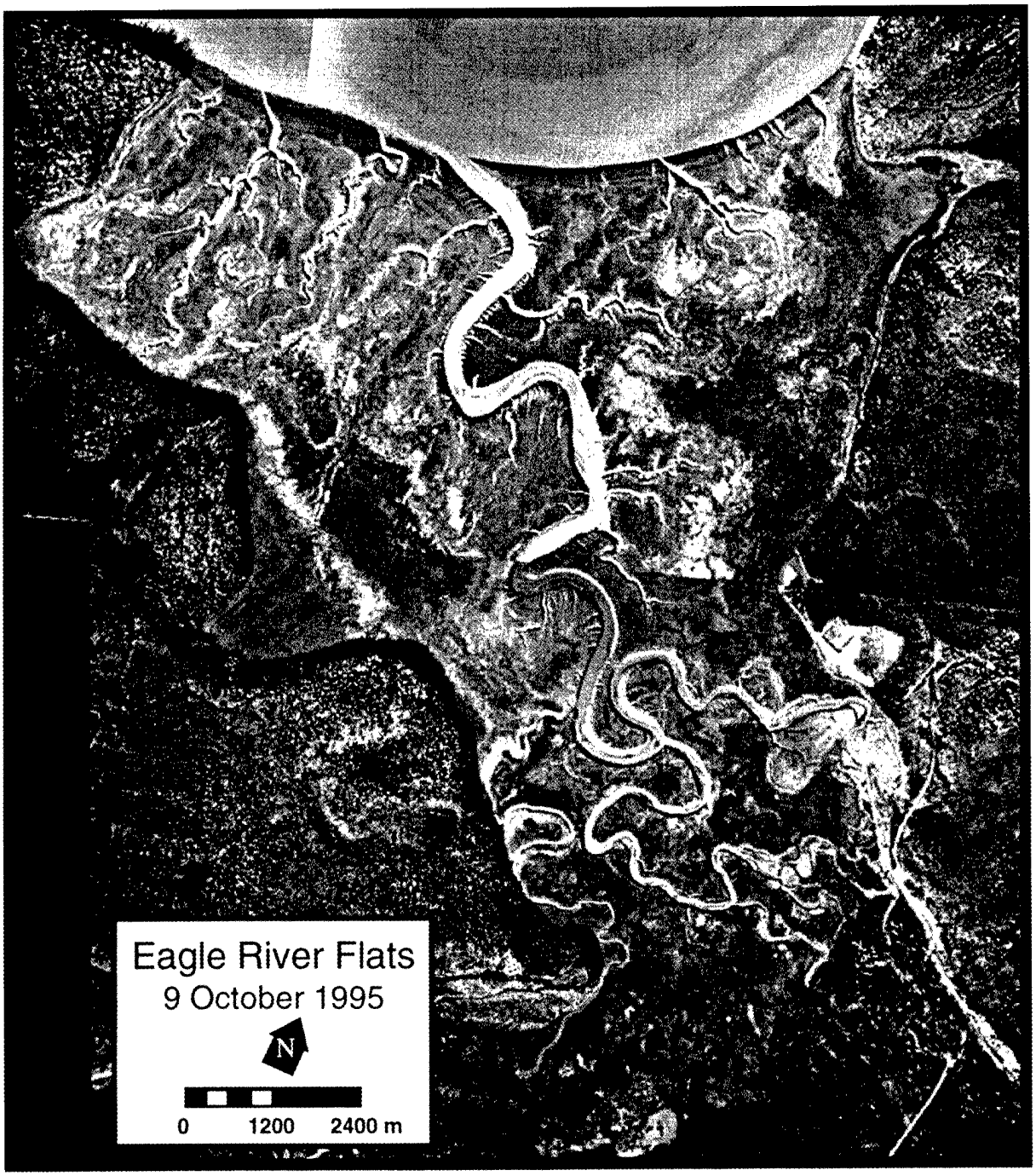

Figure 2. 1995 aerial photograph of ERF showing the dendritic drainage network.

uplands adjacent to ERF (Fig. 4, Racine et al. 1993). They commonly vary in location by elevation and thereby are related to the landforms of ERF as a function of flooding frequency, salt tolerance, drainage capacity and sedimentation rates. Levees, mudflats, marshes and shallow ponds (to 50 cm depth) are aligned approximately parallel to the Eagle River and coastline (Racine et al. 1992a). Freshwater ponds or shrub bogs bordered the upland along the northeast and southwest portions of ERF.

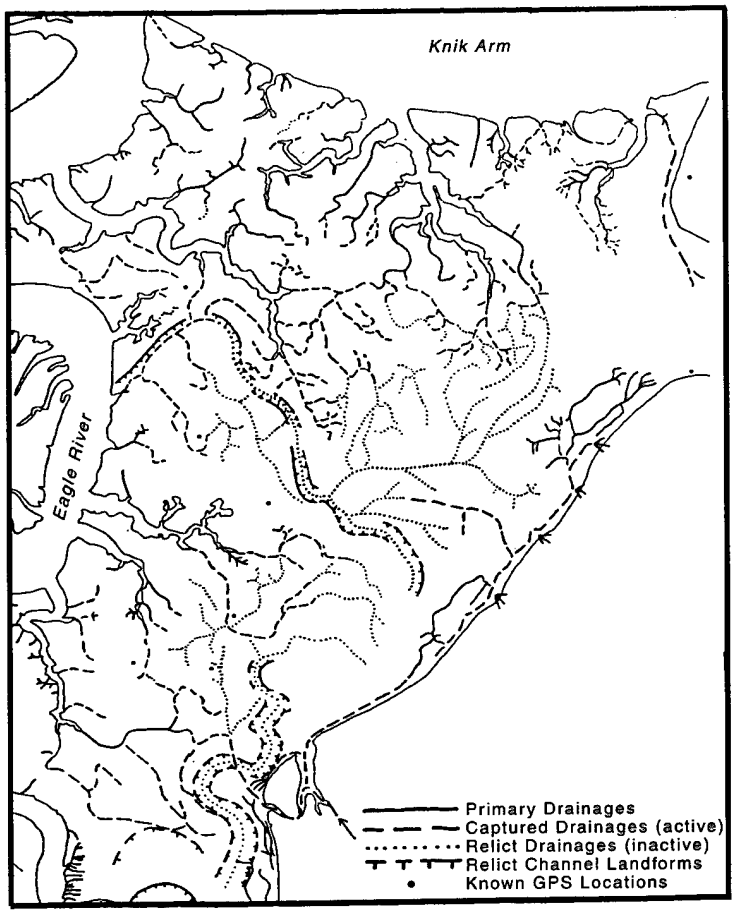

Figure 3. Drainage network in the C and D areas of ERF.

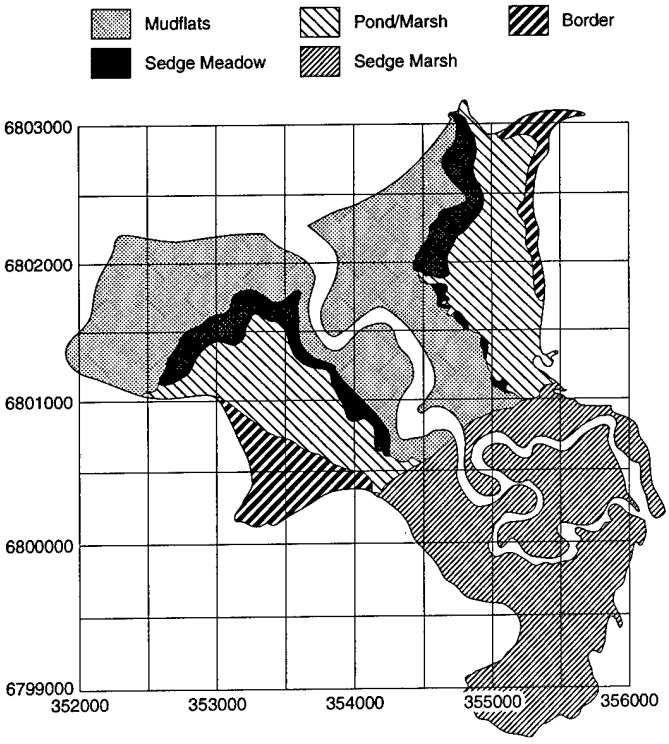

Figure 4. Distribution of primary landform–vegetation units (after Racine et al. 1992a).

RESULTS OF PREVIOUS PHYSICAL SYSTEM INVESTIGATIONS

Our previous investigations have focused on characterizing the processes and factors affecting the physical environment of ERF (Tables 1 to 4) and evaluating the fate and transport of WP, both of which are critical to developing a conceptual model for identifying appropriate methods of WP remediation and site restoration (Lawson et al. 1996).

The processes of erosion, transport and deposition vary across ERF, with responses to multiple internal and external factors over seasons, years and decades (Table 1). External controls on the physical system are difficult to define because their effects may last several decades or more and exert considerable control on internal factors that influence process relationships. The effects of earthquakes and other tectonic activity are difficult to predict; however, their impact on the ERF physical system may be enormous.

The 1964 Alaskan Earthquake (magnitude 9.2 on the Richter scale) resulted in both sedimentary and tectonic subsidence, which modified the site's elevation and the processes operating therein (e.g., Ovenshine et al. 1976a; Brown et al. 1977; Combellick 1990, 1991, 1994; Savage and Plafker 1991). A tectonic drop of about 0.6–0.7 m relative to mean sea level was recorded in the Anchorage region (Brown et al. 1977). Subsidence caused by sediment liquefaction and solidification during the earthquake probably reduced the pond bottom elevations an additional, but unknown, amount, as it did in the Portage area of Turnagain Arm (Ovenshine et al. 1976a). Post-seismic adjustments have resulted in an episodic uplift (Savage and Plafker 1991), which, according to tide-gauge data, was initially rapid

Table 1. Controls on physical processes.

Factor
Internal
River
Tides
Glacial sediment–water sources
Substrate material properties
Vegetation
Sediment influx–efflux
Weather–climate
Human activity
Ground water conditions
External
Earthquakes
Tectonic activity
Eustatic sea level rise
Isostatic rebound
Subarctic climate
Glaciers
Surface and ground water systems

Table 2. Erosional processes.

a. Summer.

Morphological unit	*Processes*	
Marshes	Currents (rare)	Wind waves (rare)
Ponds	Wind waves	Tidal currents
	Wind currents	Debris impacts (e.g., logs)
	Ducks and other bottom-feeding organisms	Bioturbation
Gullies	Currents	Ground water
	–tidal	–piping
	–runoff	–sapping
	Overland flow	Gravitational slope processes
	–sheet	–slump
	–rill	–block collapse
	Wind waves	–sediment gravity flow
Mudflats	Currents	Debris impacts (e.g., logs)
	–wind	Rain drop impact
	–tidal	Bioturbation
	Overland flow	
	–sheet	
	–rill	
Levees	Currents	Debris impacts
	–tidal	Wind waves
	–river	
Coast	Current scour	Debris impacts
	Wind waves	Overland flow

b. Winter.

Marshes	Ice plucking
Ponds	Freeze-on and ice plucking
	Ice shove
	Ice scour
Gullies	Plunge pool undercutting
	Freeze–thaw cycling
	Ice segregation and thaw
	Ice directed current scour
Mudflats	Ice plucking
	Ice shove (floating–expansion)
	Ice scour
	Ice cover confined scour
	Freeze–thaw cycling
Levees	Ice scour
	Freeze–thaw cycling
	Ice shove
	Ice-directed current scour
Coast	Ice plucking
	Ice shove (floating–expansion)
	Ice scour
	Ice block confined scour
	Freeze–thaw cycling
	Current scour
	Wind waves

(~2 cm/year; Brown et al. 1977) and now may be in the range of about 1.0 mm/year (Savage and Plafker 1991).

Long-term responses of the physical system to these changes in elevation, and hence base level relative to sea level, are unknown. An increase in flooding volume and duration may lead to an increase in pond sedimentation (e.g., Ovenshine et al. 1976a); however, the increased tidal prism (depth and volume) over the Flats might provide more energy for erosion as water is funneled into gullies during ebb tide. These responses remain under investigation.

Tidal dynamics and river hydrology control the amount of sediment that enters and drains from ERF, as well as the locations and rates of erosion and sedimentation. The amount of sediment transported in tidal flood waters is also a primary factor determining scour and sediment transport during ebb (Tables 2 and 3). Flooding tides transport large volumes of sediment onto the Flats during the summer, but the volume decreases substantially during the fall (Lawson et al. 1996). Transport changes seasonally as glacial input to Knik Arm decreases at freezeup and ambient air temperatures drop. During winter months, sediment and water discharge in the Knik, Matanuska, Susitna and Eagle river catchments decrease. This reduces the sediment available, despite lower water temperatures that increase its density, transport capacity and potential for movement of sediment into and within ERF.

Peak tidal flood heights across ERF, in the Eagle River and at the coast are delayed 20 to 40 minutes relative to the peak predicted at Anchorage (Lawson et al. 1996). The height is also generally 0.5 m or more greater than the Anchorage datum, reflecting, at least in part, the funneling of water out of Cook Inlet into the narrower Knik Arm (i.e., Syvitski et al. 1987). Tidal flooding of the Bread Truck, C, A and Racine Island areas may be

Table 3. Transport processes.

Summer	*Winter*
Currents (river)	Ice floes
–suspended load	–freeze-on
–bedload	–freeze-in
–saltation	–ice shove
Wind currents (pond–mudflats)	Frazil ice
–suspended load	–anchor ice
–sedload	–freeze-on
Gravitational slope processes	–freeze-in
Currents (tidal–gully)	
–flood	
–ebb	
Ground water	
–piping	

Table 4. Depositional processes.

Morphological unit	*Summer*	*Winter*
Ponds	Suspension sedimentation –settling-out –vegetation trapping	Ice entrapment and in-situ melting
Gullies	Suspension sedimentation –settling-out Bedload deposition Sediment gravity flows Slumping	Ice growth entrapment and in-situ melting Ice cover confined settling out
Mudflats	Suspension sedimentation –settling-out –vegetation trapping	Ice freeze-on and in-situ melting Snow filtering and in-situ melting Ice growth entrapment and in-situ melting Ice cover confined suspension settling
Marshes	Suspension sedimentation –vegetation trapping	
Levees	Suspension sedimentation –settling-out –vegetation trapping	Ice freeze-on and in-situ melting (sediment–organics) Snow filtering and in-situ melting Ice growth entrapment and in-situ melting Ice cover confined suspension settling out

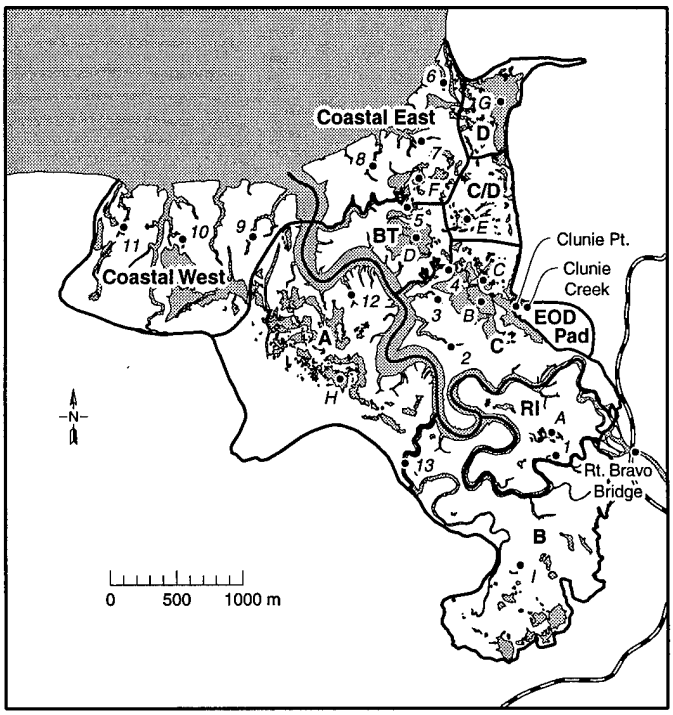

Gullies	Ponds	Areas
1—Racine	A—Racine	B—B-area
2—B-Gully	B—C-Pond	RI—Racine Island
3—Parachute	C—Lawson's	C—C-area
4—In-Between	D—Bread Truck	EOD Pad
5—Bread Truck	E—C/D-Pond	C/D—C/D-area
6—Coastal 1	F—Pond Beyond	BT—Bread Truck
7—Mortar	G—D-Pond	D—D-area
8—Coastal 4	H—A-Pond	Coastal East
9—Coastal 5	I—B-Pond	Coastal West
10—Coastal 6		A—A-area
11—Coastal 7		
12—Tanker		
13—Otter Creek		

Figure 5. Locations of gullies, ponds and areas.

enhanced seasonally by the discharge of the glacially fed Eagle River, particularly by snowmelt and precipitation in the river's watershed (Fig 5). In contrast, inundation along the coast is a function of tidal height, which may be influenced by the direction and velocity of the wind, ice cover and storm-driven surges in Knik Arm.

Tidal current measurements indicate that velocities are higher during ebb than during flood, and thus sediment transport and channel erosion are potentially greatest during ebb (Lawson et al. 1996). Peak velocities within gullies ranged from about 0.8 to 1.9 m/s in 1994 and varied from site to site and with the elevation of tidal flooding. The velocity variations reflect differences in gully width, depth, roughness and network configuration.

The Eagle River provides access for tidal waters to inundate the innermost reaches of the Flats. High tides increase river stage by tidal damming and reversing flow in the river. Sedimentation in the northern two-thirds of ERF is tidally dominated, whereas the southern one-third appears to be river dominated. Tidally dominated sedimentation ranges from several millimeters per year on levees, to 10–15 mm/year on mudflats, and up to 20–40 mm/year in ponds. Sedimentation has formed an alluvial fan at the head of ERF (Fig. 6), indicating that deposition here is mainly derived from overbank flooding of the river.

Suspended sediment concentrations measured in 1994 in the Eagle River, tidal gullies draining the ponds and mudflats, and Knik Arm show that most of the sediment is derived from Knik Arm tidal waters (Lawson et al. 1996). The Total Suspended Solids (TSS) in the waters of ERF vary with tidal stage, location, source and season. TSS values in the glacially fed Eagle River vary seasonally from peaks of 100–700 mg/L between breakup in May and freezeup in October. Apparently, there are two seasonal highs each year, the first during snowmelt runoff and the second during the peak glacial melt season. In contrast, TSS values of Knik Arm water range from about 1000 to 2800 mg/L from May to October. The high TSS values of Knik Arm reflect its source from large glacial rivers (e.g., Susitna, Knik and Matanuska), which have higher sediment discharges than the Eagle River. During a tidal cycle, TSS measurements at gully sites increase steadily through the flooding tide and decrease at a slower rate during the ebb. Seasonally, TSS values in gully and Knik Arm waters increase from spring to fall; the cause of this increase is unknown.

Gullies are actively extending into the mudflats and ponds in the Bread Truck, C, A, D and C/D

Figure 6. Aerial photograph of Racine Island taken 16 August 1995 showing remnant channel surrounded by overbank deposits.

areas (Fig 5). Headwalls and adjacent lateral walls receded at variable rates: 0.1 to 4.9 m during summer 1992, 0.4 to 6.3 m during winter 1992–93, 0.0 to 9.8 m during summer 1993, 0.0 to 2.3 m in winter 1993–94, and 0.0 to 2.6 m in summer 1994. Large tidal floods in 1993 and 1994 caused the highest headwall recession rates. Two gully headwalls, one on the western side of Bread Truck Pond and the other near the pond complex between Bread Truck Pond and C-Pond, were advancing at a mean rate during 1993–1994 that was sufficient to cause increased drainage of these ponds in 15 to 20 years (Lawson et al. 1996).

Surveying of longitudinal profiles of tidal gully thalwegs revealed nonuniform gradients that reflect their progressive and episodic elongation into the mudflats and ponds, and a lack of equilibrium with present conditions. Gully gradients are

relatively steep near their mouths, but are reduced in the lower and mid-reaches. Channel gradients then steepen in the uppermost reaches up to a nearly vertical headwall that ranges in height from 1 to 2.5 m. Incipient drainageways from ponds and mudflats into tidal gullies have very low gradients. Several sharp increases in gradient (knickpoints) occur in each gully, marking channel adjustment as the tidal gully progressively extends into the mudflats and ponds.

Aerial photographs from 1950, 1967 and 1993 reveal changes in the distributary channel pattern entering ERF (Fig. 7). Three main channels entered the Flats in 1950, but by 1967 the westernmost channel was abandoned and the eastern and middle channels diverged just northeast of the Route Bravo bridge. These two primary channels were characterized in 1967 by partial braiding and a divergent pattern characteristic of an alluvial fan (Fig. 7b). Sediments in the fan area are relatively featureless overbank materials deposited by Eagle River flooding. Only the center of the Racine Island area (Fig. 6) is characterized by intertidal ponds and an abandoned gully. The westerly channel was abandoned in September 1995, during flooding of the Eagle River as channel scour shifted the easterly channel to the northeast.

The northern two-thirds of ERF has landforms typical of tidal flats near river mouths (e.g., Ovenshine et al. 1976b) that consist mainly of levees, vegetated marshes and abandoned channels and point bars. Significant changes in the relatively tight meander loops in this lower section of the river have also taken place over the last 40 years. Channel changes are a natural progression resulting from the erosion and recession of the outer banks of meander bends, deposition of sediments as point bars in the inner parts of each bend, and a general downstream migration of the channel (e.g., Allen 1982). Meander scars, abandoned meander loops, and point bar deposits are common along the length of the active channel and are evidence of such changes in the past.

Tributary channels with dendritic patterns, herein called vegetated drainageways, drain water from the mudflats and ponds into the tidal gullies (Fig. 3 and 8). A second set of channels, intercepted by the active tributary system, unconformably crosses other landforms, including ponds (such as C and Bread Truck). Their pattern is irregular and unrelated to the active gully drainage system. These secondary channels are parts of former drainageway and gully systems that are now inactive and therefore relict. Their fragmentary presence is a sign of significant changes to the drainage system in the past. The cause of such change is unknown, but events such as river avulsion, channel migration or earthquake-induced subsidence may cause abandonment of drainageways and gullies.

Chemical analyses of a limited number of sediment trap and plankton net samples indicate that WP undergoes suspension, transport and redeposition in ERF, as well as transport through tidal gullies into the Eagle River and Knik Arm. Tidal and wind-driven currents can scour pond bottoms, resuspending and transporting WP, whether as individual particles or sorbed to sediment. Erosion and scour of vegetated drainageways and gullies can also entrain sediment containing WP and transport it in suspension or as bedload. In addition, pond and mudflat sediments can freeze to the base of the ice cover during its growth, and subsequently be rafted during tidal inundation. Bathymetric profiling offshore of ERF shows no evidence of deposition of ERF sediments as a delta at the mouth of the Eagle River. WP entering Knik Arm is potentially diffused by tidal and river currents, but there are several sites where WP-contaminated sediment might be deposited (Lawson et al. 1996). These sites include intertidal bars and nearshore deposits where waterfowl may feed.

Previous investigations suggest that natural attenuation of WP contamination is possible, but that further work is needed to assess the length of time over which this may happen and to identify specific locations where natural attenuation is the remedial method of choice. The relative importance of erosion and deposition processes varies from area to area in response to tidal and river hydrology; however, changes in the system over seasons, years and decades are possible.

Pond sedimentation rates appear to be sufficiently high in some areas to bury WP, thereby reducing the exposure risk for waterfowl naturally. The drainage system is also changing as tidal gullies expand across mudflats into ponds. Certain ponds are likely to drain in 20 years or less. Drier conditions will permit in-situ degradation and natural remediation of WP contamination. Erosion will, however, continue to release WP from mudflat and pond sediments over time, while ice and water transport mechanisms will move WP into tidal gullies, the Eagle River and

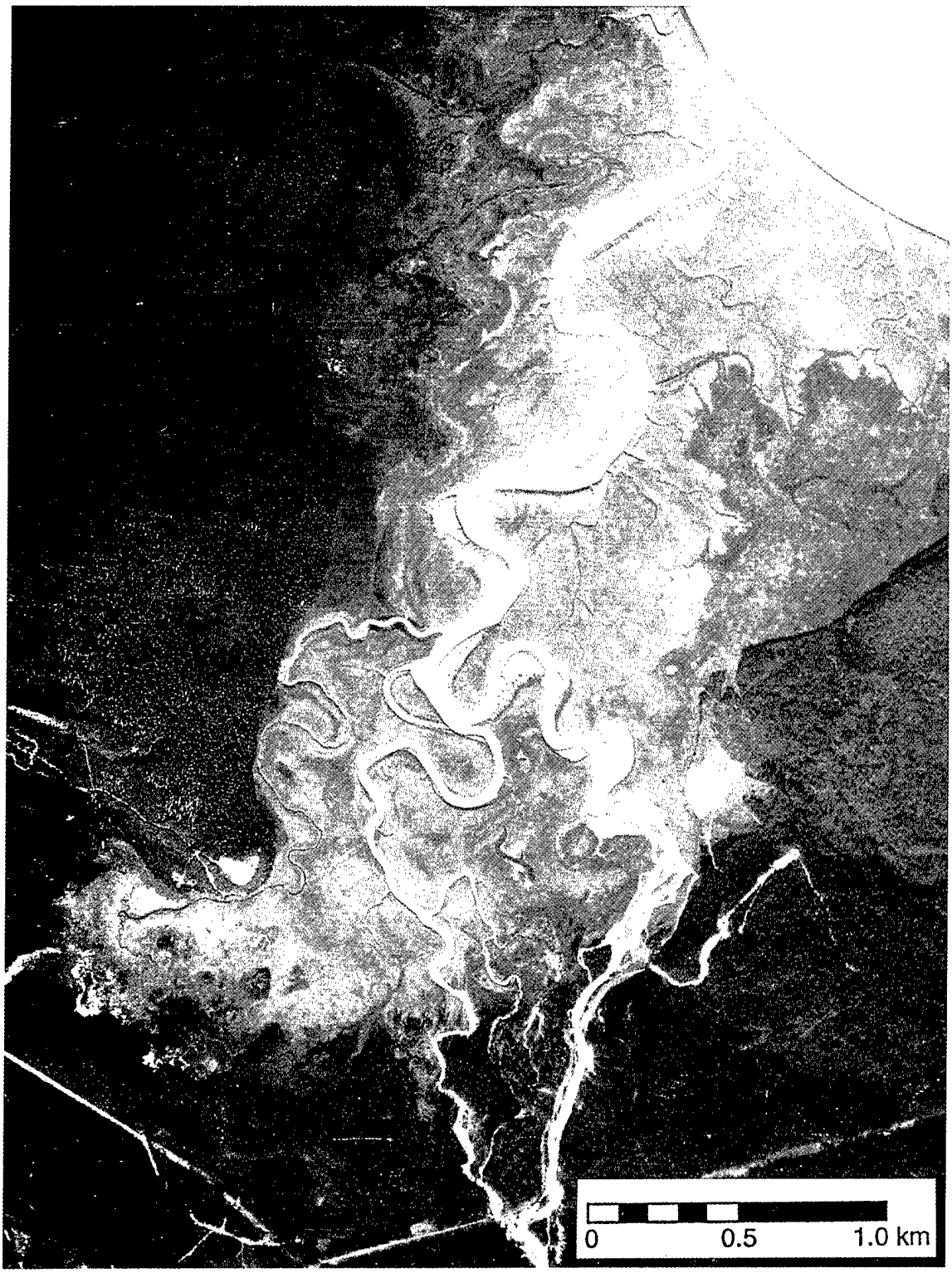

a. 1950.

Figure 7. Aerial photographs of ERF.

b. 1967.

Figure 7 (cont'd).

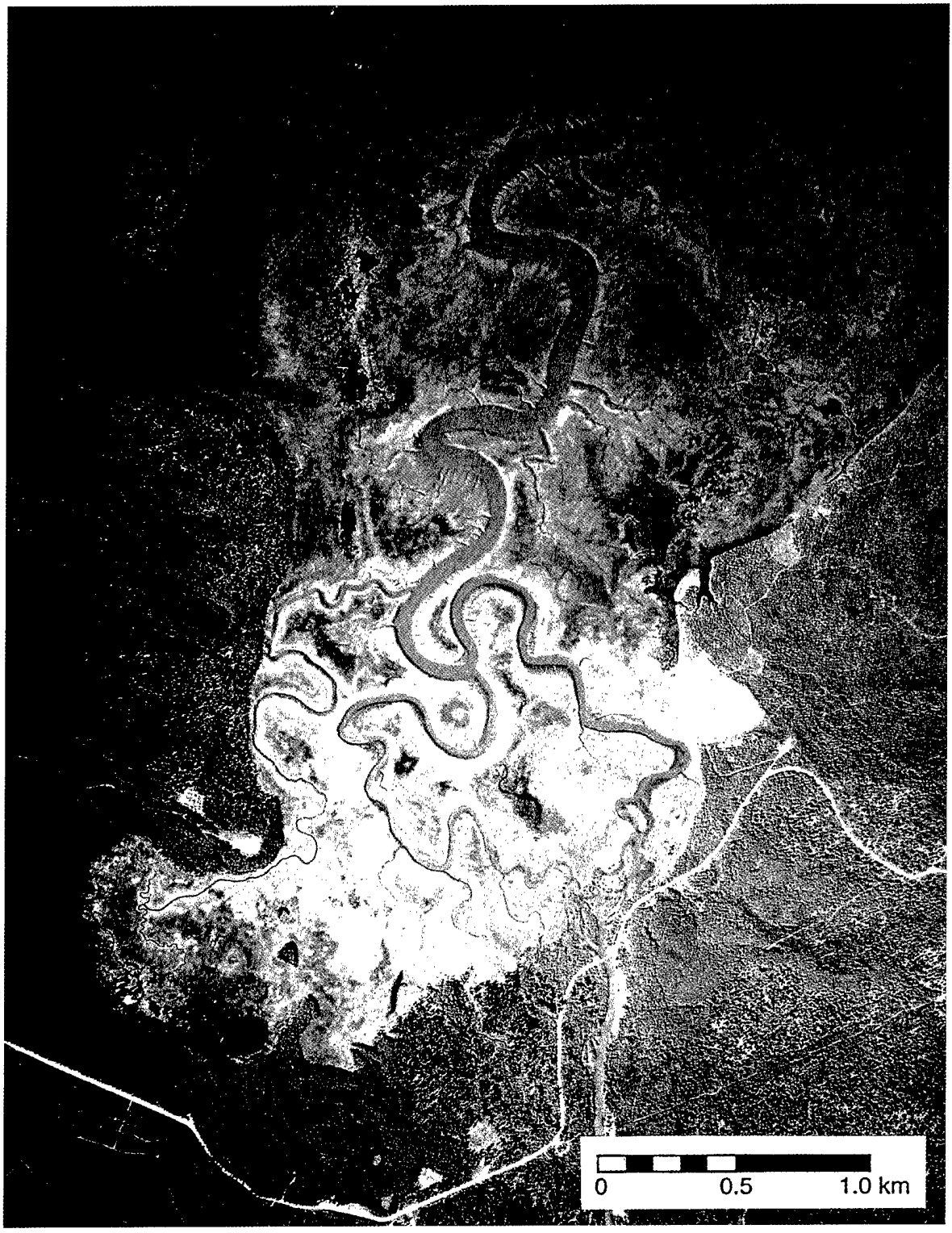

c. 1993.

Figure 7 (cont'd). Aerial photographs of ERF.

Figure 8. 1992 aerial photograph of northeastern ERF.

subsequently Knik Arm. Sediment entering Knik Arm may be widely dispersed by estuarine processes, or concentrated in bars and other deposits. Which will happen is unknown. In addition, whether WP survives transport to actually persist in Knik Arm is unknown. Laboratory flume tests of WP particle abrasion could determine if transport destroys such particles.

STUDY SITES AND METHODS

Sedimentation transects

Sedimentation rates were measured along transects across representative landforms of ERF, with 11 transects being set out in May 1992 (Lawson and Brockett 1993), 1 in June 1993 and 11 in 1994 (Fig. 9). Their locations and elevations were

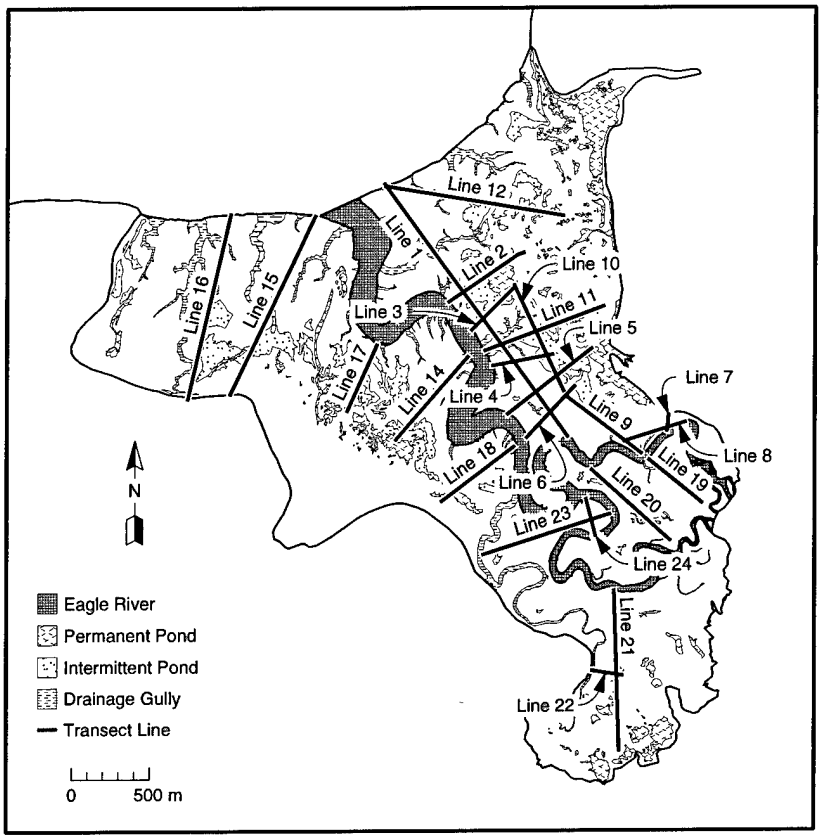

Figure 9. Mudflat sedimentation transect locations.

surveyed using an electronic theodolite. Grab samples of surface sediment (to 5 cm depth) were taken at each survey point along the transects, and their grain size distributions were analyzed using standard sieving and hydrometer techniques. These data delineated textural trends in surface materials and the relative importance of tidal and river sediment sources to sedimentation and landform development (Lawson and Brockett 1993).

Sedimentation stakes were used to measure surface aggradation or erosion on transects where the surface was wet or standing water was temporarily present (Fig. 10). These stakes consisted of a rod and a square, rigid plate (about 7 cm^2) that slides freely on it, following Ovenshine et al. (1976a,b) in Turnagain Arm, Alaska. Erosion depth is defined by the increase in distance between the top of the rod and the top of the plate, as measured periodically to the nearest 0.5 mm. The amount of accretion is the thickness of sediment deposited on the plate surface. The difference between these two readings defines the net sedimentation (or erosion) rate. Rates were measured in July, August and September 1992 following each monthly period of tidal flooding, while seasonal rates were measured in May and September 1993, 1994 and 1995.

Sedimentation on levee and mudflat surfaces was monitored by spraying an area (~30 × 30 cm) on the ground surface with pavement-marking paint and locating the corners of this area with wire survey flags (see also Vince and Snow 1984). Paint was applied at certain sites in June and August 1992, August 1993, and May–June 1994. Net accumulation was measured by cutting and removing a block of sediment with a putty knife or spatula (Fig. 11). The thickness of sediment above the paint layer was then measured to the nearest 0.5 mm. In contrast to the sedimentation stakes that were commonly broken or removed by ice during winter, the wire flags and buried paint horizons enabled us to acquire a continuous record of net sedimentation rates.

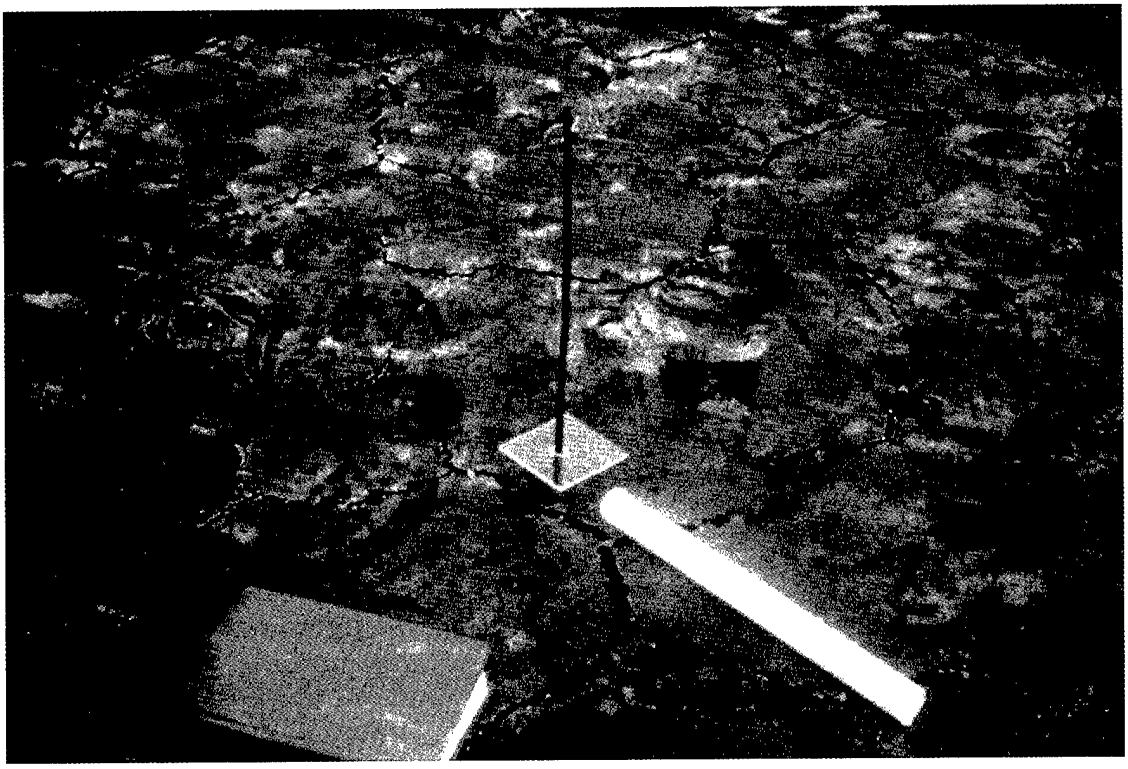

a. Sedimentation stake with plate.

b. Wire flags mark an area of painted ground.

Figure 10. Sedimentation measurement techniques.

Figure 11. Wedge-shaped sediment block used to measure vertical accretion. Note subhorizontal laminations.

Pond sedimentation measurements

Sedimentation rates in permanent ponds and marshes are difficult to measure accurately because a slight disturbance of the water column can resuspend the fine-grained materials covering their bottoms. Transects were established in May 1995 for detailed measurements of sedimentation rates in six ponds (Fig. 12), while isolated sites were previously established in 1992, 1993 and 1994. Two orthogonal transects were usually established in each pond, with traps located about every 20 m along them. Two methods were used in permanent ponds, one to measure gross sedimentation rates and another to evaluate resedimentation caused by resuspension of pond and marsh sediments by wind, waterfowl and other processes.

Gross (total) sedimentation rates in ponds were measured at 18 sites following tidal inundations in June, August and September 1992, and in May and September 1993, 1994 and 1995 (Fig. 13). Gross deposition from tidal and river inundation, as well as resuspended bottom sediments, was measured in a sediment trap consisting of a 4-in.-diameter (10.2-cm-diameter) schedule-40 PVC pipe end cap glued to a short length of 2-in.-diameter (5-cm-diameter) schedule-40 PVC pipe at the isolated pond stations, and a 16-cm-diameter end cap at pond transect stations. The pipe was inserted into pond sediments until the bottom of the cup was in contact with the bed (Fig. 14). Sediment trapped in the cup included new sediment brought into the ponds by tidal inundation and river currents, and materials resuspended by wind waves, dabbling ducks or other mechanisms. The thickness of accumulated sediment was measured to the nearest 0.5 mm by inserting a graduated scale into it at three places. After measurement, the sediment in the cup was cleared or saved for analysis of WP concentration.

Net sedimentation rates at isolated sites and transect sites were measured using a thin, rigid plastic plate of about 30 cm square that was pushed gently into the pond bottom until its surface was flush with the bottom surface. The corners of the plate were secured by aluminum tent pegs (Fig. 14). Sediment in suspension settled onto

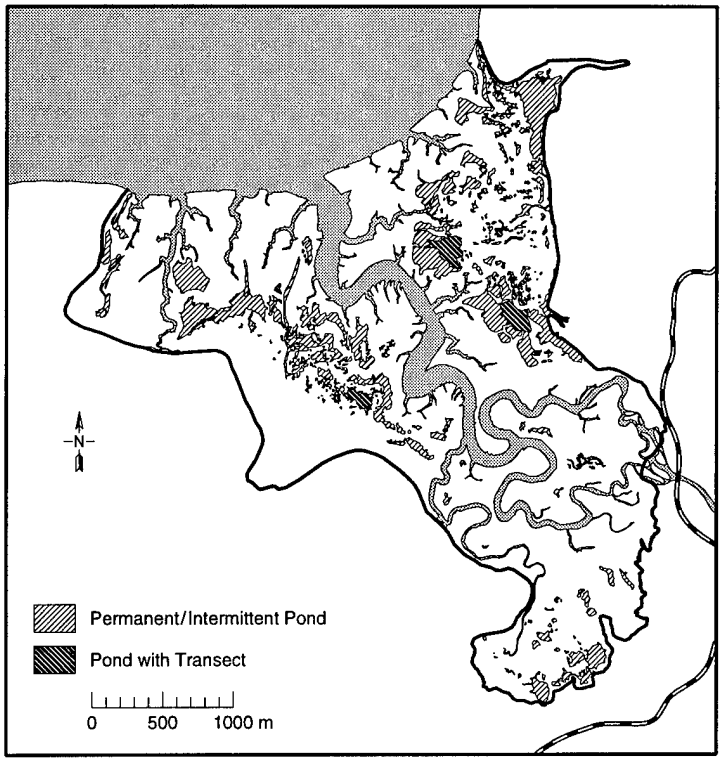

a. Locations of pond transects.

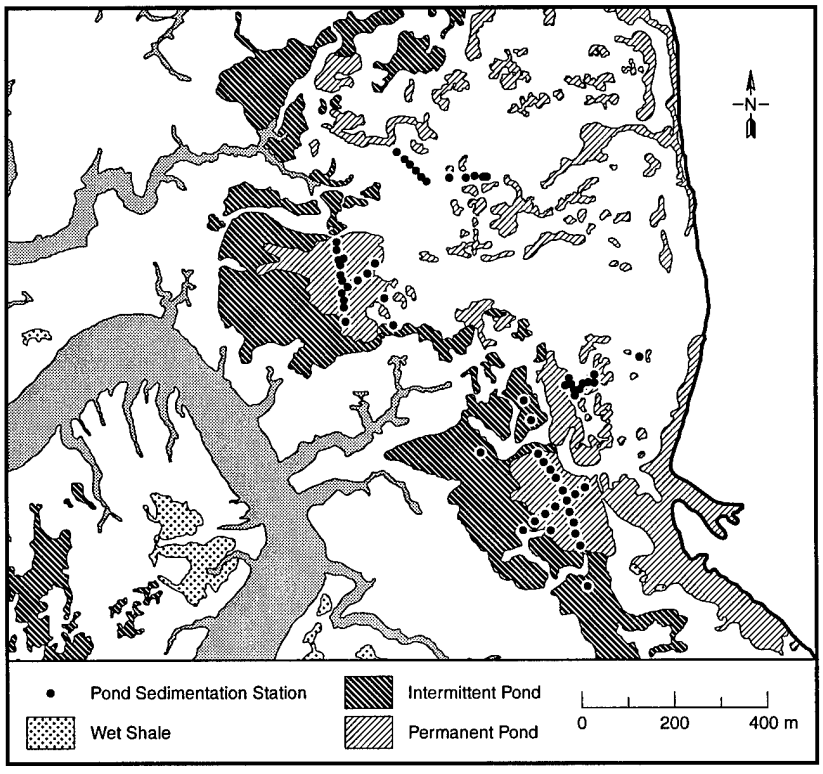

b. Transects in Bread Truck, C/D, C and Lawson's ponds.

Figure 12. Pond sedimentation measurement locations.

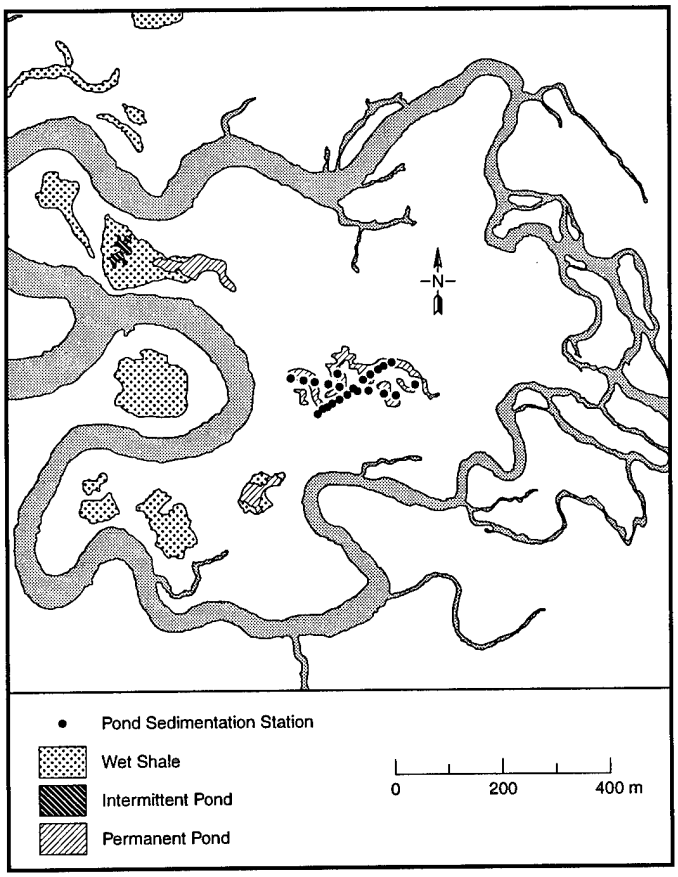

c. Racine Island Pond transects.

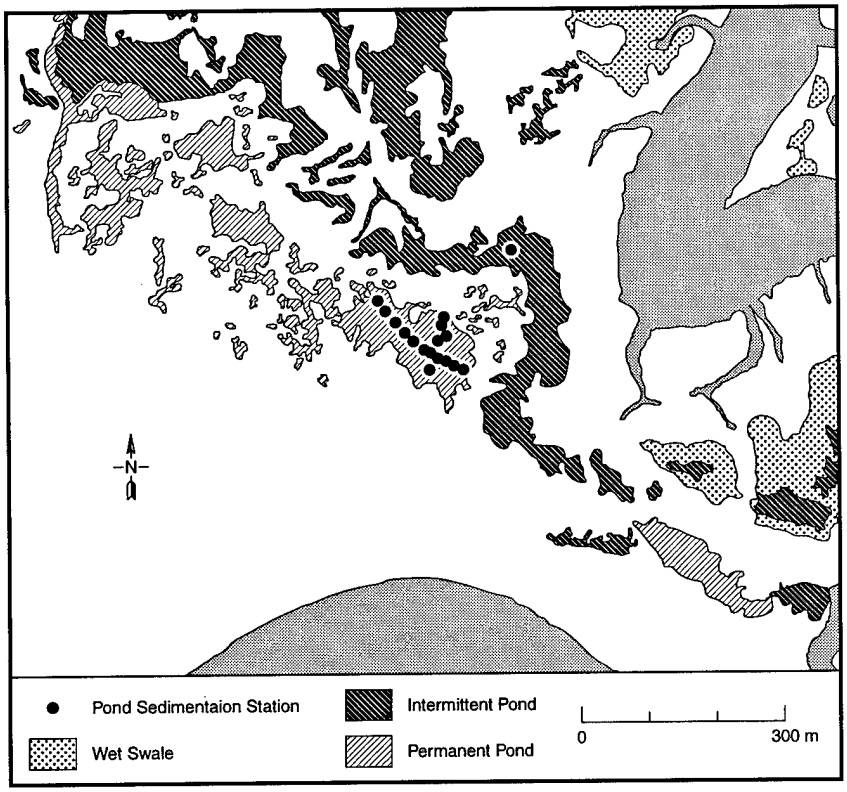

d. A-Pond transects.

Figure 12 (cont'd). Pond sedimentation measurement locations.

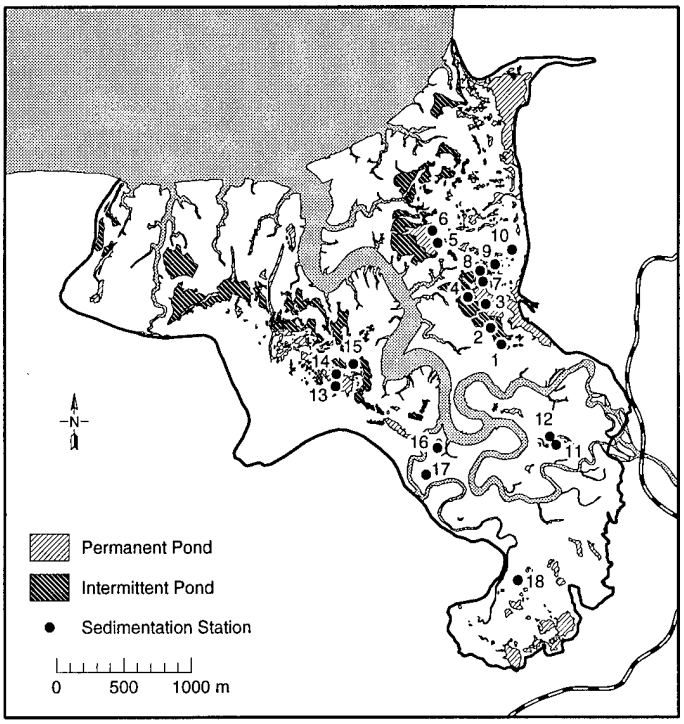

Figure 13. Locations of 1992–1994 pond sedimentation stations.

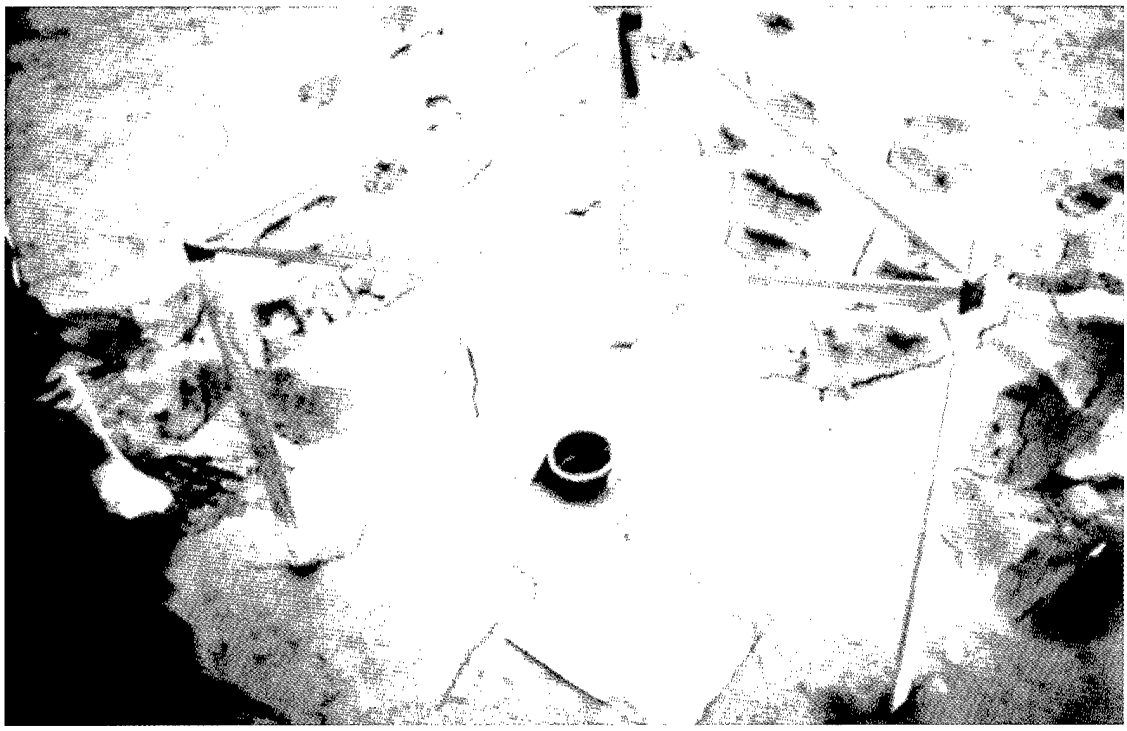

Figure 14. Example of sedimentation station at an intermittent pond location showing layout of cup and plate sampler.

Figure 15. Example of layout of hub and line stakes at River-North erosion site.

this plate, but this sediment can also be reworked and resuspended by wind or other mechanisms, thereby delineating a net rate. The thickness of sediment at three locations was measured to the nearest 0.5 mm using a graduated scale.

Gully erosion and headwall recession

Tidal gullies draining ponds and mudflats are actively extending inland by erosion at their heads. We established 86 sites between June 1992 and May 1995 to evaluate retreat rates. At each site, stakes were driven into the ground along a line at known distances from one another, typically parallel to the crest of the gully scarp, and a "hub" stake was set at a known distance from this stake line (Fig. 15). The distance between the hub and the crest of the gully scarp was measured across the top of each line stake with a tape measure. The position of the gully scarp crest was identified by lowering a plumb bob on a string from the tape measure, so that the horizontal distance could be read where the string and measuring tape met. Flagged wire stakes were then placed at each point of measurement along the headwall. We periodically relocate the stakes when scarp recession takes place (Fig. 16) and either removes or threatens them. Repeated measurements using this technique allow us to monitor changes in scarp geometry with time, as well as the rate of gully recession.

Recession rates were measured in September 1992, 1993, 1994 and 1995, in May 1993, 1994 and 1995, in November 1994 and late October 1995. The September measurements delineate summer rates, while those of May or June delineate winter rates. The October 1995 and November 1994 data show the amount of erosion since the end of summer measurements and the initial period of freezeup. Repeated measurements at points without any retreat (as indicated by the continuing presence of wire flags) indicate that they are reproducible to ±2–5 cm. Their accuracy, however, is limited by how well the crest of the gully scarp can be defined, the shape of which is highly irregular. In the worst case, accuracy is probably limited to ±10 cm.

Recession data are presented as a range of maximum recession rates measured orthogonally to the gully or river at each site. This method differs from previous years' method, where erosion measurements were reported as collected in the field and did not account for apparent distances created by the method (Lawson and Brockett 1993; Lawson et al. 1995, 1996). These rates tended to be higher than actual wherever hub to line measurements were made at an acute angle to the scarp, thus recording an oblique distance. Measurements reported herein were taken from scaled summary plots and summarize the range in recession rates,

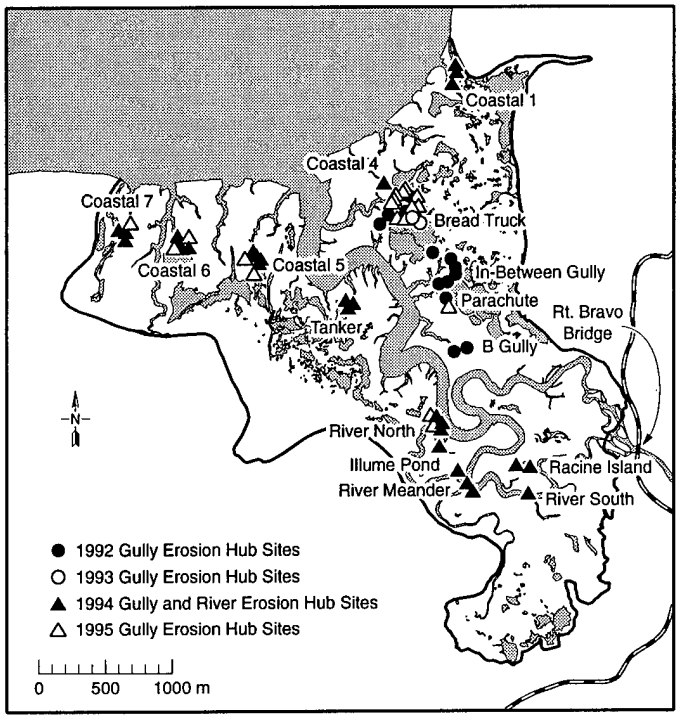

Figure 16. Location of gully headwall and lateral wall erosion sites.

not absolute values based upon each hub to line stake measurement.

Historical aerial photographic analyses

During 1995, multiple sets of aerial photographs were acquired to increase our historical coverage of Eagle River Flats (Table 5). Our current aerial photography archive provides a 45-year record of surficial changes at ERF from 8 August 1950 to 9 October 1995. The images are of variable quality and range from the highly blurred 1967 black and white images to the high resolution natural color photographs of 9 October 1995.

We measured historical changes by studying aerial photographs taken at approximately decade intervals (1950, 1960, 1972, 1984–86 and 1995). The actual photography set used was determined by our ability to detect gully headwall scarps. The headwalls of B-Gully, Parachute Gully, In-Between Gully, Bread Truck Gully, Mortar Gully and Coastal 5 Gully were mapped to document their recessional histories.

Average rates of headward recession were calculated by transposing the position of the gully headwall scarps onto gully base maps produced from the 9 October 1995 aerial photographs. The distance of headward recession was measured as the centerline distance within each gully between known points. The average rates were then determined by dividing the distance of centerline recession by the number of years between each measure.

Water quality parameters

Various types of water quality data have been collected at multiple sites to assess the surface hydrology and water quality of ERF. The majority of sampling sites were in small plunge pools at the heads of tidal gullies; three were newly located in ponds in 1995 in some of the most heavily contaminated locations of Eagle River Flats (Fig. 17). The site at Mortar Gully receives tidal waters directly from Knik Arm, whereas Bread Truck, Parachute, B and In-Between gullies are located in drainages that flow into the Eagle River and therefore have mixed fresh and tidal water sources. Racine Island Gully receives most of its water influx from the Eagle River during the summer. The three pond locations where measurements were recorded—C, A and Racine ponds—are distributed in the eastern, western and southern sections of ERF. The two remaining sites represent the primary source waters: the Eagle River up-

Table 5. Historical aerial photography of Eagle River Flats.

Year	*Date*	*Type*
1950	8 August	B/W
1953	27 June	B/W
1957	12 July	B/W
1960	30 August	B/W
1962	17 May	B/W
1967	Unknown	B/W
1972	July	False color IR
1972	9 August	B/W
1974	7 May	B/W
1977	Unknown	False color IR
1978	August	False color IR
1984	12 August	False color IR
1986	5 October	True color
1986	12 September	LANDSAT TM (Digital)
1988	4 August	B/W
1991	21 June	Color IR
1992	22 May	Color IR
1992	2 August	Color IR
1993	8 July	B/W Orthophotograph
1994	30 August	Color IR
1995	16 August	Color IR
1995	9 October	True color

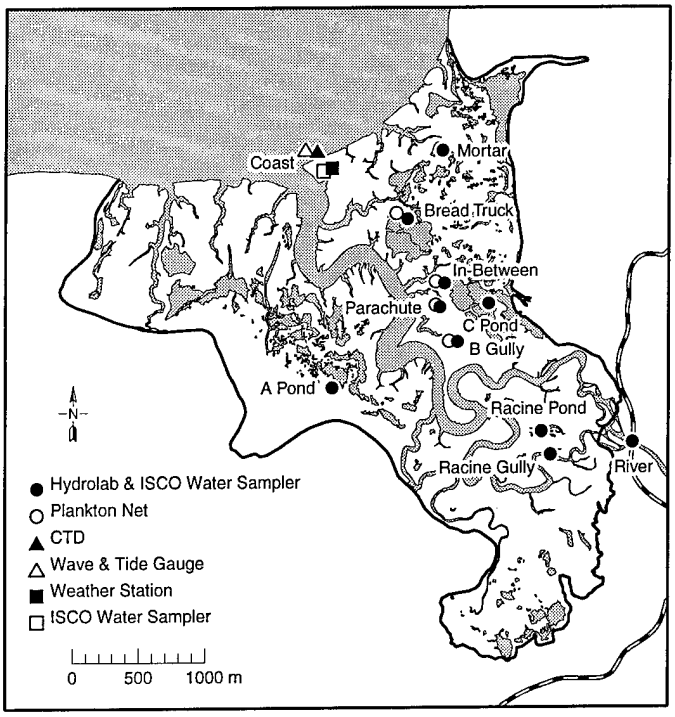

Figure 17. 1995 locations of instrumentation recording water quality parameters and water depths. Locations of weather station and plankton net sampling sites are also shown.

stream of where it enters ERF, and in Knik Arm in the nearshore zone, about 200 m north of the Eagle River mouth.

A suite of water characterization data was collected at 4-minute intervals at each site. These data include salinity, pH, redox, dissolved oxygen, turbidity and water surface elevation (Table 6). Figure 18 shows the times of data collection since 1993. Water samples were collected with an ISCO suction sampler automatically at various intervals before, during and following flood tides. The sampler was programmed to obtain 500-mL water samples at specific intervals through the flood and ebb cycles. These samples were processed for TSS concentration using vacuum techniques and 45-µm glass microfiber filters, generally following procedure 2540D in *Standard Methods for the Examination of Water and Wastewater* (APHA, AWWA, WEF 1992). Modifications to this procedure were described in Lawson et al. (1996).

A Marsh–McBirney electromagnetic flow probe was used to measure current velocity during ebb and flood in selected tidal gullies. A unit was also installed in C-Pond to

Table 6. Specifications of sensors used in water quality parameter measurements.

Instrument type	*Sensor*	*Accuracy*	*Resolution*
Hydrolab	Temperature	± 0.15°C	0.01°C
(H_2O Multiprobe)	pH	± 0.2 units	0.01 units
	Specific conductance		
	Fresh water	± 0.0015 to 0.1 mS/cm*	0.001 mS/cm
	Salt water	± 0.15 to 1.0 mS/cm*	0.01 mS/cm
	Salinity	± 0.2 ppt	0.1 ppt
	Dissolved Oxygen	± 0.2 ppm	0.01 ppm
	Redox	± 20 mV	1 mV
	Depth	± 0.45 m water	0.1 m water
CRREL thermistor	Temperature	± 0.02°C	0.01°C
Druck (PDCR 950)	Pressure (water depth)	± 0.008 m water	0.001 m water
D&A OBS-3	Turbidity	± 100 mV	1 mV
	5 V = 2000 FTU		
Marsh-McBirney	Water current (velocity)	± 6.10 cm/s	2.13 cm/s
(model 512)			
Campbell Ultrasonic	Distance (water depth)	± 1 cm	0.05 cm
(model UDG01)			
Seabird Wave/Tide	Pressure (water depth)	± 0.003 m water	0.0015 m water
(model SBE 26-03)	Temperature	± 0.02°C	0.01°C
Seabird CTD	Pressure (water depth)	± 0.75 m water	0.045 m water
(model SBE 16)	Temperature	±0.01°C	0.001°C
	Conductivity	± 0.001 S/m	0.0001 S/m
	Dissolved oxygen	± 0.1 mL/L	0.01 mL/L
	pH	± 0.1 units	
	OBS [5 V=2000 FTU]	± 100 mV	3 mV

* Depends on which of three auto-adjusting ranges is employed.

measure tidal and wind currents. The sensor was mounted about 1 m above the bed in gullies at the Bread Truck, Parachute, In-Between, Mortar and B sites (Fig. 17). Ultrasonic sensors were used to measure flooding on the mudflats near the Mortar, Bread Truck, Parachute, In-Between and Racine gullies, and at the weather station coastal sites.

The same suite of water quality parameters was collected at the Knik Arm coastal site using a Seabird SBE 16 Profiler. In addition, a Seabird SBE 26 wave and tide gauge was located here to record water depth and temperature in Knik Arm (Table 6). The same location was used in 1993 and 1994 (Fig. 17).

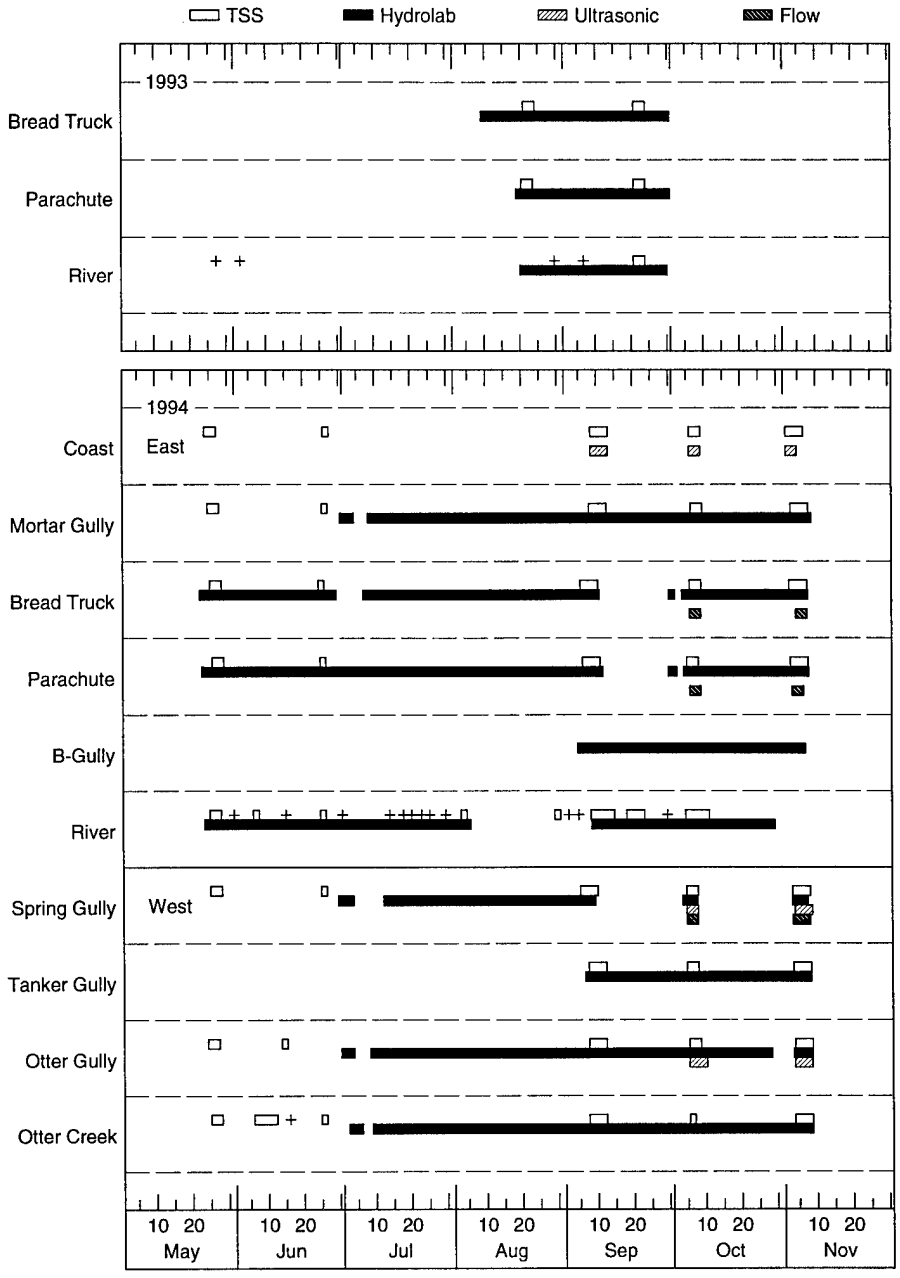

Figure 18. Extent of data collection at hydrostation sites from 1993–1995.

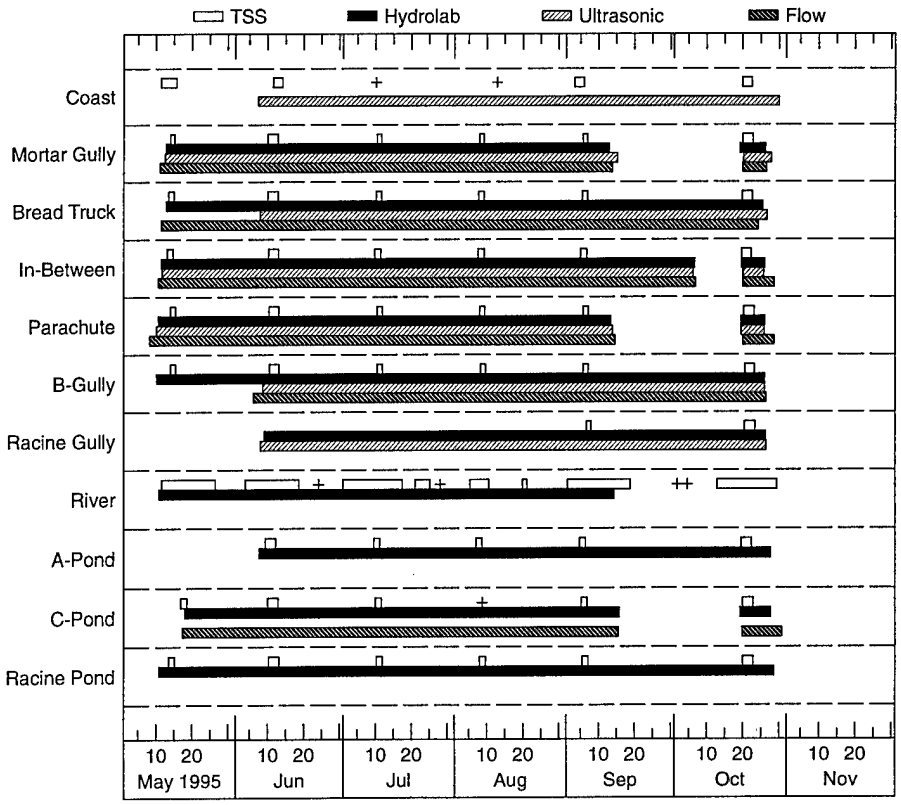

Figure 18 (cont'd). Extent of data collection at hydrostation sites from 1993–1995.

Hydrostation configuration

The instrumentation and samplers for water quality analyses were identically set up at each gully and pond site (hydrostations). Sensors and the suction sampler intake screen were mounted on a stake driven into the bottom of the pond or gully under investigation. Mounting hardware was identical at each hydrostation to permit us to precisely position them in the water column. Sensors in gully sites were placed in plunge pools to keep them wet at all times, usually about 15 to 45 cm above the bed. Current probes were mounted about 1 m above the bed on separate stakes located downstream of the plunge pool within a reasonably symmetrical gully cross section. Ultrasonic sensors were mounted on an arm attached to a metal stake located about 10 m from the platform. Each was aimed downward towards the mudflat surface, upon which a plate was pinned to provide a stable, reflective surface.

Instrumentation, including the ISCO sampler, was located on a floating platform either on the mudflat next to gully sites or within the ponds (Fig. 19). Each platform was constructed of a 4-ft (1.2-m) square plywood deck mounted on a 2- × 8-in. (about 5- × 20 -cm) wood frame. Large metal eyehooks were screwed into the frame on each corner. Five-foot (1.5-m) sections of 0.75-in. (2-cm) -diameter steel pipe were mounted vertically in 20-gal. (75.7-L) cans filled with concrete, and the eyehooks mounted on the platform's wood frame lowered over them. Foam filling the inner space of the deck framework provided flotation so that the platform could move vertically up and down the steel pipes during tidal flood and ebb, keeping the datalogger and related devices dry during the highest flood levels. Dataloggers were installed in NEMA plastic enclosure boxes mounted on 2-in. (about 5-cm) vertical steel pipes. Solar panels of 18-W output were fastened to the pipes above the dataloggers to recharge the 12-V external battery.

WP transport and resuspension

Plankton nets of 3-m length with an opening of 1 m and a mesh size of 80 μm were placed at four gully sites, three of which were previously monitored in 1994 (Fig. 17). The plankton net was tied

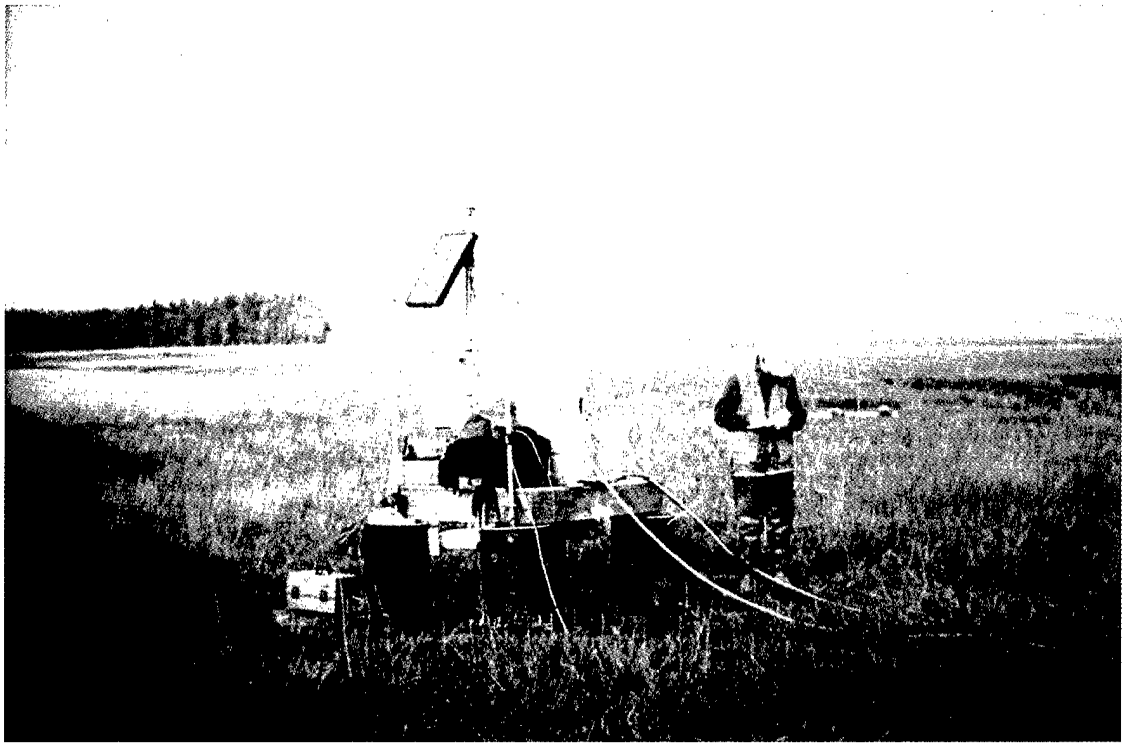

a. Platform and instrumentation at Bread Truck Gully.

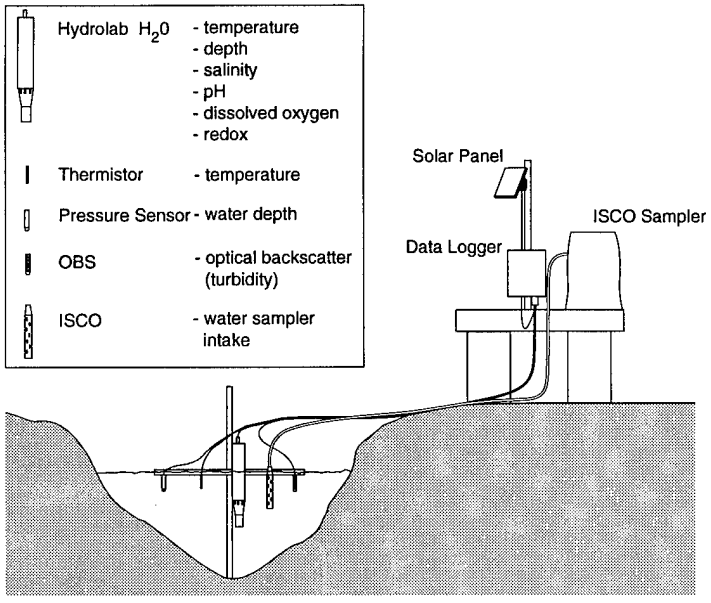

b. Schematic showing layout of intrumentation in water and collection devices on a floatation platform.

Figure 19. Hydrostation layout at a gully location.

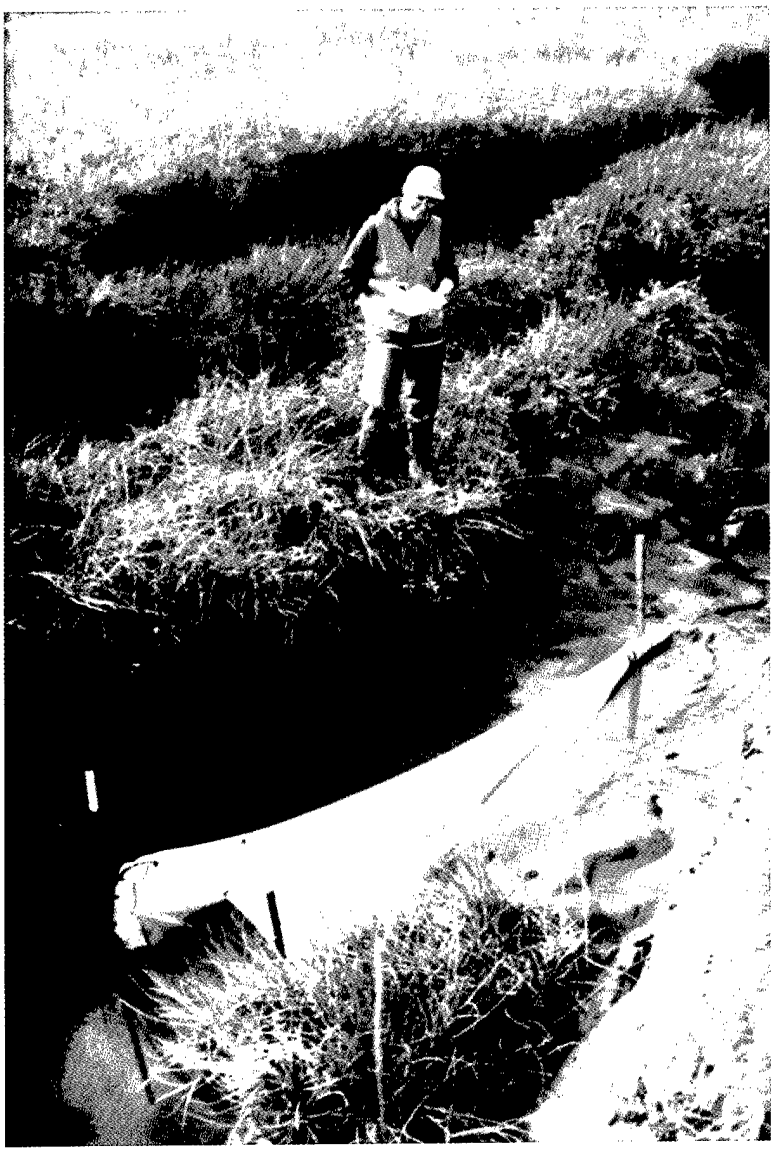

Figure 20. Plankton net used for collecting WP in water transport.

to stakes driven into the gully bottom and extended down-channel in the direction of ebb (Fig. 20). A cup at the apex of the net collected the sediments that were transported into it. Each net was in place during multiple flooding tides each month (Fig. 21). Sediment was collected following each ebb tide during a monitored tidal cycle and analyzed by a commercial laboratory for WP following standard laboratory methods (USEPA 1995).

Sediments collected in sediment traps from transects within C, A, Racine Island, C/D and Lawson's ponds were also analyzed for WP (Fig. 12). These analyses provide data on resuspension of WP by wind, tidal currents and waterfowl activity.

Data acquisition record

Figure 21 summarizes the periods when various types of field data were acquired. The multiple starting dates for acquisition reflect both the implementation of new methods and expansion to additional sites in ERF. Gaps in the records of water quality sensors, other than during the winter, resulted from either instrumentation failure or disruption by natural processes.

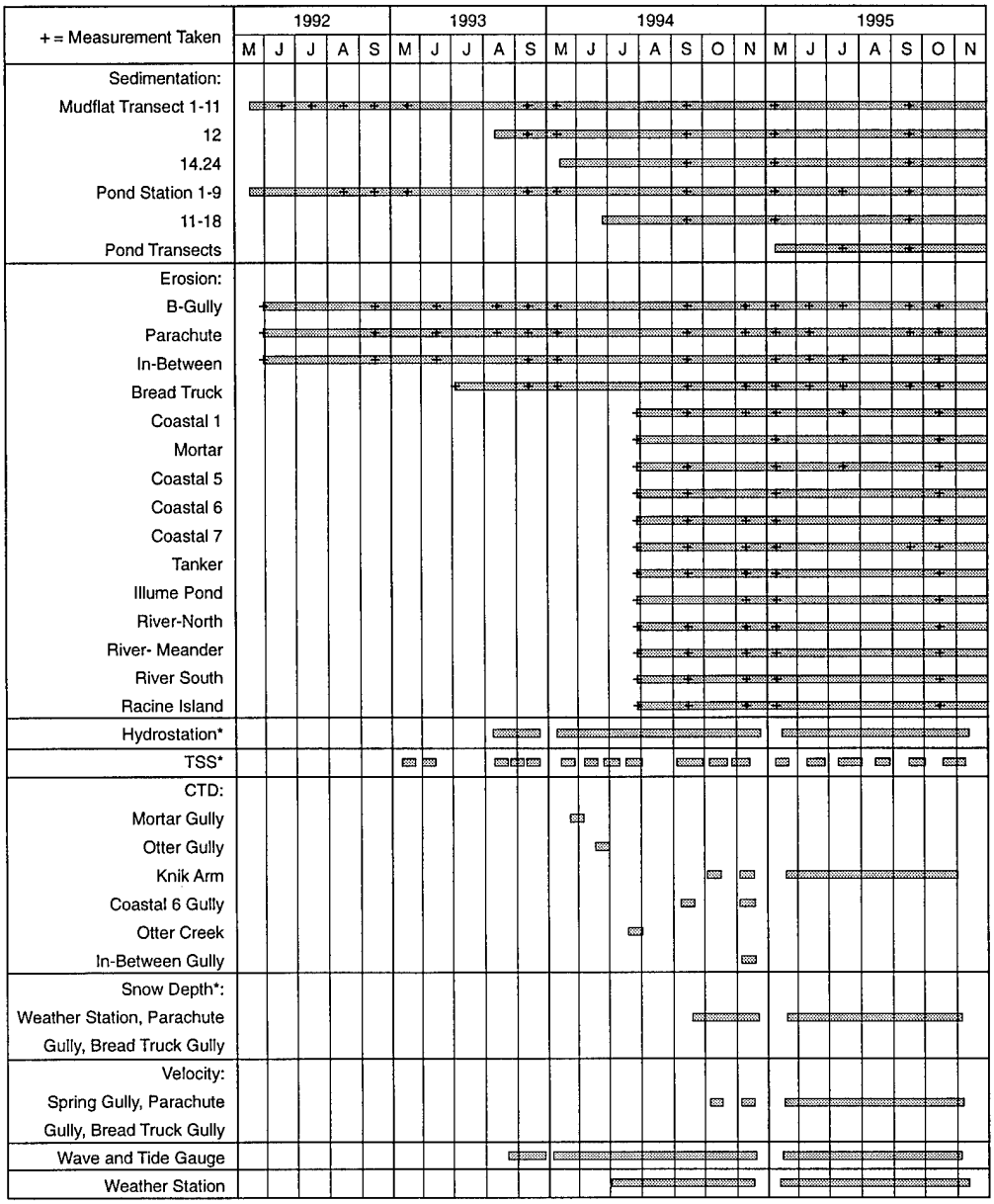

*See Figure 18

a. Continuous data.

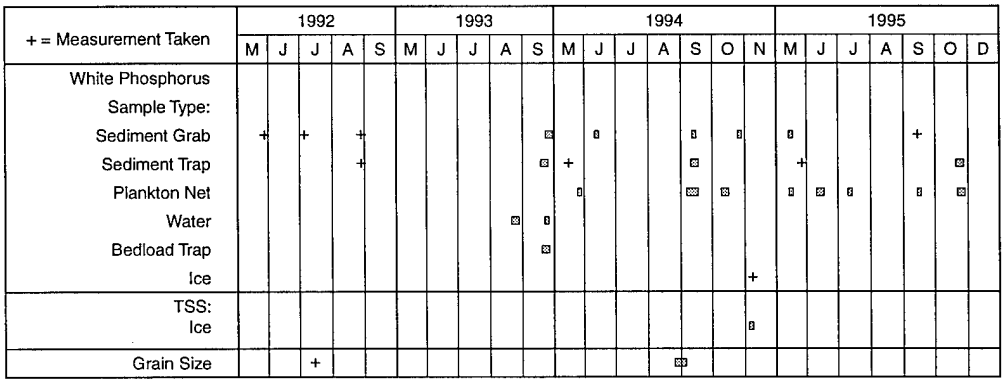

b. Discontinuous data.

Figure 21. Sampling coverages for various types of field data.

INTRINSIC REMEDIATION: POND DRAINAGE BY GULLY EROSION AND EXTENSION

Erosion and the inland extension of tidal gullies are among the most visible mechanisms currently modifying the ERF physical system. This activity is critical because our initial assessments (Lawson et al. 1996) suggested that gully extension could drain contaminated ponds, create drying conditions conducive to in-situ WP degradation (Walsh et al. 1995), and result in a natural attenuation in a relatively short time. The length of time for drainage to occur will be a function of several factors and may vary across the Flats. The 1964 Alaskan Earthquake appears to have had the single greatest effect on ERF, compared to all other external and internal factors. It significantly altered the hydrological system, which in turn has initiated major changes in drainage, gully erosion and extension, and pond and mudflat sedimentation.

External forcing

The effects of major tectonic events in the greater Anchorage area are reasonably well known and best documented following the 1964 earthquake (Hansen 1965, Plafker et al. 1971). Stratigraphic analyses of coastal marshes indicate that large earthquakes ($>M_w = 9.0$) have a recurrence interval of 600–800 years (Combellick 1993, 1994), while magnitude 8.0 or greater earthquakes are more frequent (230–460 years; Nishenko and Jacob 1990). Tectonic disturbance associated with such events causes co-seismic subsidence or uplift (depending on site position relative to local displacement), which is followed by a post-seismic recovery in the opposite direction (e.g., Savage and Plafker 1991). These crustal movements cause adjustments in surficial processes, which are manifested at ERF by the interactions of the internal factors listed in Table 1.

Leveling data collected over the decade following the earthquake of 1964 show that Anchorage subsided 60–70 cm during it (Brown et al. 1977). Brown et al. (1977) estimated that there had been about 20 cm of post-seismic recovery by 1975, although this is not apparent in the tide gauge records (Savage and Plafker 1991). Cohen et al. (1995) and Cohen (1996) suggest that uplift in the first decade following the earthquake was rapid and has subsequently decreased; Savage and Plafker (1991) estimate the current uplift rate to be around 1.0 ±2.2 mm/yr. Considerable research is still required to resolve the absolute magnitude and nature of the tectonic response to the 1964 earthquake.

The complex way in which the physical system of ERF responded to this disturbance is difficult to reconstruct. In a previous report, we speculated that the recent erosion and stepped profile in the gully gradients reflected a dynamic equilibrium related to changes in base level vs. mean sea level (Lawson et al. 1996). However, it is questionable as to whether or not the physical system would respond in such a dynamic manner to a 0.6- to 0.7-m change in base level given the macrotidal range of 9–11 m for Knik Arm. We now feel that erosion and sedimentation rates are a response to increased tidal flooding, coupled to sedimentary subsidence. Both the increase in frequency of flooding and larger volumes of water inundating the Flats are important factors that would increase the amount of sediment entering ponds while also increasing the volume and intensity of drainage during ebb.

Gully erosion and discharge

The volume of water that flows through each gully is controlled by the height and duration of tidal flooding, as supplemented by river discharge and the additive effects of wind, ice and other factors. The range and magnitude of ebb velocity is critical to determining both the flux of sediment and water into and out of the ponds and mudflats, and the ability of those currents to scour and resuspend pond, mudflat and gully sediments.

The velocity of tidal flood and ebb currents at Mortar, Bread Truck, B, Parachute and In-Between gullies ranges between 0.75 and 2.07 m/s (Table 7). The peak velocity at each site changes with the height of flooding (Fig. 22), the lower peak and range in velocities occurring during the lower elevation flooding tides. Flow velocities are greatest at B-Gully, with moderate values recorded at Bread Truck, In-Between, Mortar and Parachute gullies.

Peak ebb velocity is greater than peak flood velocity (Table 7, Fig. 22). This asymmetry in flow velocities, and therefore discharge, determines when erosion and sediment transport will take place and to what magnitude. During tidal flooding, gully water levels rise passively before spreading out onto the mudflats and suspended sediment loads increase as Knik Arm waters flood the gullies, mudflats and ponds. In contrast, higher velocities during ebb dictate an increase in turbu-

Table 7. Summary of gully velocity and discharge data.

Gully	Tide stage	Monthly range in average velocity (cm/s)	Peak velocity (cm/s)	Average TSS (mg/L)	Peak TSS (mg/L)	Monthly range in average water discharge (m^3/s)	Monthly range in average sediment discharge (kg/s)
B	Flood	8.50–15.83	42.39	280–780	2251	0.50–0.94	0.14–0.53
	Ebb	9.04–75.41	207.5			0.54–4.47	0.20–1.81
Parachute	Flood	7.63–26.67	66.96	422–972	2518	0.96–3.36	0.30–1.99
	Ebb	4.56–52.47	96.02			0.57–6.60	0.18–2.79
In-Between	Flood	2.23–15.45	75.16	292–999	2787	0.16–1.11	0.08–1.04
	Ebb	3.46–25.07	97.29			0.25–1.81	0.12–1.62
Bread Truck*	Flood	22.6–29.9	71.1	170–1186	2152	1.24–1.64	0.23–1.95
	Ebb	74.0–81.0	146			4.07–4.46	1.95–3.60
Mortar	Flood	2.75–3.26	15.34	251–856	1973	0.12–0.15	0.03–0.12
	Ebb	7.75–9.93	31.62			0.35–0.45	0.08–0.30

*Based on 1994 measurements.

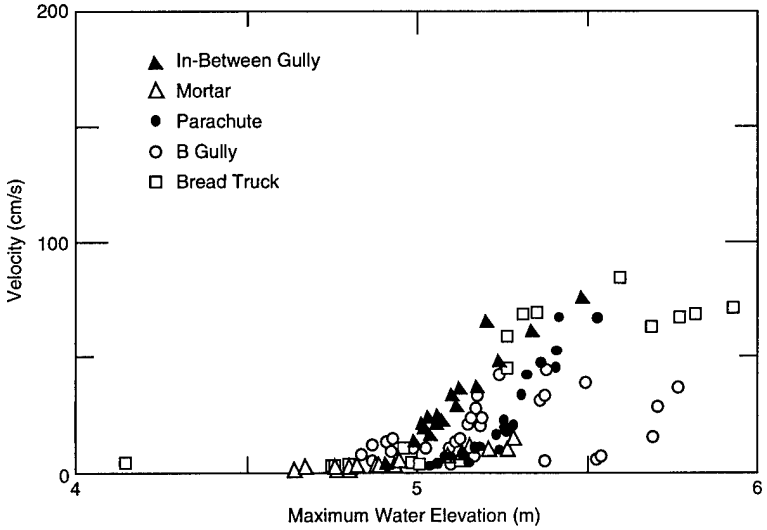

a. Flood currents

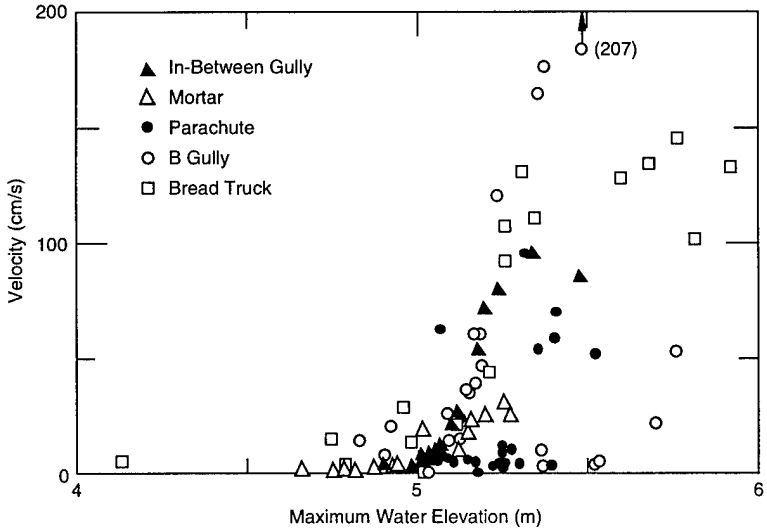

b. Ebb currents

Figure 22. Relationship between peak velocity and maximum water elevation at selected sites.

Table 8. Summary of scarp recession (m).

a. Seasonal.

Site	Summer 92		Winter 92–93		Summer 93		Winter 93–94		Summer 94		Winter 94–95		Summer 95		1992–1995	
	H	*L*	*H*	*L*	*H*	*L*	*H*	*L*	*H*	*L*	*H*	*L*	*H*	*L*	*H*	*L*
B	—	0.1–0.3	—	0.2–0.3	—	0.3–0.8	—	0.1–0.6	—	0.1–1.1	—	0.1–0.8	—	0.2–0.8	—	1.0–5.3
Parachute	0.3–3.2	0.2–0.5	0.5–1.3	0.6–0.7	0.1–3.3	<0.1–0.2	0.6–2.7	0.6–0.7	1.7–2.0	0.7–1.2	0.3–1.7	0.1–2.3	0.1–3.4	0.3–0.6	1.1–12.1	1.3–1.8*
In-Between	<0.1–1.0	<0.1–0.5	<0.1–0.8†	<0.1	<0.1–0.8	0.8	0.1–0.3	<0.1	0.1–0.6	~0.8	<0.1–0.2	<0.1–0.5	<0.1–1.2	<0.1	0.2–2.8	0.2–1.2
Tanker									<0.1	0.1–0.8	<0.1	<0.1–0.3	<0.1–0.5	<0.1–0.5	<0.1–0.5	0.3–0.9
Bread Truck							0.3–5.0	0.1–0.3	0.1–>1.1	0.1–2.2	1.0–11.7	0.1–0.3	0.3–20.0	0.1–2.0	2.0–33.3	0.6–3.0
Coastal 5									0.3–1.5	<0.1–0.6	0.4–6.4	0.6–1.0	0.3–16.9	0.5–0.7	0.6–25.9	1.0–1.7
Mortar											0.3–1.7	0.5–1.1	0.3–1.3	<0.1–1.2	~1.1–1.6	0.5–2.2
Coastal 6									~0.9	1.0–1.8	~0.3	0.3–0.4	0.7–1.2	0.9–1.1	~1.9	1.1–2.7
Coastal 1									1.5–1.7	<0.1–0.3	0.5–0.8	<0.1–0.7	1.1–1.4	<0.1–0.3	0.8–3.1	<0.1–0.7
Coastal 7									1.0–1.2	0.3–1.0	0.4–0.9	~0.6	0.2–0.8	~0.5	1.3–2.4	0.9–1.1
River-North									—	~3.2	—	3.6–4.6	—	1.1–2.5	—	3.3–7.4

H = Headward; L = Lateral.

* Maximum total erosion measured from scarp outline of May 1992; local lateral erosion was greater where associated with lateral expansion accompanying headward migration of headwall.

† Shallow trough (<0.5 m deep) extended ~ 40 m.

b. Annual.

Site	1992–1993		1993–1994		1994–1995		1992–1995	
	Headward	*Lateral*	*Headward*	*Lateral*	*Headward*	*Lateral*	*Headward*	*Lateral*
B	—	0.1–1.5	—	0.1–1.1	—	0.2–0.8	—	1.0–5.3
Parachute	0.8–4.5	0.3–0.7	0.4–2.8	0.6–1.0	0.3–2.0	0.6–3.2	1.1–12.1	1.3–1.8*
In-Between	<0.1–1.1	<0.1–0.5	0.1–0.8	0.1–1.1	<0.1–1.3	~0.1	0.2–2.8	0.2–1.2
Tanker					<0.1–0.5	0.3–0.7	<0.1–0.5	0.3–0.9
Bread Truck			0.3–5.0	0.2–2.2	0.8–31.7	0.3–1.3	2.0–33.3	0.6–3.0
Coastal 5					0.4–7.6	0.9–1.0	0.6–25.9	1.0–1.7
Mortar					1.1–1.6	0.5–2.2	~1.1–1.6	0.5–2.2
Coastal 6					0.6–1.0	1.0–1.8	~1.9	1.1–2.7
Coastal 1					0.8–2.0	<0.1–0.7	0.8–3.1	<0.1–0.7
Coastal 7					0.8–2.0	~1.0	1.3–2.4	0.9–1.1
River-North						1.1–7.4	—	3.3–7.4

* Maximum total erosion measured from scarp outline of May 1992; local lateral erosion was greater where associated with lateral expansion accompanying headward migration of headwall.

lence and the potential for transporting greater amounts of sediment. Perhaps more importantly, additional energy is released from the stored potential energy of the elevated flood waters, causing scour and sediment entrainment. Thus, tidal discharge during ebb is more erosive than during flood.

Discharge (Q) was estimated for each monitored gully using the peak and mean velocities by

$$Q = VA$$

where V is velocity and A is the cross-sectional area.

Average discharge values calculated for each gully ranged from 0.12 to 3.36 m^3/s during flood and 0.25 to 6.60 m^3/s in ebb (Table 7). Peak ebb discharge at each site ranged from 1.16 to 12.30 m^3/s. Peak and average TSS concentrations collected over the same time intervals provide rough estimates of flood and ebb sediment fluxes through gullies (Table 7).

These data indicate ebb sediment flux is greater than the flood sediment flux, with average sediment flux ranging from 0.03 to 1.99 kg/s during flood and 0.08 to 2.79 kg/s during ebb (Table 7). This difference in flux reflects the ebb and flood asymmetry. The significance of the data in terms of sediment transfer is not as clear. These data suggest that, over time, there should be a net transfer of sediment into Knik Arm. However, they do not account for sediment flux via flood waters that overflow the Eagle River and gully banks and levees and, therefore, may be misleading.

Gully erosion and scarp recession rates

Gully erosion and recession were monitored to assess current rates of extension into ponds and the potential for pond drainage and in-situ WP degradation. These short-term rates were compared with long-term trends analyzed on aerial photographs of selected gullies. These historical rates also define variations in gully extension across ERF and are an independent check on field measurements.

Modern rates

The amount of recession of scarp crests is highly variable within a particular gully, as well as among all gully sites (Table 8). Maximum recession rates ranged from 0.3 to 3.2 m during May–September 1992, 0.1 to 1.3 m during September 1992 to June 1993, and 0.1 to 3.3 m during June–September 1993. During the winter of 1993, erosion rates ranged from 0.1 to 5.0 m, 0.1 to 2.0 m in the summer of 1994, 0.1 to 11.7 m during the winter of 1994, and 0.1 to 20.0 m during the summer of 1995. Net headward recession ranged from 0.1 m to about 33 m between 1992 and 1995, with a maximum of 33 m occurring since the spring of 1994 at Bread Truck Gully (Fig. 23a). At each site, however, some parts of the scarp crests did not retreat at all.

Extension of the hub to scarp distance was measured where tension cracks developed at an

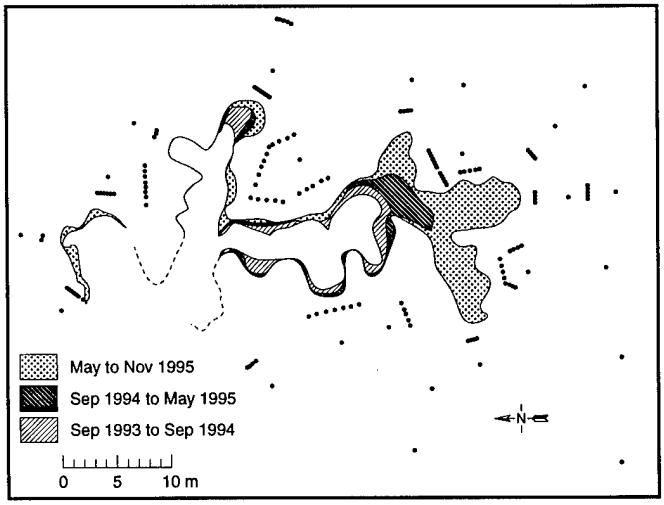

a. Bread Truck Gully.

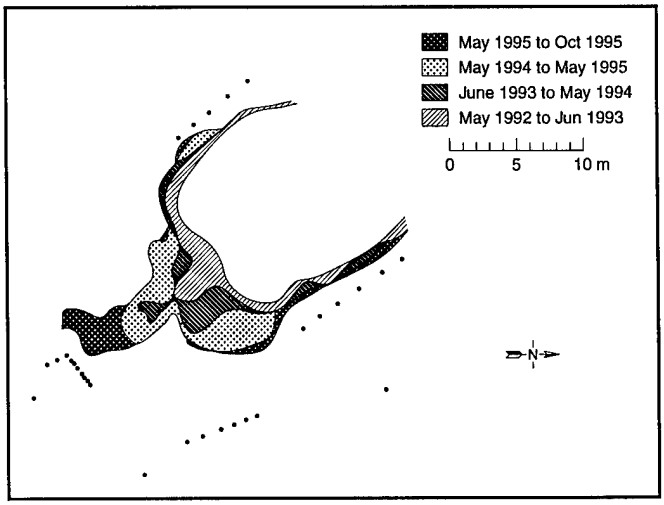

b. Parachute Gully.

Figure 23. Summary of gully scarp recession.

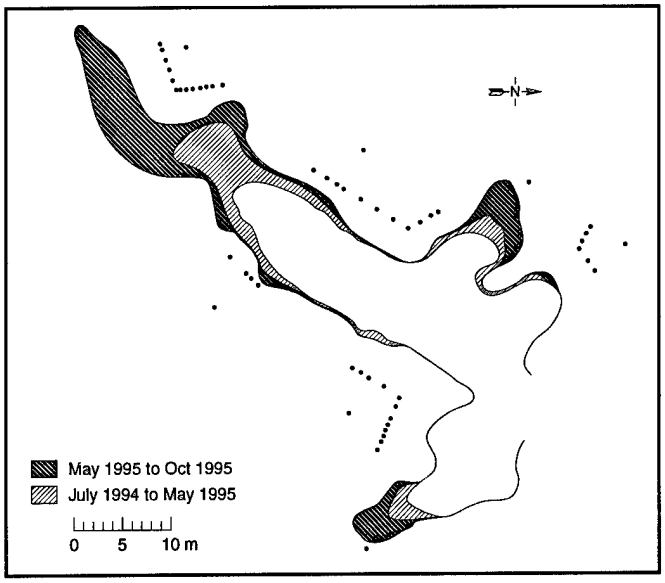

c. Coastal 5 Gully.

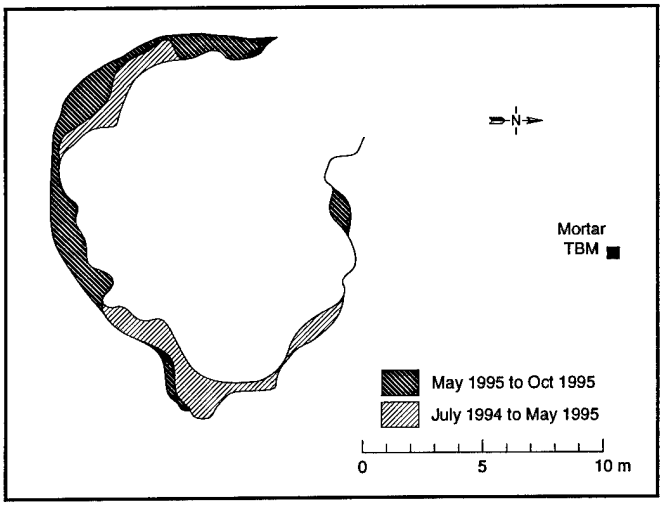

d. Mortar Gully.

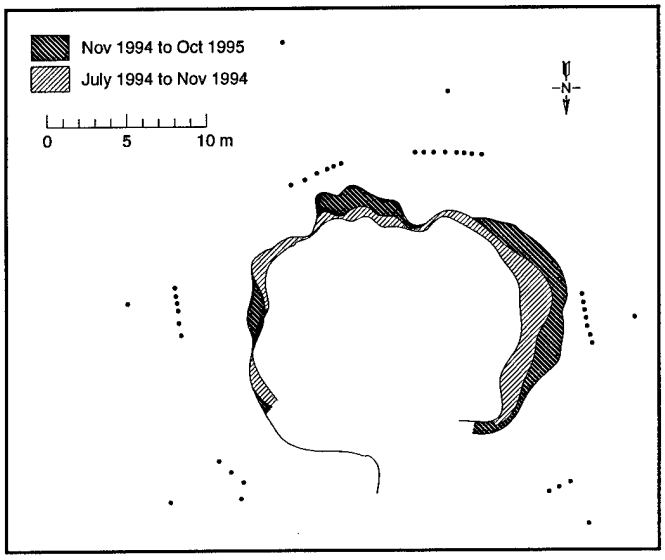

e. Coastal 6 Gully.

Figure 23 (cont'd). Summary of gully scarp recession.

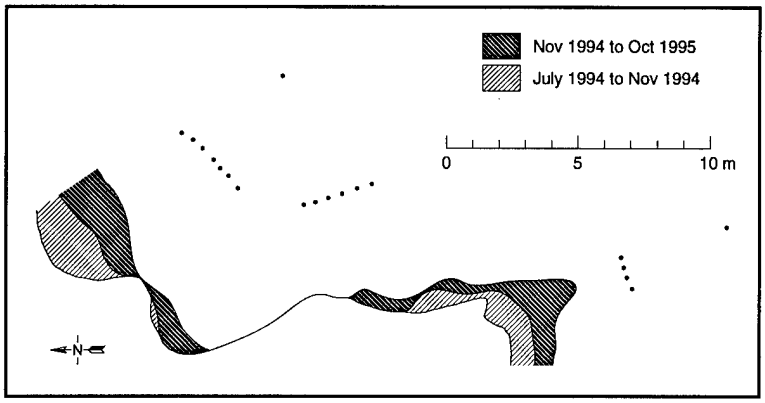

f. Coastal 1 Gully

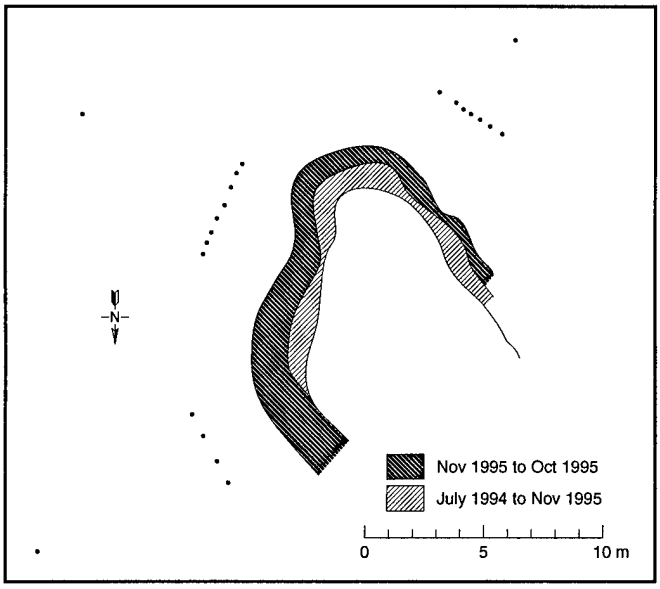

g. Coastal 7 Gully.

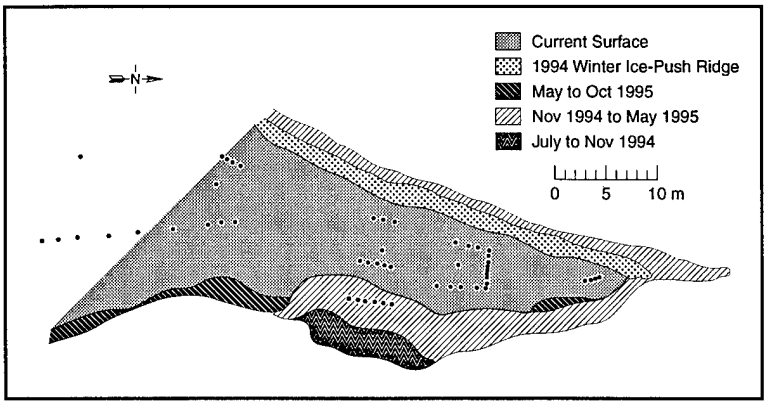

h. River-North site.

Figure 23 (cont'd).

a. North view showing extension crack in foreground.

b. Rotational slump blocks visible to right of scarp.

Figure 24. Measurements of bank erosion along Eagle River at the River-North site.

early stage of collapse (Fig. 24). This extension was particularly evident in May of 1995 following the first tidal flooding cycle (15–17 May 1995) after thawing of the ground began. A shallow snow cover in the winter allowed frost to penetrate deeply. Intermittent flooding and subsequent pond drainage are favorable to ice growth (Fig. 25). The subsequent freezing of interstitial water and growth of needle ice, as well as ice shove, probably reduced the cohesiveness of the bank sediments and increased their susceptibility to erosion during the May flood and ebb cycles.

The spatial variability in recessional rates is evident in the plots showing the sequential recession of scarp crest location through time (Fig. 23). One of the first gullies monitored at ERF was

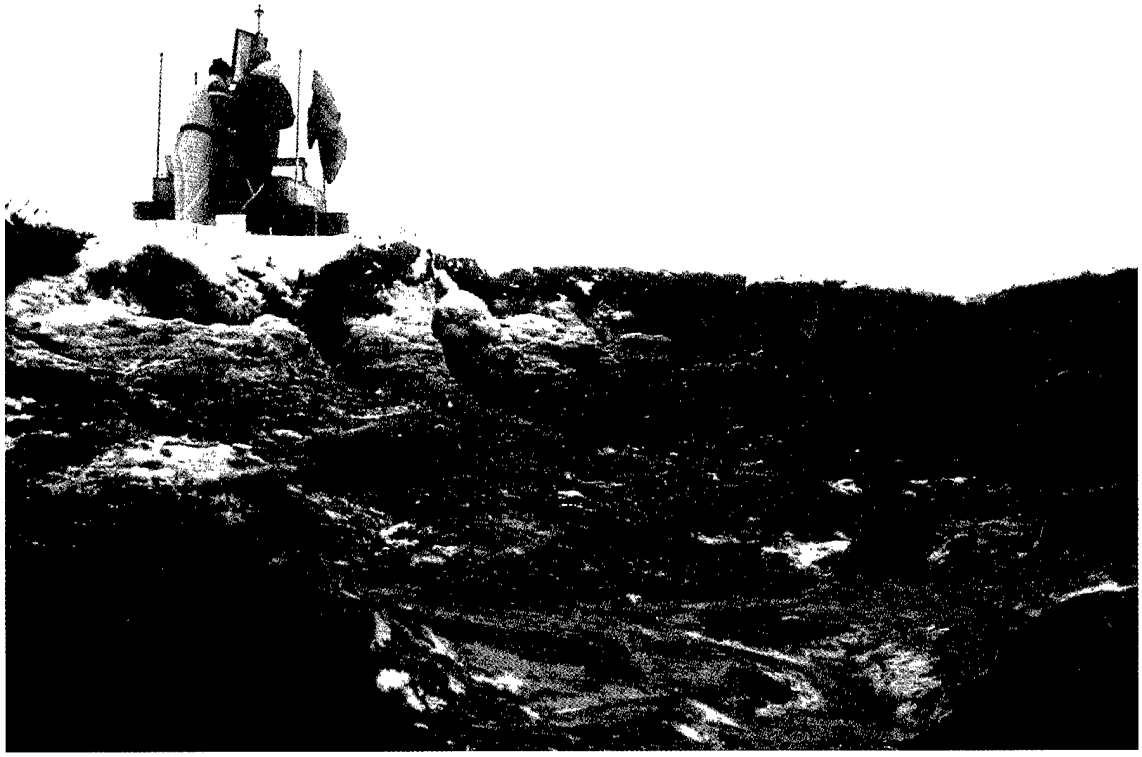

a. Lateral wall view. Ice armor is caused by repeated flooding and subsequent freezing in gully.

b. Headwall view showing ice coating formed by freezeup of waters flowing into gully.

Figure 25. Bank of Bread Truck Gully showing ice growth formation.

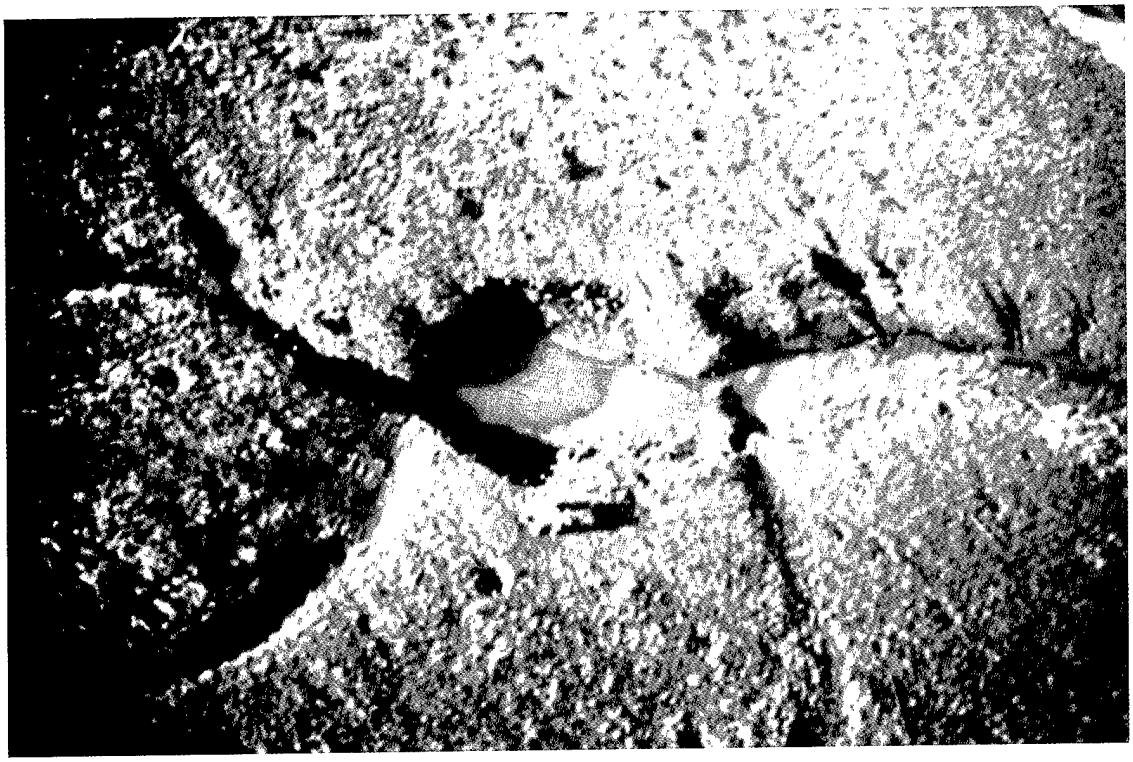

Figure 26. Aerial view of Parachute Gully in October 1995 showing accelerated headward recession that has accompanied capture of flow through craters.

a. Area A.

Figure 27. Aerial view of gullies where recession and ebb flow have been modified by surface craters.

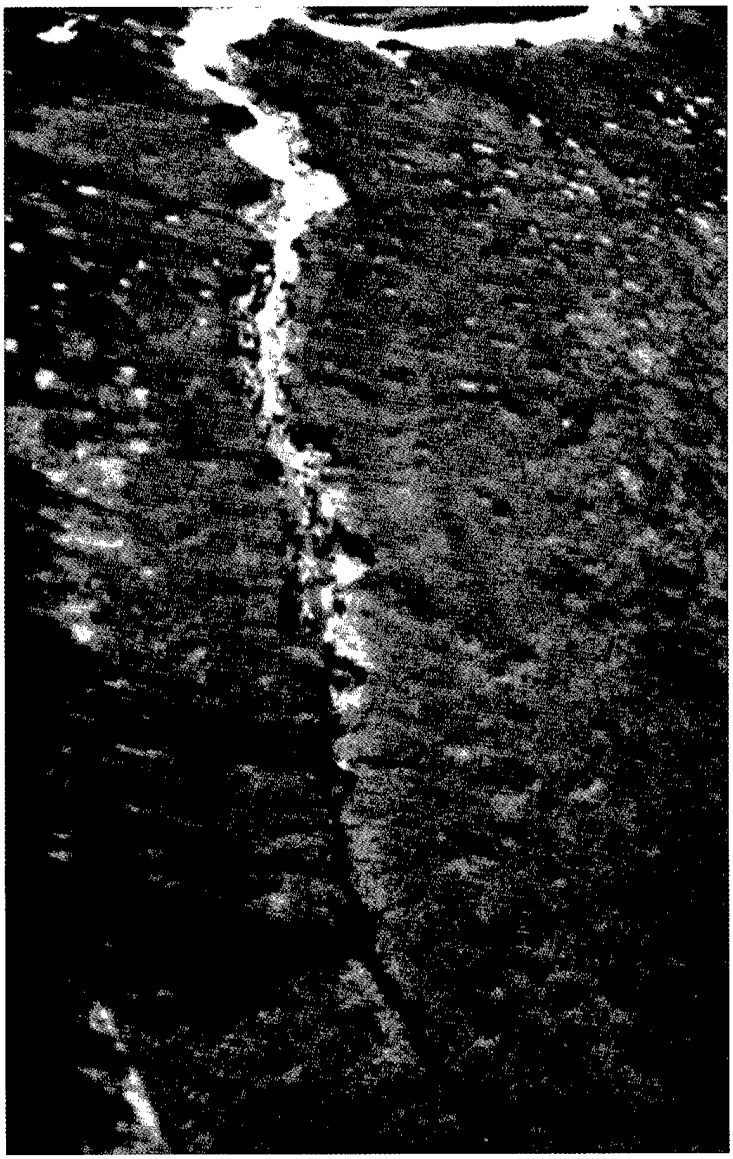

b. B-Gully.

Figure 27 (cont'd).

Parachute Gully on the west side of Area C (Fig. 16). Since monitoring began in 1992, Parachute Gully (Fig. 23b and 26) has undergone up to 12.1 m of headwall recession but only 1.8 m of lateral recession (Table 8). Recession has centered around a drainageway that has become incised and enlarged where multiple craters were once situated. In this situation, the craters became hydraulically connected by localized scour during ebb; the direction of gully extension is dictated by their presence. There was similar enhanced erosion along drainageways in Area A (Fig. 27a) and B-Gully (Fig. 27b).

Bread Truck and Coastal 5 gullies bracket the mouth of the Eagle River and are the sites with the maximum rates of headward recession (Fig. 16, 23a and c). Bread Truck Gully (Fig. 28 and 23a) was first monitored in 1993 when headward recession ranged from 0.3 to 5.0 m and lateral recession was on the order of 0.2 to 2.2 m (Table 8a). In 1995, headward recession accelerated to 11.7 m during the May 1995 flooding tide (representing the winter 94–95 erosion column of Table 8a) and an additional 20 m during the 1995 summer season. These rates do not appear to be exceptional or unique; Coastal 5 Gully receded by 17 m during the summer of 1995 and a total of about 26 m since the hub and line stakes were established in July of 1994.

Recession at the B-gully site, monitored since 1992, is the result of lateral erosion. The monitored section lies along the margin of a peninsula

Figure 28. Aerial view of Bread Truck Gully in October 1995.

between two tributaries to the main gully, about 75 m downchannel of the gully headwall. Gully erosion is characterized by the formation of cuspate embayments that have gradually enlarged since 1992, with a maximum of 5.3 m change (Table 8, Fig. 29). This site is significant because we have repeatedly detected WP in transport within ebb waters (Lawson et al. 1995), as well as in fauna sampled within the gully (Bouwkamp 1995). The source of this WP is unknown at this time; however, it is likely to have either eroded out of the gully headwall or been flushed from C-Pond.

Data (Tables 8) indicate that, in general, lateral recession is lower (often by an order of magnitude) than headward recession. The exceptions are Mortar and Coastal 6 gullies, where wide plunge pools below their respective headwalls are expanding laterally through bank collapse and rotational slumping (Fig. 23d and 30).

Figure 23h shows one section of the monitoring network at the River-North site, where slope processes are consuming mudflat sediments and introducing material directly into the Eagle River (Fig. 24). Rapid lateral erosion on the order of 3.2 m was recorded at this site between July and November of 1994, and there was up to 7.4 m of recession by late October 1995. Erosion occurs along large rotational slumps that fail because of river undercutting and removal of sediment supporting the toe of the slope (Fig. 24b). Prior to failure, large extension cracks develop parallel to the scarp, gradually leading to catastrophic failure (Fig. 24a). The location of the crack becomes the new scarp of the riverbank.

Recession rates are variable because the erosional processes are rapid, short-duration events (Table 2). Recession appears to be caused mostly by currents scouring the lower, unvegetated portion of the gully walls during ebb tide when water velocities are highest. Because the uppermost 20–30 cm of material is consolidated and root-bound (Fig. 30), this soil and root mat are undermined and only fail after an erosional niche of approximately 0.5 m or deeper is cut below it. In the gullies themselves, current scour during ebb tide removes material from the toe of the slope, thereby removing the base of the slope and causing slumping and sediment flow (Fig. 31).

Eroded sediments form deposits in the gullies that are eventually transported into the Eagle River. Along steep scarps, blocks of consolidated, root-bound sediments fall and roll into the gully bottoms and remain intact until currents eventually break them apart. The lateral walls of gullies, which tend to develop low-angle slopes as headwalls recede inland, fail mainly by rotational slump flow, or by creeping slowly as a mudflow into the gully channel. On gentler slopes, blocks of root-bound material remain intact as they are trans-

Figure 29. Eastward view of eroding cuspate embayments at B-Gully.

Figure 30. Thick laminated peat layer at Coastal 6 forms the threshold to channel downcutting and headward recession.

ported downslope by slow-moving mudflows that are active in the latter stages of the ebb cycle.

Historical rates

Historical rates of gully extension by headward erosion have been reconstructed for B, Parachute, In-Between, Mortar, Bread Truck and Coastal 5 gullies (Fig. 32; Table 9). Long-term average recession rates over the past 45 years range from 3.6 m/year at Mortar Gully to 13.7 m/year at the Coastal 5 Gully. Recession ranged from 1.1 to 3.5 m/year between 1950 and 1960 and increased to between 2.1 and 14.7 m/year between 1960 and 1972. Recession continued to increase between 1972 and 1986, when rates ranged from 5.1 to 23.6 m/year. In the decade of 1986 to 1995, recession rates have remained high but have in general slowed slightly, ranging from 3.9 to 21.6 m/year.

The aerial photographic record suggests that there was little physical change before the 1964 earthquake. At four of the six locations studied, recession rates reached their peak between 1972 and 1986. The recent high rate of recession at In-Between Gully reflects a rapid, shallow distributary that advanced into the mudflat by about 40 m during the 1992–93 winter (Lawson et al. 1996), which increases the 9-year average by 4.4 m/year. Therefore, the last decade of recession at In-Between Gully may be best represented by a rate of 2.9 m/year (Table 9). The other gullies that have shown a recent acceleration of recession are those of Bread Truck, which has been the site of considerable monitoring (see below), and Coastal 6. Recession at Bread Truck Gully has been accelerating in an unpredictable manner as the gully headwalls have encroached on Bread Truck Pond and entered into unvegetated mudflats that are intermittently ponded.

Recent vs. long-term rates of recession

The modern rates of net headward and lateral recession measured using the hub and line stake technique are depicted in Figure 33 to show the spatial patterns in gully erosion along a transect from the mouth of the Eagle River inland to the head of the Flats. Nearest the coast, sites Coastal 1 and Coastal 7 have experienced more headward than lateral recession. In the mid-coastal regions, Mortar and Coastal 6 have experienced similar rates of lateral and headward recession, with lateral erosion dominating slightly as these gullies have been widening by bank collapse and slumping. Slightly inland from the mouth of the river, Bread Truck and Coastal 5 gullies have been experiencing drastic, yet rather

Figure 31. Sediment flow at Bread Truck Gully. Saturated sediment fails when erosion during ebb tide removes material from the slope toe.

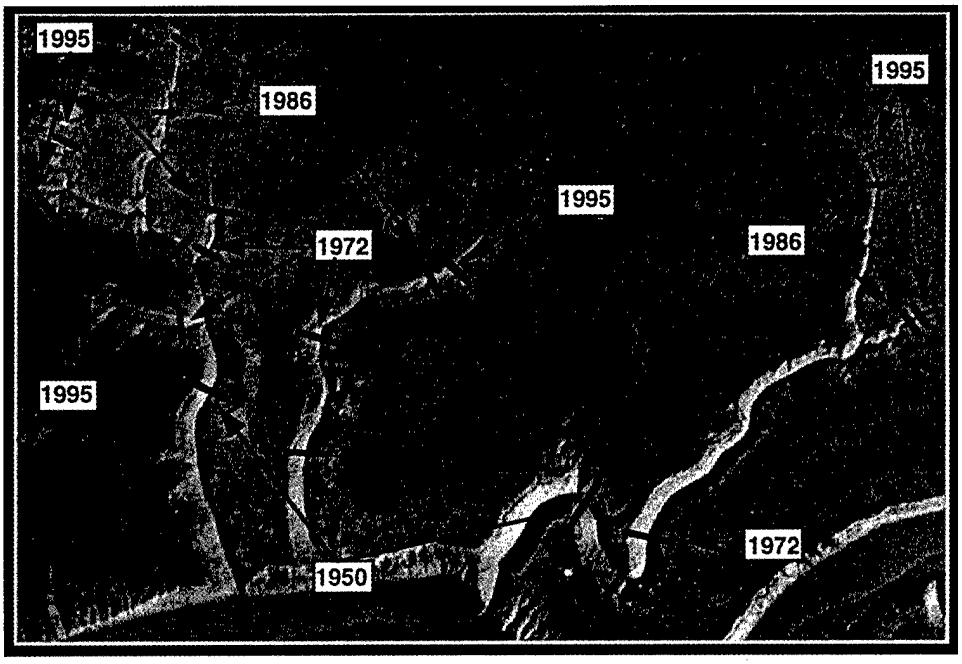

a. B-, Parachute and In-Between gullies.

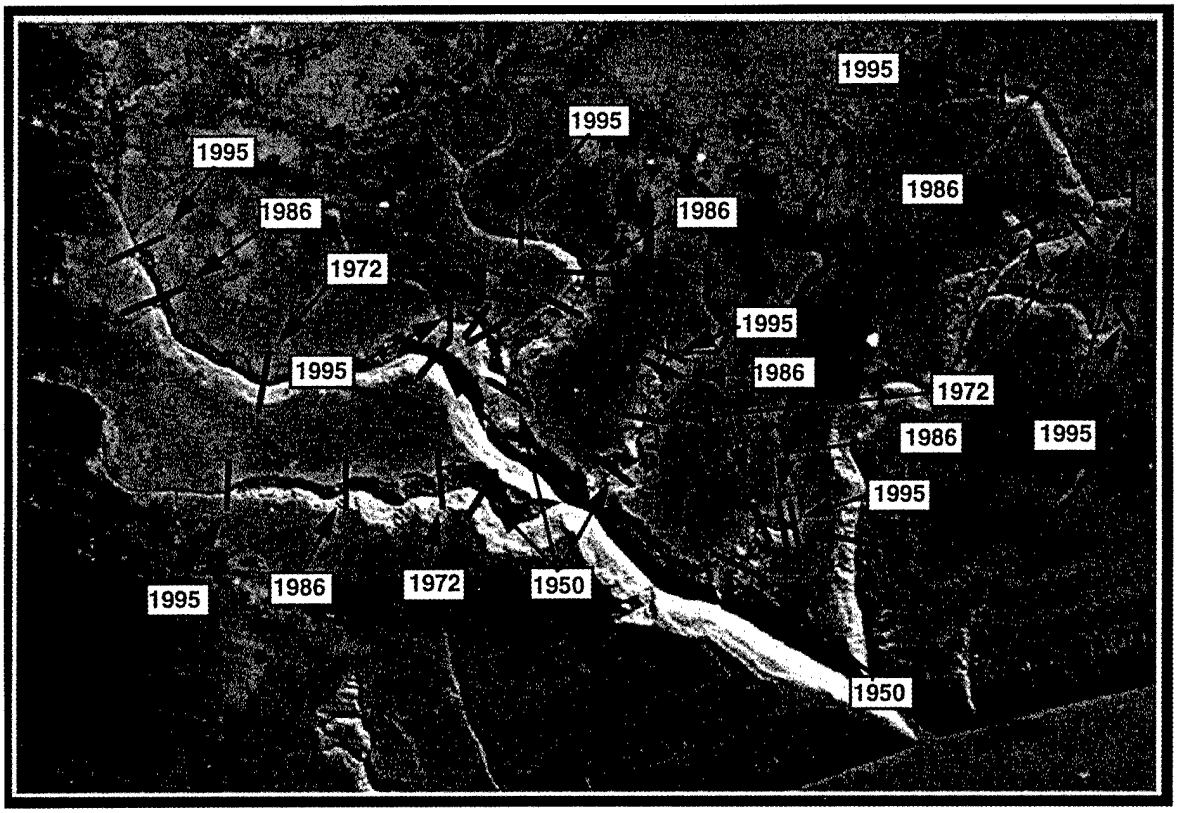

b. Mortar Gully.

Figure 32. Historical gully recession (see Table 9 for corresponding recession rates).

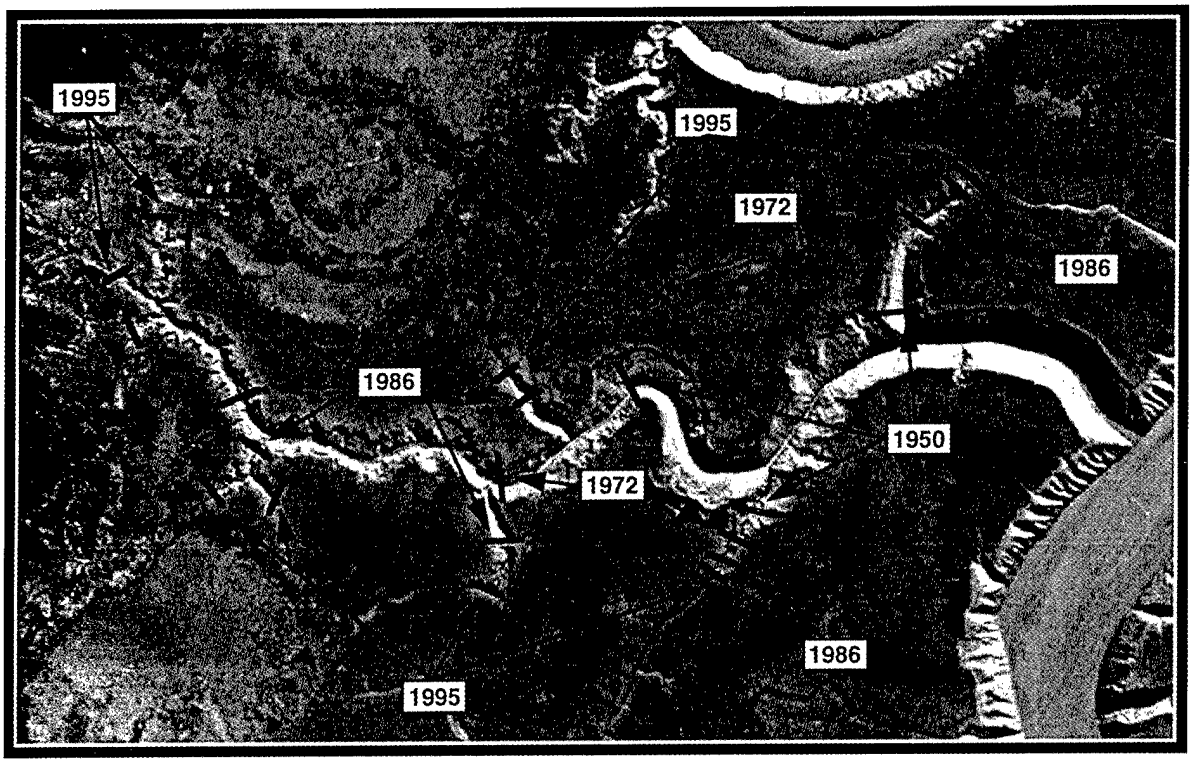

c. Bread Truck Gully.

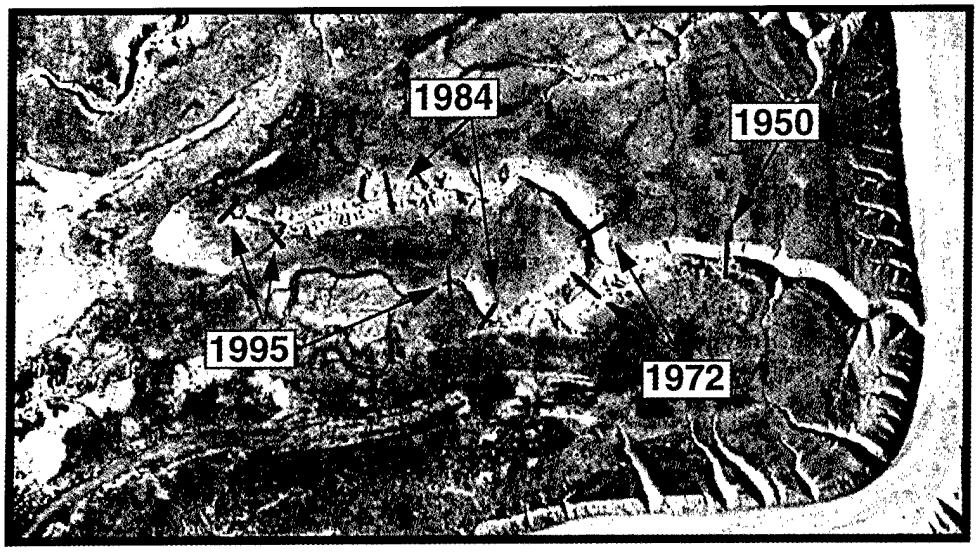

d. Coastal 5 Gully.

Figure 32 (cont'd). Historical gully recession (see Table 9 for corresponding recession rates).

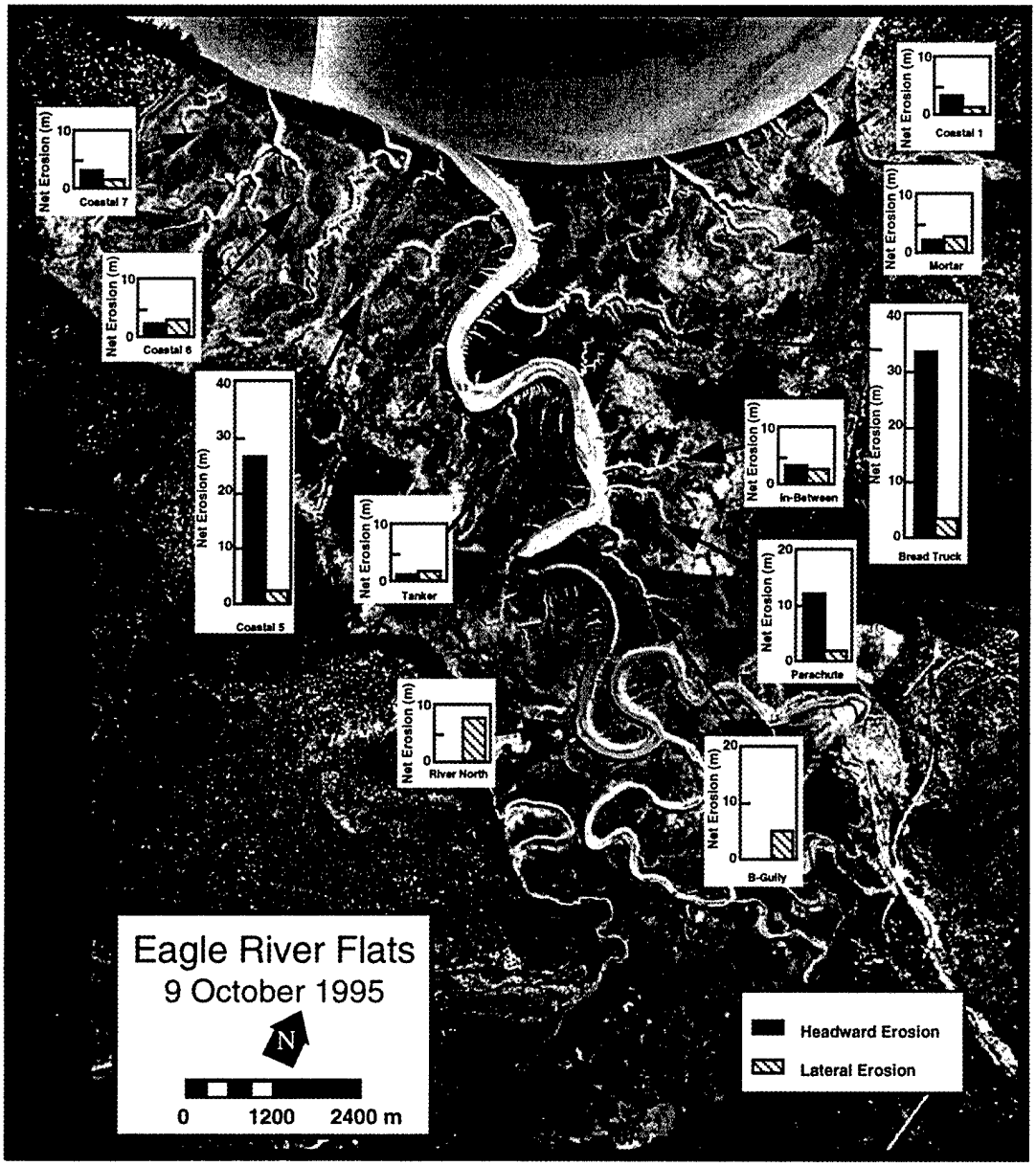

Figure 33. Spatial comparison of headward and lateral recession monitored at selected hub-line stake erosion sites.

symmetrical, retreat patterns governed by rapid headwall recession. Moving further inland, Tanker and In-Between gullies have also experienced unequal headward and lateral erosion and recession. The rates of erosion at sites north of Parachute Gully appear to be mirrored on either side of the Eagle River. The reasons for this symmetry are unknown, but are probably related to the nature of flow patterns during ebb drainage and how effectively water is channeled into incipient feeder channels inland of the gully heads.

Comparison of the recent erosion (Table 8) and historical data (Table 9) shows considerable annual variability over the short term, but over the long term (approximately decades), rates appear relatively consistent. The high rates of headwall recession at Bread Truck (33 m in approximately 2 years) and Coastal 5 (26 m in approximately 1.5 years) are close to the 11-year average rates of 21.6 and 18.4 m/year, respectively, as determined from historical photograph analyses (Fig. 32). Similarly, the headward recession of 12.1 m in 3 years

Table 9. Summary of long-term gully erosion rates at selected sites.

Gully		*Duration (years)*	*Distance (m)*	*Rate (m/yr)*
B	1950–60	10	35.4	3.5
	1960–72	12	70.8	5.9
	1972–86	14	330.4	23.6
	1986–95	9	35.4	3.9
	Total	45	472.0	10.5
Parachute	1950–60	10	11.8	1.2
	1960–72	12	82.6	6.9
	1972–86	14	70.8	5.1
	1986–95	9	35.4	3.9
	Total	45	200.6	4.5
In-Between	1950–60	10	23.6	2.4
	1960–72	12	99.1	8.3
	1972–86	14	94.4	6.7
	1986–95	9	66.1	7.3
	Total	45	283.2	6.3
Mortar	1950–60	10	21.4	2.1
	1960–72	12	25.2	2.1
	1972–86	14	82.0	5.9
	1986–95	9	35.3	3.9
	Total	45	164.0	3.6
Bread Truck	1950–60	10	34.3	3.4
	1960–72	12	34.3	2.9
	1972–86	14	251.5	18.0
	1986–95	9	194.3	21.6
	Total	45	514.4	11.4
Coastal 5	1950–60	10	11.4	1.1
	1960–72	12	175.8	14.7
	1972–84	12	225.1	18.8
	1984–95	11	202.6	18.4
	Total	45	614.9	13.7

at Parachute Gully (Tables 8) is almost identical to the 3.9-m/year average since 1986; the 1.6-m rate observed at Mortar is lower than the 11-year average of 3.9 m/year (Fig. 23d, 32b; Table 8b). Since our hub and line stakes at B-Gully record only lateral erosion, the current rates are not comparable to the 11-year average of 3.9 m/year of headward recession.

Historical analysis of the drainage system

The surface morphology and drainage patterns of ERF have undergone significant change over the last 45 years, with large scale changes particularly evident since the 1964 earthquake. The photographic coverage from 8 August 1950, 27 June 1953 and 30 August 1960 shows an apparently stable environment prior to 1960. The only indicators of on-going change are the incised meanders of the Eagle River where vegetation was absent and some slumping was evident. Small, low-relief channels drained into tidal gullies, which were eroding slowly into the mudflats (Table 9).

During the 1950s and early 1960s, the mudflat areas of Racine Island were largely undissected and had a mostly complete cover of vegetation (interior sedge meadow; Racine and Brouillette 1995a). The C, C/D and D areas were mostly vegetated (halophytic herb meadow; Racine and Brouillette 1995a), except where dissected by narrow, relict drainageways that extended into freshwater marsh (bulrush) in the areas where the C-, Bread Truck and Pond Beyond ponds now occur (Fig. 3, 4 and 5). Open or standing water covered the drainageways that feed Mortar, Bread Truck, Parachute and B gullies in the early 1960s. In Parachute and B gullies, open water covered what now are gullies to within about 100 to 150 m of the Eagle River. At Mortar and Bread Truck, the narrow relict drainageways were arranged in a dendritic pattern penetrating into emergent sedge marsh (Racine and Brouillette 1995a). They formed a tight drainage network along the boundary of what is now Bread Truck Pond and Pond Beyond, and where there is at present standing water. Relict drainageways directed water flow through an abandoned meander present in Bread Truck Pond. Small abandoned pools are also apparent in several of these relict gullies in locations where headwall recession is active

Open water first became evident on photos in 1967 in the areas near Clunie Creek and Clunie Point (Fig. 5). There were also several small bodies of water in the C/D and D areas, where small sedge bogs are now located. The major gullies of Bread Truck and Mortar were also actively eroding into the mudflats by 1967 (Fig. 7, 32b and c; Table 9). By 1974, areas in C-Pond, the channel in Bread Truck Pond, and large relict drainages in Pond Beyond and C/D-Pond had additional open water and, by 1984, ponds had dimensions similar to the present. Pond expansion and gully recession rates (Table 9) appear to have been greatest during the late 1970s and early 1980s at a time when isostatic uplift rates were high (~1.5 cm/year; Brown et al. 1977).

The Eagle River exhibited major changes only where it enters ERF; these changes are probably related to floods of the river, rather than tidal inundation. In 1950, two well-developed channels, which bifurcated about 850 m southeast of the Route Bravo Bridge, entered ERF (Fig. 34a). The northern channel was straight and confined by the uplands, while the south channel appears slightly subordinate in discharge volume and had a meandering pattern. Between 1957 and 1960, the south channel had eroded and captured

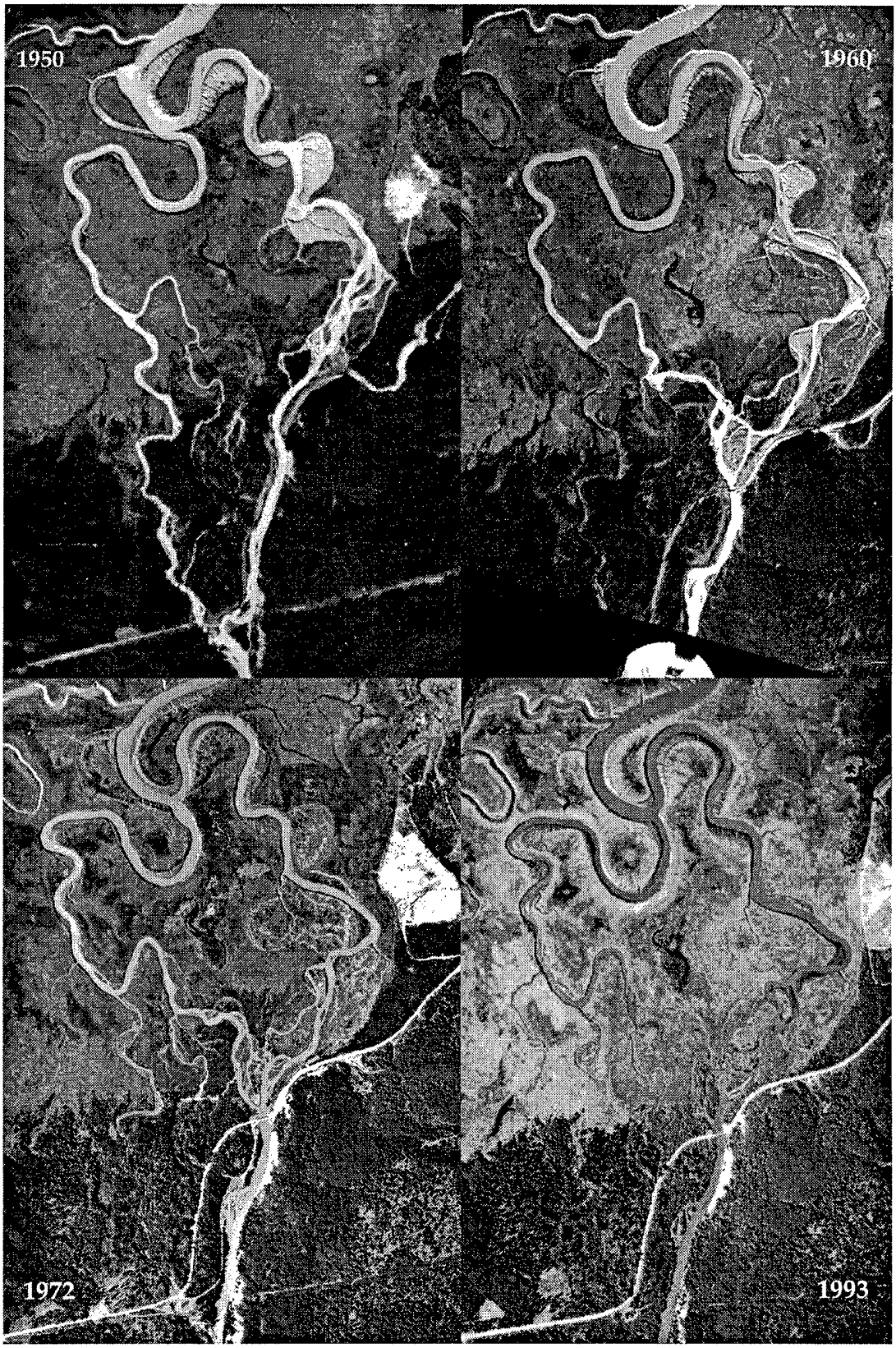

Figure 34. Aerial photographs depicting the morphologic changes in the Eagle River where it enters the ERF.

all of the flow in the Eagle River; the north channel was inundated only during tidal flooding (Fig. 34b). The southern channel remained the principal discharge until sometime between 1967 and 1972, when flow was reestablished in the north channel (Fig. 34d). Multiple channels then remained active throughout the 1980s and 1990's (Fig. 34c); however, in September 1995, flooding of the Eagle River resulted in abandonment of the southern channel as the northern channel was deeply scoured and eroded eastward into the upland bluffs.

Natural attenuation by pond drainage

Given the combined short-term and long-term recessional data, we revise our previous prediction of how long it will take for the ponds to be drained naturally (see Lawson et al. 1996). These refined recessional data (Tables 8 and 9) indicate that Bread Truck pond will start to drain in 2 to 3 years or less. In about 6 to 7 years, In-Between Gully will drain parts of C and Lawson's ponds, and in about 14 to 16 years, Parachute Gully will drain parts of C-Pond (Fig. 35a). Previously, more limited short-term data suggested that that Bread Truck Pond would begin to drain in 35 to 50 years, while the In-Between and Parachute gullies would begin to drain C-Pond in 17 to 20 years and 25 to 30 years respectively (Fig. 35b). The drastic change in our predictions reflects the increase in data obtained on the highly variable short-term rates of erosion, and the longer-term historical rates. The historical data average the variability seen in the short-term observational data and are considered more accurate for predicting future gully behavior.

Gullies are routes for pond outflow and therefore potential pathways for WP transport. As the gullies continue headward erosion into WP-con-

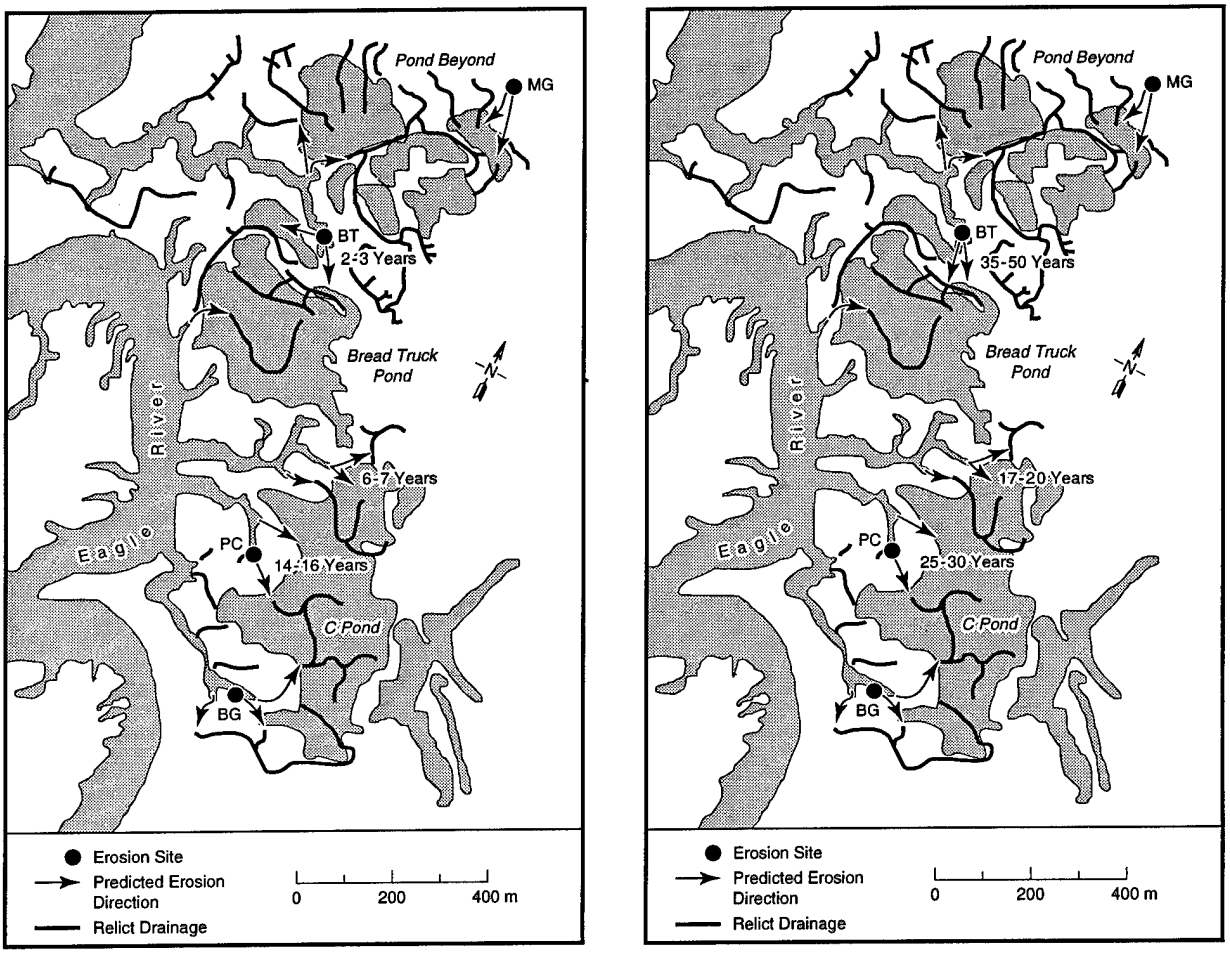

a. 1995. *b. 1994.*

Figure 35. Predictions for pond drainage by selected gullies in Areas C, Bread Truck and C/D.

taminated areas, fresh sediment will be exposed and introduced into them, potentially increasing the amount of WP in ebb discharge. Gully erosion may also threaten the integrity of other remedial methods. For example, capping measures (i.e., geotextiles and AquaBlock) may be undercut and damaged. Similarly, hydrological and physical changes to the ponds and mudflats may result from dredging and cause rapid extension of the gullies into the dredged areas.

SEDIMENTATION AND NATURAL ATTENUATION OF WP BY BURIAL

Suspension settling through flocculation takes place during slack high tide and through the early stages of the ebb cycle. In ponded areas, it also happens between tidal floods when turbulence is low, allowing fine-grained particles to settle out of the water. Therefore, the longer calm conditions can be maintained, the greater is the time over which deposition can occur. The mixing and exchange of tidal flood water with existing pond and marsh water increases the amount of suspended sediment in the ponds and marshes, and provides the primary source for deposition.

Controls on sedimentation rates at any particular location include elevation, vegetation that traps sediment (e.g., Reed 1995), and the frequency, height and duration of inundations by sediment-laden waters (e.g., Vince and Snow 1984; Reed 1989, 1995; Reed and Cahoon 1992; French and Spencer 1993). The distance from the source also plays a role in some areas, as sediment can be deposited or eroded during flood and ebb, altering the amount in suspension. Large amounts of sediment may be deposited locally from ice rafting of materials plucked from other locations within the Flats (Fig. 36).

Tidal inundation

Several factors (see Lawson et al. 1996) influence the timing, magnitude and duration of tidal flooding and runoff, which in turn control sediment influx into ponds. The typical tidal flooding cycle begins with a rise in the water level in the Eagle River and the gullies. This water gradually floods over the banks of the gullies and river,

a. Sediment layer frozen onto an ice block transported during the November 1994 flooding tides.

Figure 36. Ice rafting at ERF.

b. Ice-rafted sediment deposited at the head of Mortar Gully.

Figure 36 (cont'd). Ice rafting at ERF.

displacing the water over a large area, and causing a decrease in the rate of water level rise (Fig. 37). River waters are dammed, causing the river to reverse its direction in the upper Flats (Fig. 38). This damming effect causes the elevation of the river to rise higher than the elevation of water in the gullies and reverses flow direction in the drainage systems. The effect may be accentuated during peak discharge of the river. Water depths measured at the hydrostations and the tide gauge in Knik Arm show that the peak elevation on the Flats exceeded the predicted tidal height for Anchorage by up to 0.7 m throughout the 1995 summer season (Fig. 39). The effect is to increase the volume of water and hence sediment available for sedimentation.

At peak flood or slack high tide, water is ponded upon the Flats. The mixing of flood waters with the existing pond and marsh waters increases the amount of suspended sediment. In those ponds such as Racine Island Pond, which have the highest proportion of fresh river water inundation, suspended sediment concentrations are less than where tidal sources dominate.

Flood waters first begin to drain near the coast at the start of ebb tide, and water levels inland progressively decrease. The duration of outflow during ebb is greater than inflow during flood.

Pond sedimentation results mainly from settling-out of sediment suspended in the water column; sediments are deposited in ponds and mudflats during and immediately following slack high tide (Fig. 37b). Its duration and the height and volume of the flood water therefore determine sedimentation rates.

The length of time available for sedimentation during tidal inundation is directly related to peak elevation and each landform's threshold for flooding. The time between the start of water rise and peak high tide was measured for each gully hydrostation and compared to the peak water elevation at each site. We found a linear relationship between water rise time and peak elevation (Fig. 40). Average elevations for tidal flooding across the Flats were estimated from surveyed transects (Fig. 9). These data indicate that most drainageways feeding ponds begin to flood at a tidal height of about 4.6 m above sea level, mud-

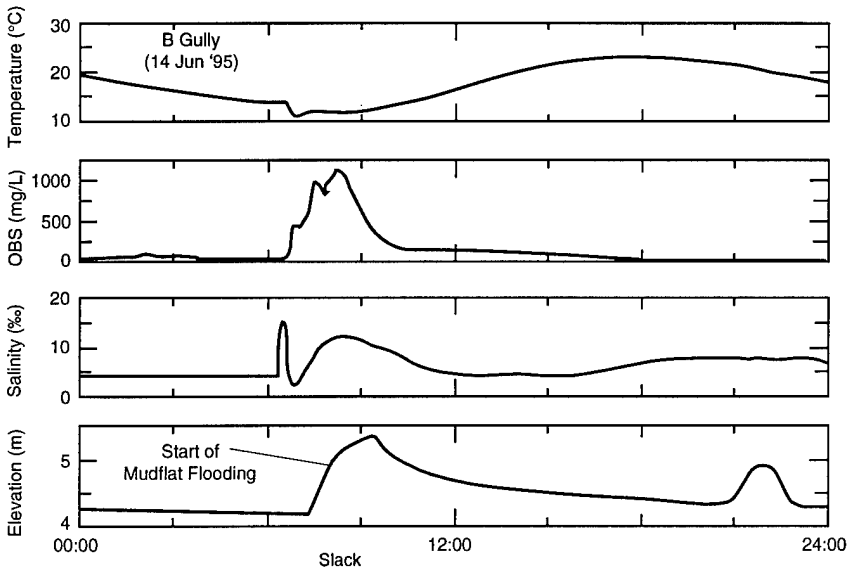

a. B-Gully on 14 June 1995.

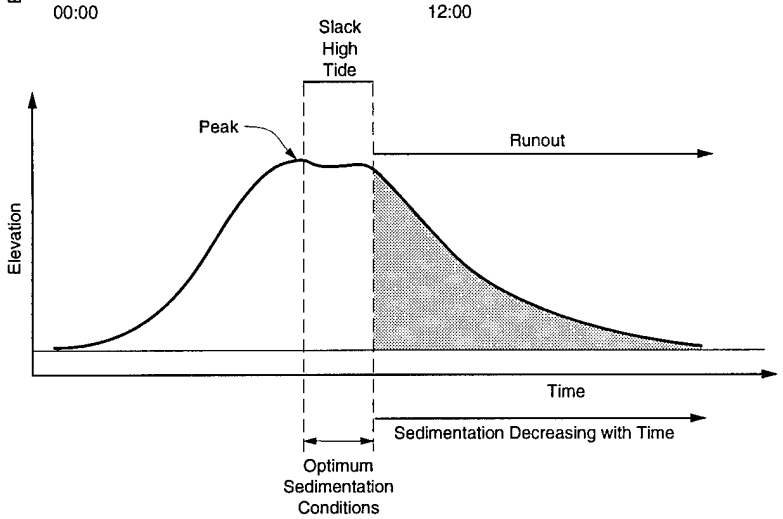

b. Schematic showing a typical tidal cycle and period of sedimentation during the ebb tide event.

Figure 37. Example of a flooding tide cycle. Note that rate of tidal rise decreases following bankfull stage when water begins to flood adjacent mudflats.

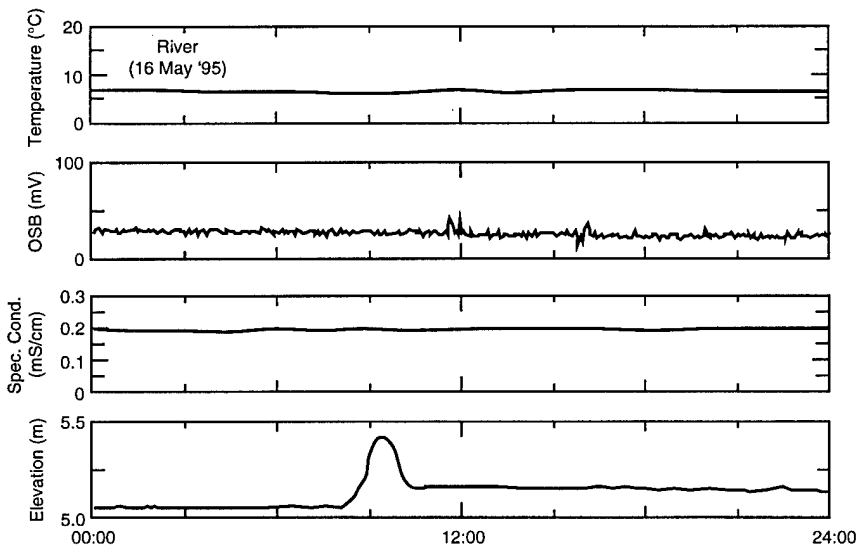

Figure 38. Water quality data from the Eagle River site showing the effect of water damming caused by a flooding tide.

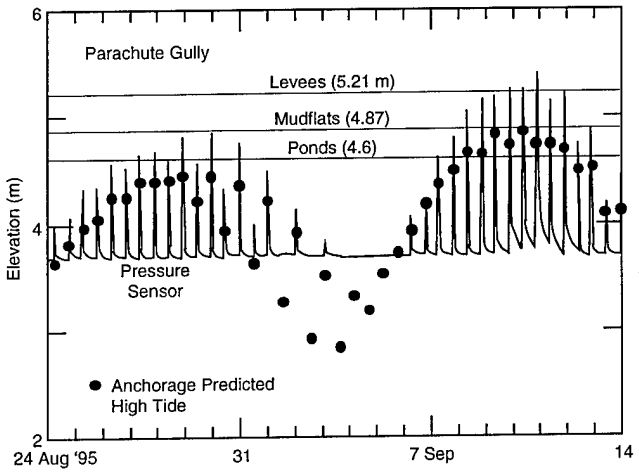

Figure 39. Water elevation record showing elevations required to flood selected landforms and tidal amplification at Parachute Gully above predicted high tide at Anchorage.

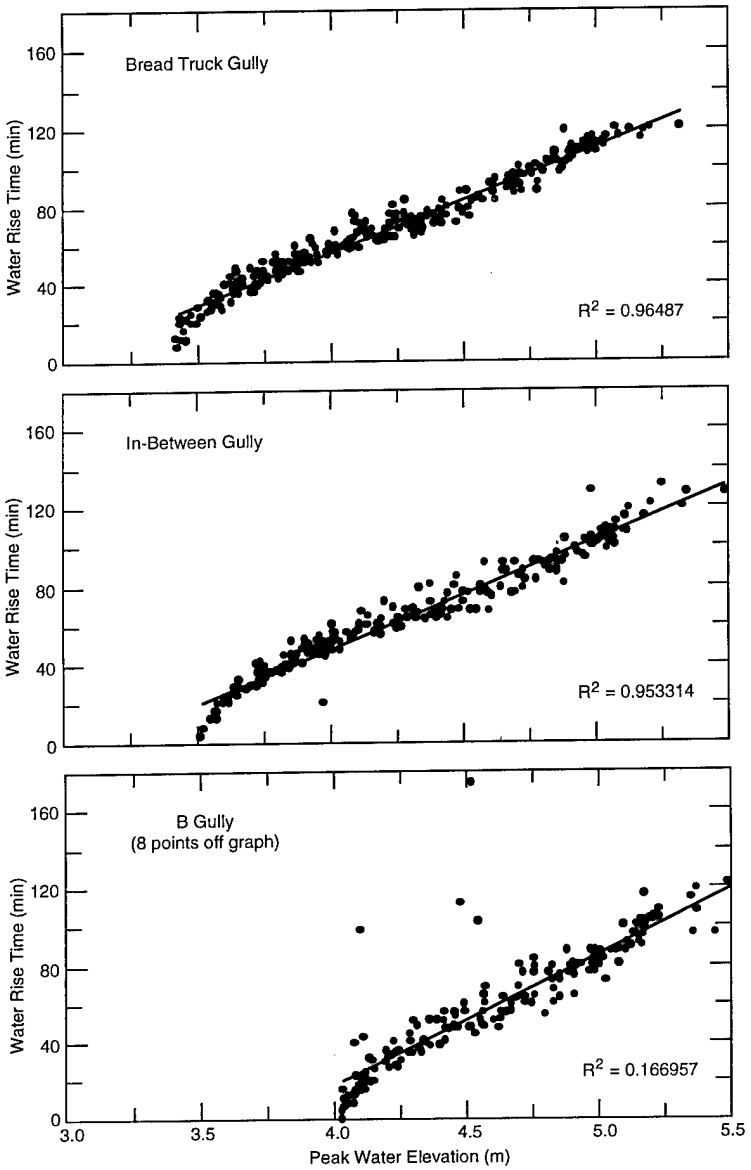

Figure 40. Relationship between water rise time and peak water elevation at several gully sites. Note that x-axis for Racine Gully differs from other graphs.

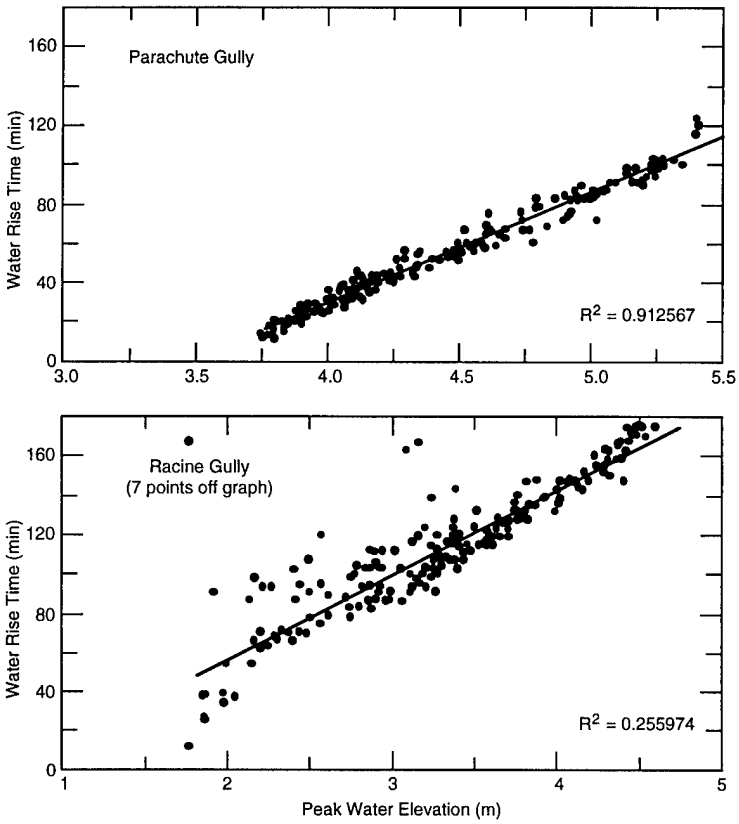

Figure 40 (cont'd).

flats are inundated at 4.9 m and levees are covered at 5.2 m (Fig. 39). Only at Racine Island was there a difference; here, survey data indicate a 4.35-m threshold for pond flooding at the south end. The former elevations also yielded a linear relationship between the period of flooding (i.e., time when water elevation was greater than 4.6 m) and peak water elevation (Fig. 41). Estimates of how often each landform is flooded in a given time period can be based upon these elevations.

The timing of flooding is controlled by the elevation of the levees and mudflats surrounding the gullies, the distance of the gully headwall from the coast, and the gully length. Water moving down the river can also alter the timing of flooding inland from the coast, depending upon its volume relative to the volume of tidal waters. Analyses show that tidal flooding is best described by a polynomial regression (Lawson et al. 1996).

Pond drainage is restricted by gully parameters (cross-sectional area, channel roughness and drainage density) that limit the volume of water that can escape from the pond. This produces a bottleneck effect where water in the pond remains dammed despite turbulent, fast flowing conditions in the gully heads. The response is a nonlinear relationship between water elevation

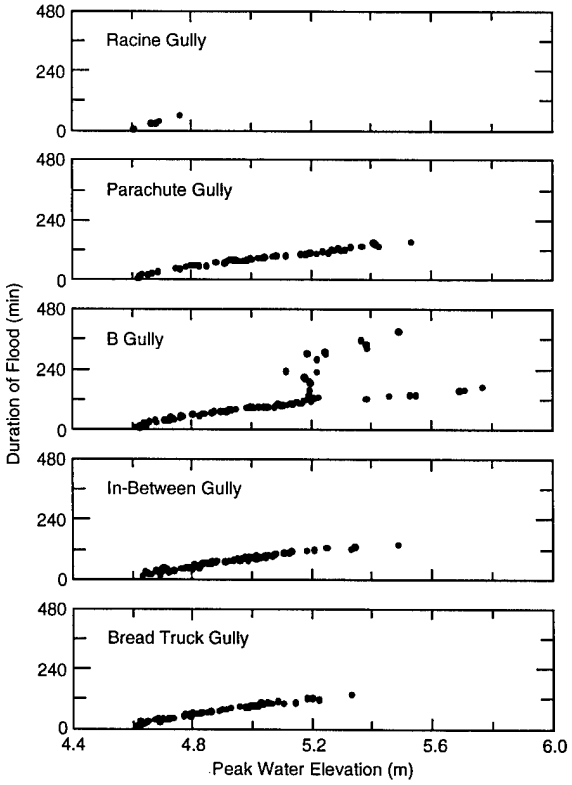

Figure 41. Tidal flooding time as a function of peak flood elevation at selected gullies.

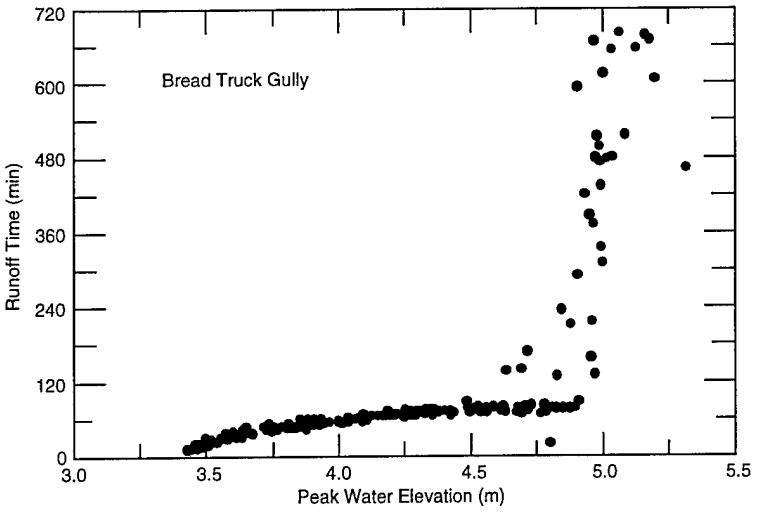

Figure 42. Runoff time vs. peak water elevation at Bread Truck Gully. The change in slope reflects the effect of pond drainage where runoff is extended once ponds are flooded.

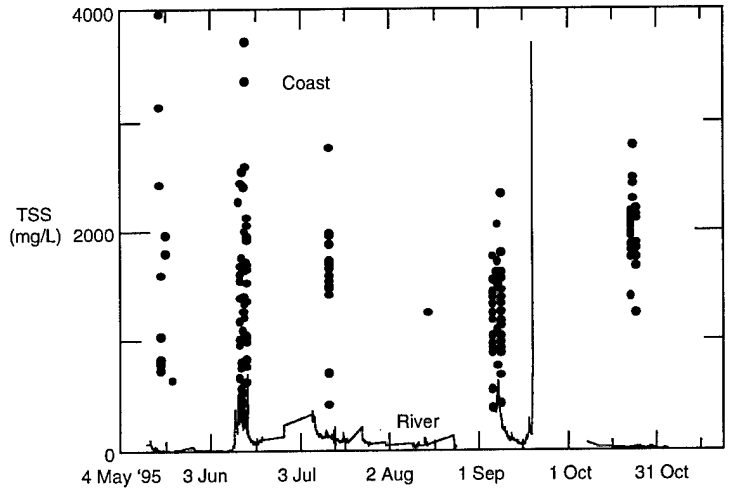

Figure 43. Coastal vs. river TSS measurements. The large spike in mid-September indicates a flooding event in the Eagle River watershed.

and runoff time (Fig. 42), which, in effect, extends the time for sedimentation. Drainage is incomplete between consecutive tides exceeding 5.0 m, furthering the time available for sedimentation.

Sediment transport and sediment sources

Sediment transported in suspension from Knik Arm is the primary source for ponds, and it varies seasonally as well as during single tidal cycles (from flood to ebb) (Lawson et al. 1996). TSS measurements in Knik Arm exceed those at the river (which are quite low) throughout the year and show a general increase in sediment concentration through the summer season (Fig. 43). In contrast, TSS concentrations vary seasonally in the Eagle River, being relatively high through June and September, with peaks in mid-June and early August during snowmelt in the mountains and maximum glacial runoff (Fig. 43; Lawson et al. 1996). The higher sediment concentrations in Knik Arm reflect the high sediment influx from the large glacierized basins of the Susitna, Matanuska and Knik rivers (Fig. 1). The increase in TSS values in Knik Arm during fall and winter probably reflect the effects of colder water and increased salinity (both of which affect its viscosity). In the Flats, reduced discharge in fall and winter from the Eagle River minimizes dilution by fresh water with a much lower sediment concentration, allowing more saline water with a greater sediment concentration to enter the ponds and mudflats.

Sediment flux into and out of the ponds and mudflats varies monthly as tidal height, flood duration and runoff time vary (Fig. 44). TSS concentrations vary among the gullies through a single tidal cycle and reflect distance inland from the coast, as well as spatial variations in runoff,

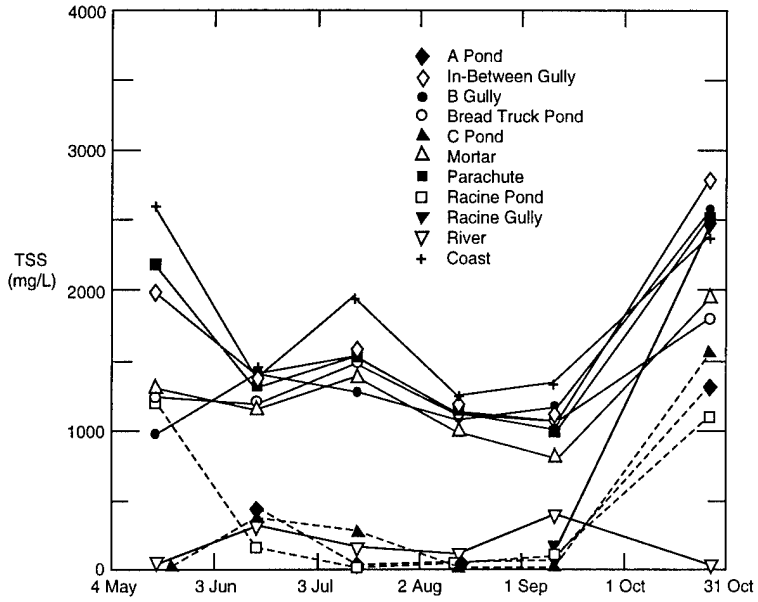

Figure 44. Maximum monthly TSS comparison at all sites. Dashed lines connect data from pond sites.

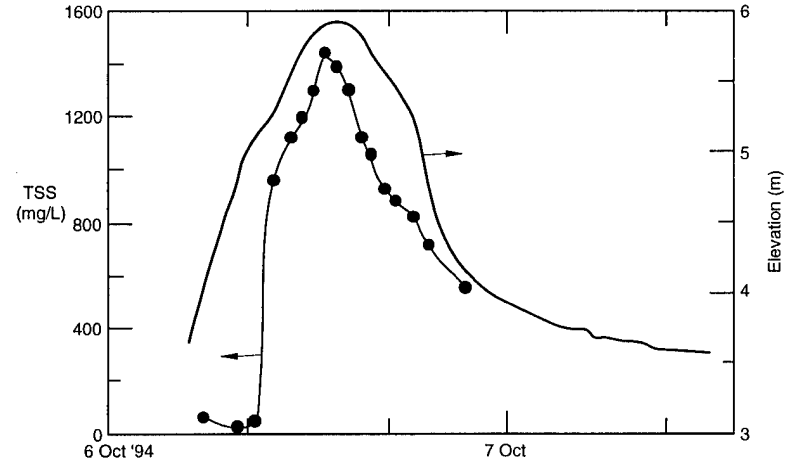

Figure 45. Typical TSS variation through a flooding tide.

pond storage capacity and the capacity of the gully to drain water from the ponds and mudflats. These differences in sediment flux into and out of the ponds and mudflats result in a spatial variability in deposition, which is compounded by the effects of localized differences in elevation and vegetation.

A typical pattern in TSS response, as measured at the heads of gullies through a flooding cycle, is a sharp increase because of the influx of highly turbid flood water from Knik Arm and resuspended gully bed sediment (Fig. 45). TSS values remain high through slack high tide and the start of ebb. TSS then abruptly decreases during ebb runoff. The duration of ebb runoff depends on the ability of the gully or network of gullies to transfer water stored in the ponds and mudflats. The greater the volume of water stored in an area, the longer it will take for gullies to effectively drain the ponds. The decrease in suspended sediment concentration during ebb reflects the loss of material by deposition on mudflats and in ponds, as well as the mixing of the tidal waters with sediment-poor pond and river waters.

Landform sedimentation rates

Sedimentation rates vary with morphology and, in a general sense, elevation (Table 10). The overall trend is an increase in rate from levees to mudflats, to ponds, to marshes and to gully bottoms, with the more heavily vegetated areas of mudflats having higher rates of accumulation than those that are not vegetated. Typical annual sedimentation ranges from about 10 to 30 mm among the various landform types.

Net accumulation is generally higher during the "winter" 8-month period from September to May than during the "summer" 4-month period from May to September. This difference probably

Table 10. Gross sedimentation rates.

	Range (mm)						
Morphological unit	*Sum. 1992*	*Win. 1992–93*	*Sum. 1993*	*Win. 1993–94*	*Sum. 1994*	*Win. 1994–95*	*Sum. 1995*
Levee	1–6	1–12	0–6	0–11	0–15	0–30	0–17
Vegetated mudflat	1–6	1–16	1–14	1–21	1–30	0–31	0–13
Unvegetated mudflat	1–13	7–12	1–8	6–10	1–17	3–21	0–17
Pond—plate	1–4	8–28	6–26	2–17	1–21	1–16	1–37
Pond—cup	2–9	8–26	6–19	1–13	2–20	9–40	1–39
Marsh	ND	ND	ND	ND	1–20	2–10	1–13
Gully	1–77	20–33*	0–19	0–16	1–19	3–50	6–60

* Based on small sample size.
Measurements for seasons through winter 1993–94 are from transect lines 1–12 only, Summer 1994 and 1995 measurements from lines 1–24 (Fig. 9).

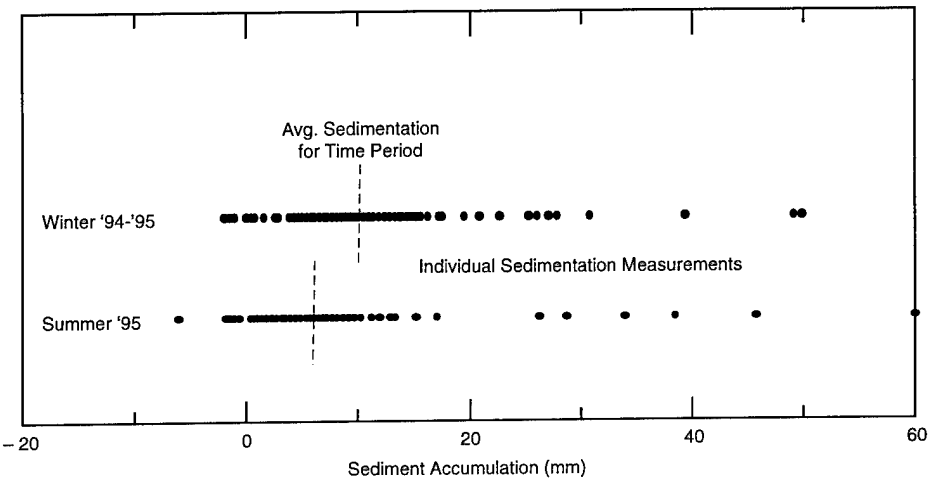

Figure 46. Net seasonal accumulation rates at sites spray-painted in the C and D areas.

reflects their respective length of measurement, the seasonal increases in TSS within the source waters during the early winter months (Fig. 44), the trapping of sediment by the snow cover, and the number of flooding events. Net accumulation measurements from the paint-layer technique vary seasonally for the periods of September 1994 through May 1995 (winter) and May 1995 through September 1995 (summer) in Area C and Area D mudflats and levees (Fig. 46). Most winter values fall in the range of 2 to 18 mm (average 10 mm), while the summer values range between –2 and +14 mm (average 6 mm).

The relationship of sedimentation rate to elevation reflects the number of times the sites are inundated. The number of measured flooding events exceeds that predicted from tidal elevations at Anchorage because of several factors, including tidal amplitude caused by the geometry of Knik Arm (e.g., Syvitski et al. 1987, p. 163), river discharge, ice cover and wind. There was significantly more tidal flooding at each hydrostation site during both 1994 and 1995 than predicted by using the Anchorage datum (Table 11). Given this scenario, floods should far exceed that number again in 1996.

During summer, about twice as many floodings occur than predicted, but fewer take place in winter, presumably because of the seasonal reduction in river discharge (Table 11). Flooding of the various landforms is therefore also affected. The number of inundations is highest for ponds, being less on mudflats and levees, thereby correlating with the general decrease in sedimentation rates that characterizes this respective sequence of landforms (Fig. 47).

The amount of vegetation covering the mudflats also influences the sediment accumulation rates (Fig. 48). Gross sedimentation rates from 1992 to 1994 had total accumulations of 6–18 mm at sites

Table 11. Comparison of predicted and measured number of flooding events reaching critical heights during summer 1994 and summer 1995.

	Number of flooding events				
	Summer 1994		*Summer 1995*		*Summer 1996*
Critical height	*Predicted*	*Measured*	*Predicted*	*Measured*	*Predicted*
Inundate ponds (4.6 m)	16	52	33	38	44
Cover mudflats (4.87 m)	8	18	10	22	25
Cover levees (5.21 m)	0	4	0	1	2

Summer 1994 is 22 May–15 September; summer 1995 is 5 May–11 September; predicted means based on Thompson tide table at Anchorage; measured means based on depth transducer at Bread Truck gully; time periods are intervals between sedimentation measurements.

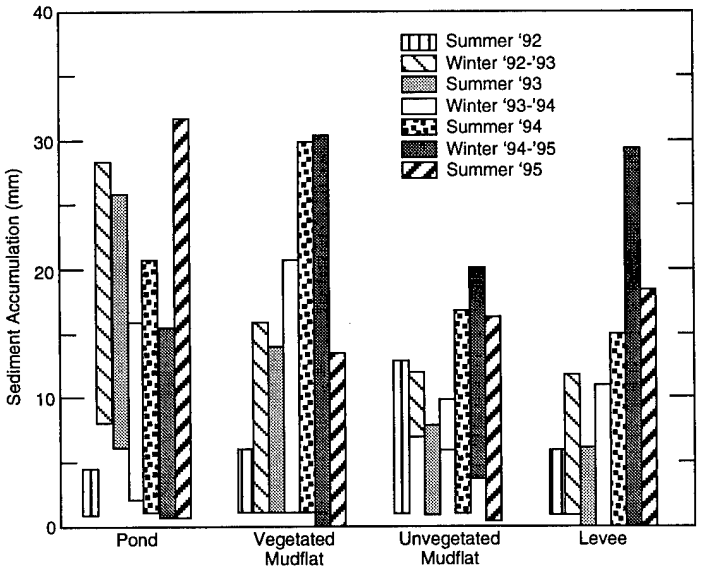

Figure 47. Variations in sedimentation rate as a function of landform type.

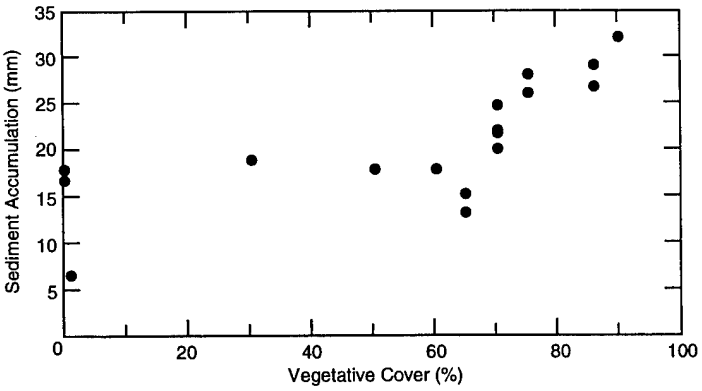

Figure 48. Relationship between total sediment accumulation and vegetation cover at sites sprayed with paint in 1992 and measured in the fall of 1994.

with less than 60–65% vegetative cover, and 26–32 mm at sites with a vegetation cover of greater than 70%.

Sedimentation rates also vary with distance from source waters. A decrease in sedimentation rate with distance inland is illustrated by transect 16 data (Fig. 49a), which extends southward from Knik Arm into coastal Area A (Fig. 9). The decreased velocities of Knik Arm waters during flooding reduce their ability to transport sediment, causing rapid sedimentation near the coast. The same effect is often seen along the scarp of many gullies where flow conditions change rapidly as flood waters overtop their banks. Sedi-

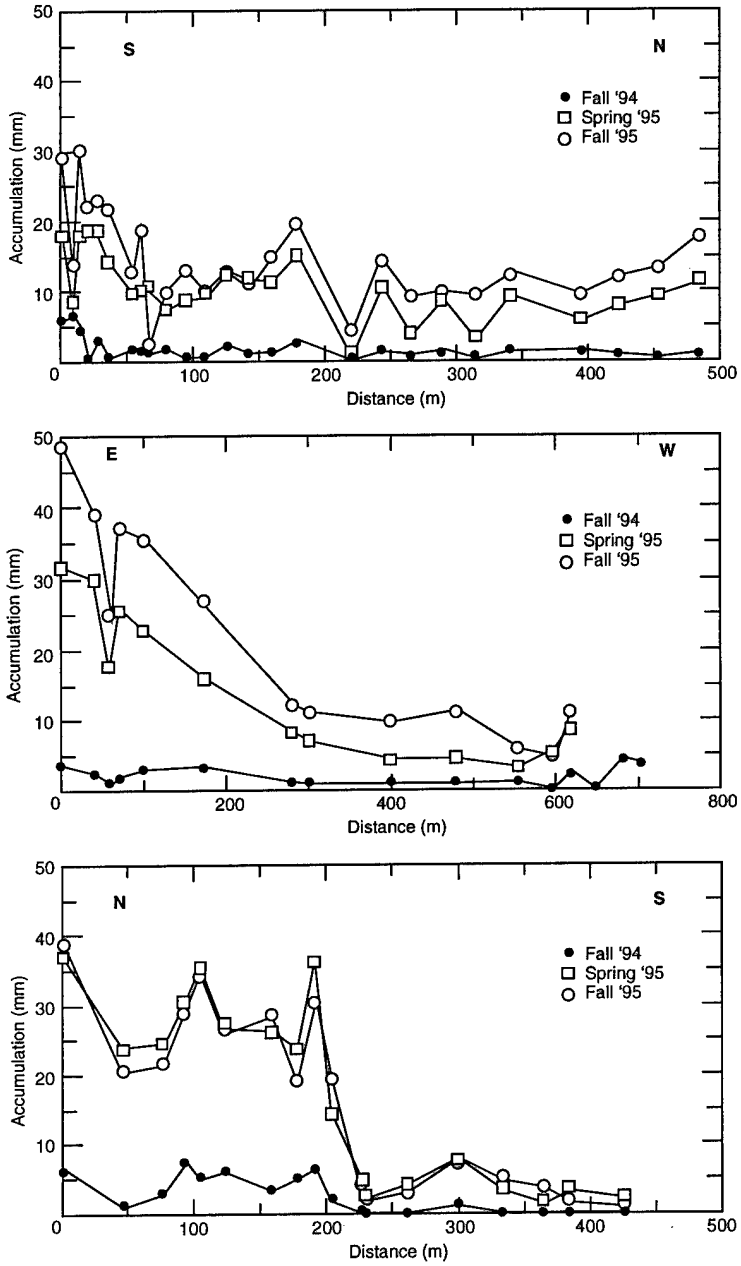

a. Transect line 16.

b. Transect line 14.

c. Transect line 19.

Figure 49. Sediment accumulation along mudflat lines sprayed with paint in early summer 1994 (see Fig. 9).

mentation rates decrease with distance from the Eagle River inland toward the marshes adjacent to the uplands (Fig. 49b). We also observed high accumulation rates at a low elevation oxbow area on the north end of Racine Island that floods more frequently than adjacent mudflats (Fig. 49c).

Pond transects and stations

Pond sedimentation transects were newly established in 1995 in Bread Truck, C/D, C, Lawson's, A and Racine Island ponds (Fig. 12). The plates and cups were measured in September at each station on these transects, except in C/D, where only cups could be measured. Sediment that accumulated at the new pond sites during this first summer was liquefied and contained a high organic fraction that we did not differentiate from the mineralogical fraction. At sites where an algal bloom was present in the water column above the measuring devices, we either gently removed or moved the material enough to see the sediment surface and obtain the measurement.

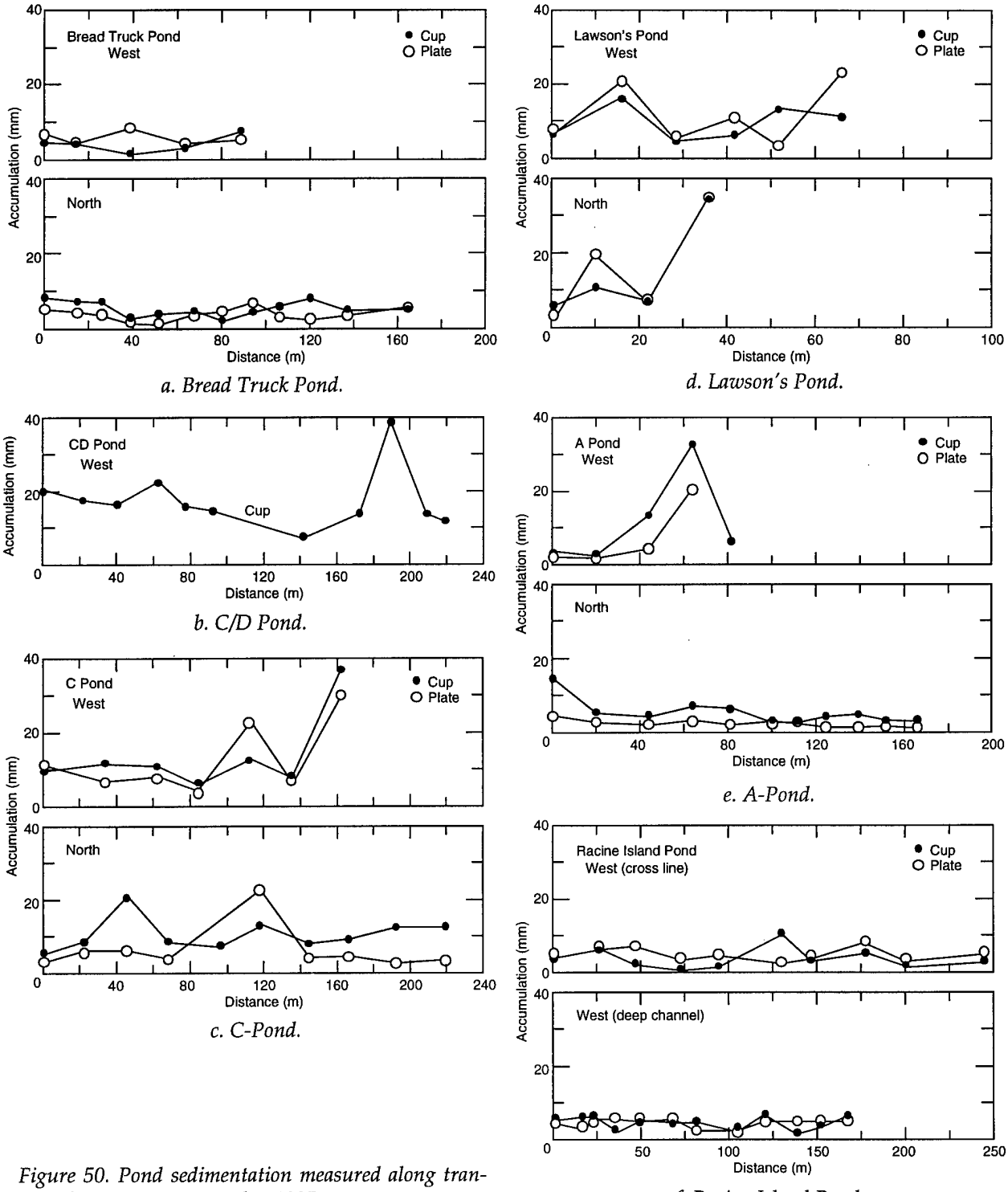

Figure 50. Pond sedimentation measured along transects from May to September 1995.

Overall, accumulation amounts were consistent along the transects, ranging from 5 to 20 mm (Fig. 50). There were only a few anomalously high readings among the otherwise consistent data, which we believe were probably the result of human or wildlife-induced disturbance.

Gross sedimentation amounts as measured by the cups, without the anomalously high data points (Table 12), indicate that Lawson's Pond, C/D Pond and C Pond have higher averages than the other three ponds (Fig. 51). Lawson's Pond and C/D Pond have less open water and more

Table 12. May to September 1995 sediment accumulation along pond sedimentation transects.

	Sediment accumulation (mm)							
	All measurements				*Without disturbance*			
	Cup		*Plate*		*Cup*		*Plate*	
Pond	*Avg*	*Std*	*Avg*	*Std*	*Avg*	*Std*	*Avg*	*Std*
Bread Truck	5.0	2.2	4.2	1.9	—	—	—	—
C/D	17.7	8.0	—	—	15.6	4.2	—	—
C	11.9	7.7	8.2	7.8	9.2	2.3	5.4	2.4
Lawson's	12.3	9.3	14.3	10.9	9.5	4.1	11.7	8.3
A	7.7	7.8	3.7	5.0	4.6	1.5	2.3	0.9
Racine Island	4.3	2.3	4.7	1.5	—	—	—	—

Left columns include all measurements; right omits sites with disturbance.

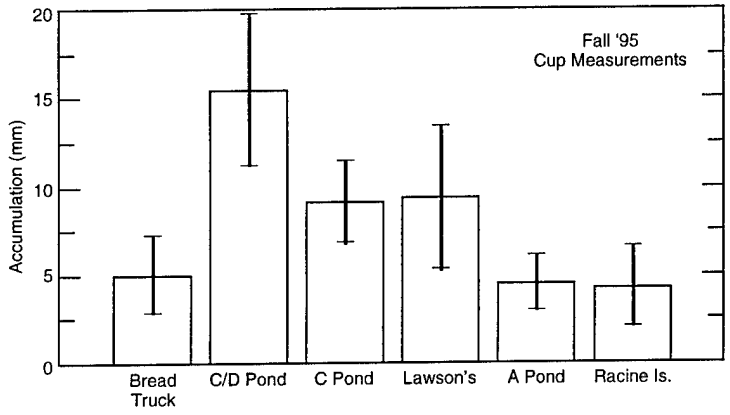

a. Fall 1995 cup measurements.

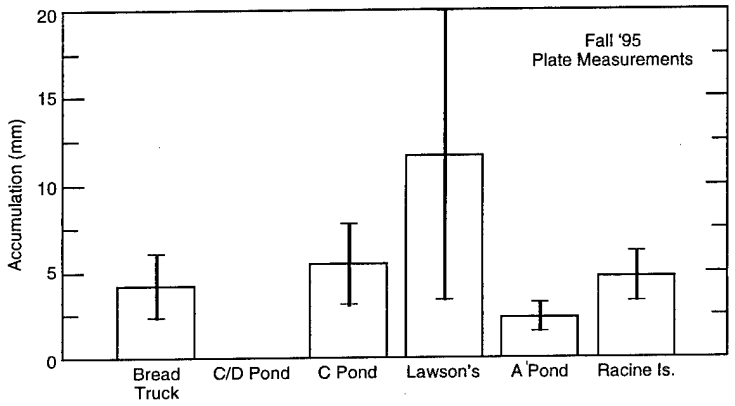

b. Fall 1995 plate measurements (no measurements made at C/D Pond).

Figure 51. Average sediment accumulation from May to September 1995 at pond sedimentation station transects, without data points suspected of disturbance. One standard deviation is shown with error bars.

vegetation to help trap sediment. Net sedimentation rates measured by the plates show that Lawson's Pond has the highest average, but with a large variability. The three ponds—Bread Truck, Racine Island and C—had similar net rates of accumulation, while A-Pond accumulations were less.

Longer-term net accumulation rates over 3 years were measured at the isolated sedimentation stations (Fig. 13 and 52). At these sites, the material in about the upper 5 mm is liquefied, while the lower portion of the accumulated sediment has undergone dewatering and compaction, resulting in a consistency that resists penetration with a millimeter rule. Accumulation amounts were somewhat higher in C Pond than in Bread Truck Pond, but in both cases, amounts appear to

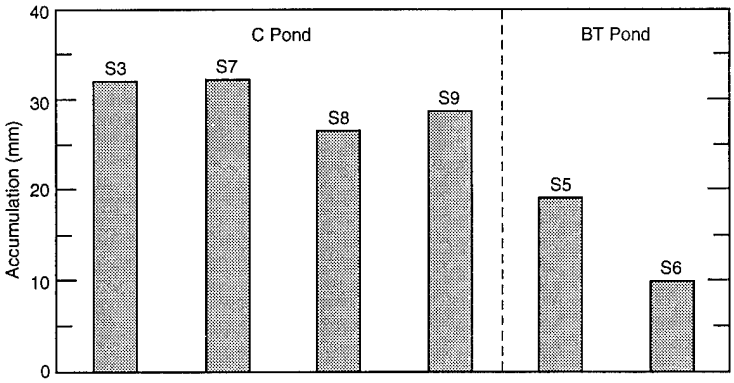

Figure 52. Fall 1995 measurements of accumulation at sedimentation stations established in 1992.

be such that, in another 6 to 9 years, the upper uncontaminated sediment should provide a barrier deep enough to keep dabbling ducks from reaching contaminated material beneath it.

WHITE PHOSPHORUS FATE, TRANSPORT AND MIGRATION

WP-contaminated sediment is eroded and transported from the ponds, mudflats and gully walls by a variety of processes operating throughout the year (Tables 2 and 3). The processes are primarily wind, river and tidal currents, and various types of slope erosion. Animals, waterfowl and humans may likewise disturb and mobilize WP in ponds.

Both ice and water entrain and transport WP-contaminated sediments. Wind and water currents in ponds can resuspend WP-contaminated sediments, as evidenced by analyses of resuspended materials in sediment traps. Gully transport during ebb moves these sediments into the Eagle River. Samples of material trapped by plankton nets record WP-contaminated sediment transport during ebb tide. Analyses of samples from sediments adhering to ice floes are evidence that ice can erode and transport WP-contaminated sediments.

Field sampling of sediment in transport in a natural setting, rather than in a controlled laboratory, is difficult in the intertidal environment and was not possible in Eagle River or Knik Arm during tidal ebb. Given the fine particle size of both the suspended and bed loads, it is likely that these sediments are transported into Knik Arm where their fate is unknown. Whether WP erosion, transport and redeposition constitute a quantitatively important biologic hazard cannot be assessed because of the limited number of samples acquired during this study and the generally random nature of WP occurrence.

We gauged WP migration by analyzing material in sediment traps within contaminated permanent ponds, and by analyzing the materials collected in plankton nets from the bedload and suspended load of gully runoff from the ponds during ebb tide. Plankton nets in the centers of gullies provide the only data available on transport and migration of WP into the Eagle River and Knik Arm. The sediment traps in ponds provide data on localized WP movement by resuspension. Sediment trap and surface samples, which were taken in previous years (Lawson et al. 1995, 1996), provide data on mudflat scour of WP during runoff. Ice samples were obtained in 1994, but weather conditions in late 1995 and early 1996 did not produce ice conditions suitable to floe analyses. Previous work indicated that ice floes cause WP erosion and transport (Lawson et al. 1996).

Plankton nets in four gullies draining contaminated ponds and mudflats were used to trap sediments during the monthly tidal flooding events of May through October (Fig. 17 and 21b). Of 138 samples, WP was detected in 44 (32%), indicating WP transport during ebb tide in all tidal flooding events exceeding 5.1 m elevation (Fig. 53). This relationship to elevation is consistent with the more limited 1994 results (Lawson et al. 1996). The quantities detected in these samples were typically less than 0.1 μg/g. The B-Gully site is the only exception to this trend, with values ranging from less than 0.1 to about 0.9 μg/g. The reasons for this difference are not clear; however, the upper reaches of B-Gully are undergoing lateral and headward erosion into a heavily cratered and highly contaminated part of the mudflats (Fig. 27) (Racine et al. 1993, Racine and Brouillette 1995b). It is therefore possible that the plankton

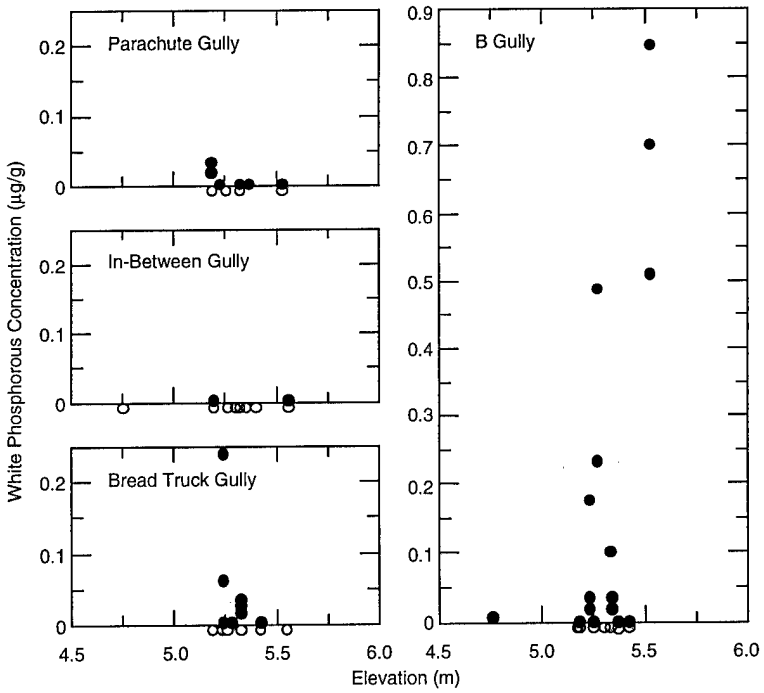

Figure 53. Relationship between WP detected in plankton net samples and peak elevation of flooding event sampled. Open circles are samples in which no WP was detected.

Table 13. 1995 positive WP results from pond sedimentation station cup samples.

Time	*Area*	*Station no.*	*Conc. (µg/g)*
May	B-Pond	S-18	0.0671
	C-Pond	S-3 Pan N	0.0175
		S-3 Pan S	0.0320
		S-8	0.0225
		S-9	0.0260
	Bread Truck Pond	S-6	0.0268
Sept.	Lawson's Pond	LP-4	0.0008
	Bread Truck Pond	BT-1	0.0003
		BT-6	0.0008
		BT-9	0.0023
	Racine Is. Pond	RI-2	0.0203

net samples are recording the erosion of these WP-bearing sediments and that the higher concentrations reflect the lack of mixing and dilution that occur during longer distance transport.

Sediments trapped in cups on pond transects revealed some internal movement of WP as the result of resuspension of pond and mudflat materials during both the winter and summer seasons (Fig. 12 and 13; Table 13). Analytical results were less than 0.1 µg/g, but quantities detected were generally greater in May samples of "winter" activity than in September samples of the "summer" season. The six WP detections in the May analyses were from a total of 12 trap samples, whereas the September analyses were from 90 samples. These detected values are consistent with those of pond sediment traps that were analyzed previously (Lawson et al. 1996).

In summary, the plankton net samples show that water is actively transporting WP in the gullies. The origin of the WP is probably contaminated sediments released by erosion of gully walls, or by resuspension and transport of pond and mudflat sediments of the C, Bread Truck, Lawson's and C/D ponds. About one-third of the samples acquired during tidal events exceeding 5.1 m in 1995 contained WP, similar to 1994. Previous samples in 1993 from the Bread Truck and Parachute gullies proved negative for WP, but were collected during tides of less than 5.03 m when the potential for erosion and transport were less.

Resuspension of WP during winter and summer tells us that we need to consider remobilization and potential movement of WP to uncontaminated areas. Data are, however, limited and the amount of WP migrating within and out of ERF cannot be quantified.

Further measurements of summer and winter transport should be made. The high level of WP found in a B-Pond sample this year is a good

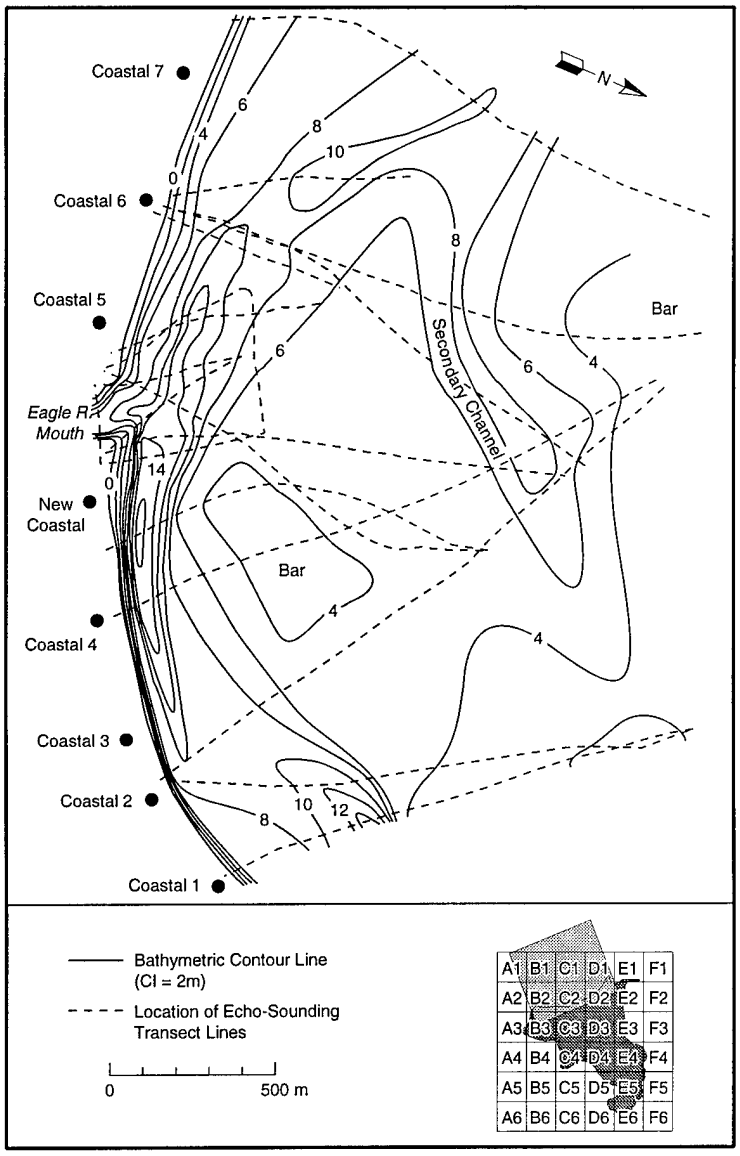

Figure 54. Bathymetry of Knik Arm near the mouth of the Eagle River and adjacent to the coast of ERF.

example of why such monitoring is important; the B-Area has been considered clean of WP and this sampling result shows that WP migration can spread contamination within the Flats.

KNIK ARM AND WP DEPOSITION

The Knik Arm near the mouth of the Eagle River is 9–10 km wide and has large tidal cycles (±9 m). At high tide, Knik Arm fills and spills over into ERF. Currents are relatively weak by comparison to those at low tide. At low tide, this portion of Knik Arm essentially becomes a braided stream system with a main channel located directly off the coast of ERF. Rapid flow in this channel produces highly turbulent conditions with large standing waves. As tidal flooding begins, conditions change rapidly, with transitory areas of severe turbulence and scour and back-eddies with minimal turbulence—conditions enhancing sedimentation.

Bathymetric analyses of Knik Arm offshore of ERF and near the mouth of Eagle River in 1994 (Lawson et al. 1996) provided data that are integral to identifying potential locations where WP may be deposited after migration out of ERF proper. These data showed various locations in Knik Arm, such as intertidal bars and other areas, where sedimentation is active. Such areas are migratory and can change extent and location over time.

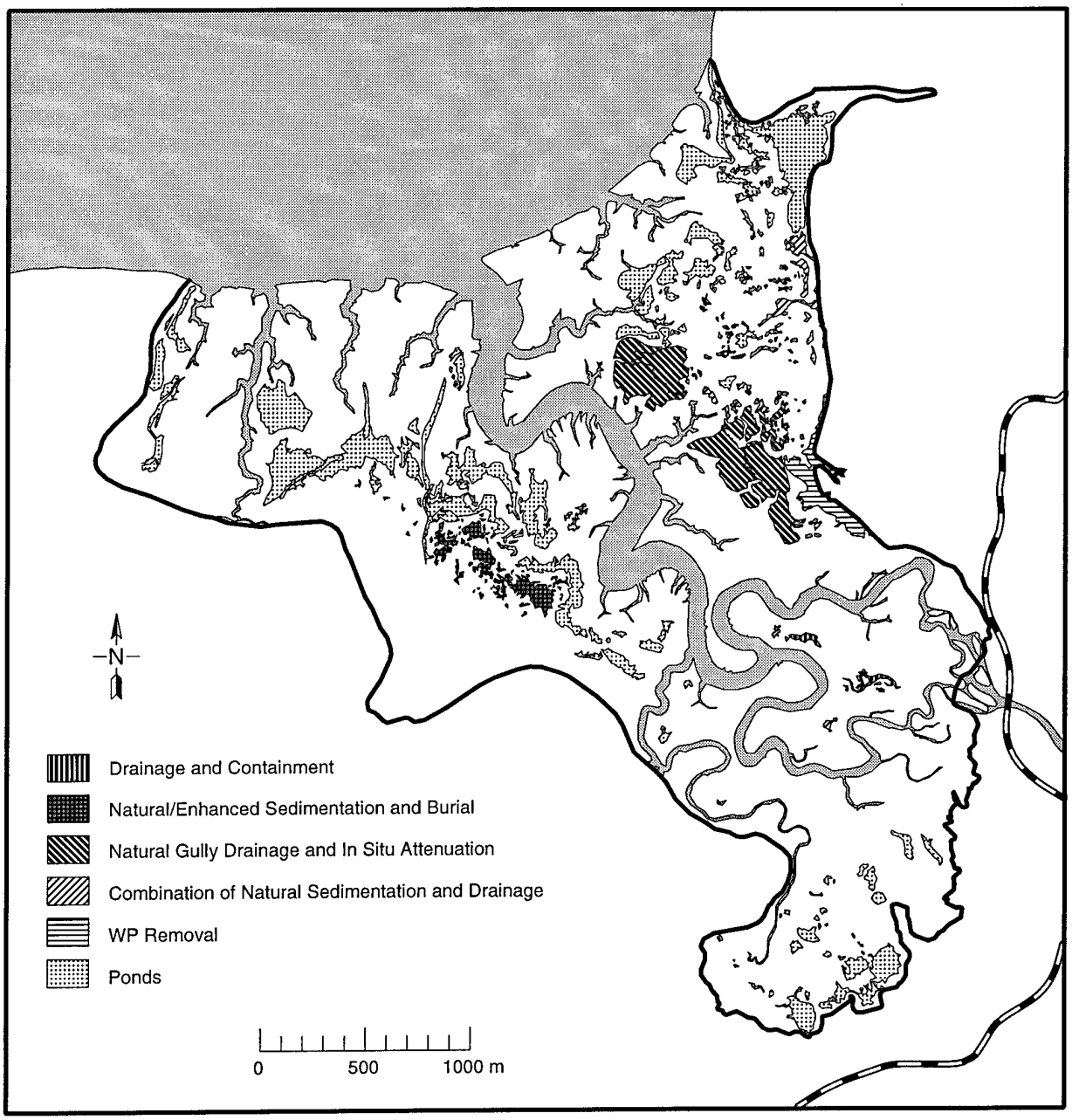

Figure 55. Recommendations for site remediation.

These areas in Knik Arm are therefore sites where samples of sediment should be examined for WP. They include two intertidal bars, a bar at the mouth of the Eagle River, and nearshore zones north and south of the Eagle River (Fig. 54). Because they are periodically exposed, these sites may be locations where receptors can find WP. Further analyses are required to evaluate whether WP is being preserved in these deposits, and, further, whether the dynamics of Knik Arm can cause potential exposure of WP to waterfowl or other receptors. Repeated bathymetric profiling could also define net rates of sedimentation or erosion in Knik Arm.

CONCLUSIONS AND RECOMMENDATIONS

Conclusions

The results of the 1995 and previous years' investigations lead to several important conclusions:

1. Physical system processes can produce a natural attenuation or in-situ degradation and removal of WP from a significant portion of the ERF ecosystem (Fig. 55).

2. Gully erosion and headwall recession will begin to drain large areas of contaminated ponds in about 1 to 10 years, potentially resulting in in-situ WP degradation and attenuation from drying; it is a cost-effective alternative to artificial remediation (Fig. 35a). Historical photographic analyses, field data and process analyses indicate that Bread Truck Pond will probably begin draining in 1 year; C/D-Pond, Lawson's Pond and a large area of C-Pond will begin draining in 10 to 15 years or less.

3. Sedimentation rates appear sufficient to bury WP in certain ponds and can reduce the risk of feeding waterfowl being exposed to WP contamination.

4. Natural sedimentation, perhaps artificially enhanced in some ponds by flocculation or other means, is a cost-effective alternative that removes WP from feeding waterfowl through burial. Areas of C/D-Pond, Lawson's Pond and A-Pond are sites where sedimentation and burial are important in reducing exposure (Fig. 55). Sedimentation and burial may be the best solution in isolated and remote ponds where other techniques would be too costly. Erosion and recession of gullies draining C/D-Pond and Lawson's Pond may subsequently drain these areas and produce permanent remediation.

5. Ice growth in ponds can be sufficiently thick that freezing extends into the sediments of the pond bottom. In so doing , it is possible that large areas of sediment, including those contaminated with WP, will be pulled from the bottom when the ice cover is lifted by incoming tides or wind. Ice floes have been observed with dimensions of over 7 to 8 m square, onto which sediments of up to 30 cm thick were frozen. Wind and water currents move these floes throughout ERF during the flooding tide and move them out into the Eagle River and Knik Arm during ebb tide. Both ice floes with pond sediments adhering to them and deposits of sediments from such ice were sampled; WP was detected in several of these samples. It is, therefore, possible that large areas of contaminated sediments (hot spots) could be entrained and transported by ice floes to other areas of ERF, as well as into Knik Arm.

6. Ice and water entrain and transport WP-contaminated sediments within the ponds, mudflats and gullies of ERF. Wind and water currents in ponds can resuspend WP contaminated sediments, as evidenced by analyses of resuspended materials in sediment traps. Gully transport during ebb moves these sediments into the Eagle River. Samples of material trapped by plankton nets record WP-contaminated sediment transport during ebb tide. Analyses of samples from sediments adhering to ice floes are evidence that ice can erode and transport WP-contaminated sediments. Field sampling of sediment in transport in a natural setting, rather than in a controlled laboratory, is difficult in the intertidal environment and was not possible in Eagle River or Knik Arm during tidal ebb. Given the fine particle size of both the suspended and bed loads, it is likely that these sediments are transported into Knik Arm where their fate is unknown. Whether WP erosion, transport and redeposition make up a quantitatively important biologic hazard cannot be assessed because of the limited number of samples acquired during this study and the generally random nature of WP occurrence in ERF.

7. Racine Island Pond has neither high gully erosion and recession rates, nor high sedimentation rates. It also floods at a relatively low tidal elevation (4.35 m). Because the pond bottom sediments are rich in organics, a longer period is required for drying. Therefore, it appears that Racine Island can be effectively remediated and readily restored through artificial drainage or pumping of the pond, following construction of a temporary berm to contain the former pond area and permit long-term drying to degrade the WP. By removing the berm after in-situ degradation is complete, the pond environment can be restored.

Recommendations

Based upon our investigations in 1995 and previous years, we recommend the following (Fig. 55):

1. Cost-effective remediation can be accomplished across a large area of ERF by allowing the physical system to remove or isolate WP contamination.

2. WP contamination of Bread Truck Pond and 50% or more of C-Pond, including Lawson's Pond, should be treated by natural (or enhanced) drainage and in-situ WP degradation by drying of the former pond bottoms.

3. Sedimentation and burial of WP will, in certain ponds, effectively remove it from feeding waterfowl over the short term. Over the long term, burial will reduce waterfowl mortality during natural pond drainage, especially in parts of C-

Pond, Lawson's Pond and C/D-Pond. It should be considered a method of natural attenuation, particularly in isolated, small, remote ponds where other methods are too costly.

4. Racine Island Pond should be remediated by artificial gully extension, pond drainage and pumping, and long-term containment with a temporary berm to permit in-situ WP degradation by drying. By removing the berm, the pond environment can be naturally restored.

5. Gully erosion and recession, pond sedimentation, pond drainage, and ground water levels and WP degradation and attenuation should continue to be monitored to ensure that remediation is taking place as predicted by the physical system analyses.

6. WP migration and contamination in Knik Arm should be evaluated, focusing on sampling areas of the nearshore zones and mid-Arm bars where there is a potential for WP exposure to receptors.

7. The potential natural attenuation of WP as the result of mechanical abrasion during transport by gully and tidal currents should be examined.

LITERATURE CITED

Allen, J.R.L. (1982) *Sedimentary Structures: Their Character and Physical Basis.* Volume 1, 2. *Developments in Sedimentology*, vol. 30A, B. New York: Elsevier.

APHA, AWWA, WEF (American Public Health Association, American Water Works Association, Water Environment Federation) (1992) Method 2540D: total suspended solids dried at 103–105°C. In *Standard Methods for the Examination of Water and Wastewater*, p. 2–56.

Bouwkamp, C.A. (1995) Evaluation of white phosphorus effects on the aquatic ecosystem. In Interagency expanded site investigation: Evaluation of white phosphorus contamination and potential treatability at Eagle River Flats, Alaska (C. Racine and D. Cate, Eds.). FY94 Final Contract Report for U.S. Army Alaska, Directorate of Public Works.

Brown, L.D., R.E. Reilinger, S.R. Holdahl and E.I. Balazs (1977) Post-seismic coastal uplift near Anchorage, Alaska. *Journal of Geophysical Research*, **82**(23): 369–378.

Cohen, S.C. (1996) Time-dependent uplift of the Kenai Peninsula and adjacent regions of south central Alaska since the 1964 Prince William Sound earthquake. *Journal of Geophysical Research*, **101** (B4): 8595–8604.

Cohen, S.C., S. Holdahl, D. Caprette, S. Hilla, R. Safford and D. Schultz (1995) Uplift of the Kenai Peninsula, Alaska, since the 1964 Prince William Sound earthquake. *Journal of Geophysical Research*, **100** (B2): 2031–2038.

Combellick, R.A. (1990) Evidence for episodic Late-Holocene subsidence in estuarine deposits near Anchorage, Alaska: Basis for determining recurrence intervals of major earthquakes. Fairbanks: Alaska Division of Geological and Geophysical Surveys, Public-data File 90-29.

Combellick, R.A. (1991) Paleoseismicity of the Cook Inlet region, Alaska: evidence from peat stratigraphy in Turnagain and Knik Arms. Fairbanks: Alaska Division of Geological and Geophysical Surveys, Professional Report 112.

Combellick, R.A. (1993) The penultimate great earthquake in south-central Alaska: Evidence from a buried forest near Girdwood. In Short Notes on Alaskan Geology (D.N. Solie and F. Tannian, Eds.). Fairbanks: Alaska Division of Geological and Geophysical Surveys, Professional Report 113, p. 7–15.

Combellick, R.A. (1994) Investigations of peat stratigraphy in tidal marshes along Cook Inlet, Alaska, to determine the frequency of 1964-style great earthquakes in the Anchorage region. Fairbanks: Alaska Division of Geological and Geophysical Surveys, Report of Investigations 94-7.

Evans, C.D., E. Buch, R. Buffler, G. Fish, R. Forbes and W. Parker (1972) The Cook Inlet environment: A background study of available knowledge. University of Alaska Sea Grant Program.

French, J.R. and T. Spencer (1993) Dynamics of sedimentation in a tide-dominated backbarrier salt marsh, Norfolk, UK. *Marine Geology*, **110**: 315–331.

Gurnell, A.M. and J.C. Clark (Eds.) (1987) *Glaciofluvial Sediment Transfer.* New York: John Wiley and Sons.

Hanson, H.C. (1951) Characteristics of some grassland, marsh and other plant communities in western Alaska. *Ecological Monographs*, **21:** 327–378.

Hansen, W.R. (1965) The Alaska earthquake, March 27, 1964: Effects on communities, Anchorage. Washington, D.C.: U.S. Geological Survey, Professional Paper 542-A.

Lawson, D.E. (1993) Glaciohydrologic and glaciohydraulic effects on runoff and sediment yield in glacierized basins. USA Cold Regions Research and Engineering Laboratory, Monograph 93-2.

Lawson, D.E. and B.E. Brockett (1993) Prelimi-

nary assessment of sedimentation and erosion in Eagle River Flats, south-central, Alaska. USA Cold Regions Research and Engineering Laboratory, CRREL Report 93-23.

Lawson, D.E., S. Bigl, J. Bodette and P. Weyrick (1995) Initial analyses of the hydrology and sedimentology of Eagle River Flats, Fort Richardson, Alaska. USA Cold Regions Research and Engineering Laboratory, CRREL Report 95-5.

Lawson, D.E., L.E. Hunter, S. Bigl, B.M. Nadeau, P. Weyrick and J.H. Bodette (1996) Physical system dynamics and white phosphorus fate and transport, 1994, Eagle River Flats, Fort Richardson, Alaska. USA Cold Regions Research and Engineering Laboratory, CRREL Report 96-9.

Nishenko, S.P. and K.H. Jacob (1990) Seismic potential of the Queen Charlotte–Alaska–Aleutian seismic zone. *Journal of Geophysical Research,* **95** (B3): 2511–2532.

Ovenshine, A.T., D.E. Lawson and S.R. Bartsch-Winkler (1976a) The Placer River Silt: An intertidal deposit caused by the 1964 Alaskan earthquake. *Journal of Research, U.S. Geological Survey,* **4:** 151–162.

Ovenshine, A.T., S.R. Bartsch-Winkler, N.R. O'Brien and D.E. Lawson (1976b) Sediment of the high tidal range environment of upper Turnagain Arm, Alaska. In *Recent and Ancient Sedimentary Environments in Alaska* (T.P. Miller, Ed.). Memoir, Alaskan Geological Society, p. M-1–M-26.

Plafker, G., E.B. Eckel, R. Kachadoorian and L.R. Mayo (1971) Effects on various communities, in the Great Alaska Earthquake of 1964: Geology. Washington D.C.: National Academy of Science, p. 489–540.

Racine, C.H. and M.C. Brouillette (1995a) Ecological inventory of Eagle River Flats, Alaska. In Interagency expanded site investigation: Evaluation of white phosphorus contamination and potential treatability at Eagle River Flats, Alaska (C. Racine and D. Cate, Eds.). FY94 Final Contract Report for U.S. Army, Alaska, Directorate of Public Works.

Racine, C.H. and M.C. Brouillette (1995b) Appendix A. Eagle River Flats map atlas. In Interagency expanded site investigation: Evaluation of white phosphorus contamination and potential treatability at Eagle River Flats, Alaska (C. Racine and D. Cate, Eds.). FY94 Final Contract Report for U.S. Army, Alaska, Directorate of Public Works, p. 634–698.

Racine, C.H., M.E. Walsh, C.M. Collins, D.J. Calkins, B.D. Roebuck and L. Reitsma (1992a) Waterfowl mortality in Eagle River Flats, Alaska. USA Cold Regions Research and Engineering Laboratory, CRREL Report 92-5.

Racine, C.H., M.E. Walsh, B.D. Roebuck, C.M. Collins, D. Calkins, L. Reitsma, P. Buchli and G. Goldfarb (1992b) White phosphorus poisoning of waterfowl in an Alaskan salt marsh. *Journal of Wildlife Diseases,* **28**(4): 669–673.

Racine, C.H., M.E. Walsh, C.H. Collins, S.R. Taylor, B.D. Roebuck, L. Reitsma and B. Steele (1993) White phosphorus contamination of salt marsh pond sediments at Eagle River Flats, Alaska. USA Cold Regions Research and Engineering Laboratory, CRREL Report 93-17.

Reed, D.J. (1989) Environments of tidal marsh deposition in Laguna San Rafael Area, south Chile. *Journal of Coastal Research,* **5**(4): 845–856.

Reed, D.J. (1995) The response of coastal marshes to sea-level rise: Survival or submergence? *Earth Surface Processes and Landforms,* **20**: 39–48.

Reed, D.J. and D.R. Cahoon (1992) The relationship between marsh surface topography, hydroperiod, and growth of Spartina alterniflora in a deteriorating Louisiana saltmarsh. *Journal of Coastal Research,* **8**(1): 77–87.

Rosenberg, D.H. (1986) Wetland types and bird use of Kenai Lowlands. Anchorage, Alaska: U.S. Fish and Wildlife Service, Special Studies.

Savage, J.C. and G. Plafker (1991) Tide gage measurements of uplift along the south coast of Alaska. *Journal of Geophysical Research,* **96**(B3): 4325–4335.

Syvitski, J.P.M., D.C. Burrell and J.M. Skei (1987) *Fjords: Processes and Products.* New York: Springer-Verlag.

USEPA (1995) Method 7580: White phosphorus (P_4) by solvent extraction and gas chromatography. Test methods for evaluating solid waste, SW-846: Update III. Washington, D.C.: Office of Solid Waste, U.S. Environmental Protection Agency.

Vince, S.W. and A.A. Snow (1984) Plant zonation of an Alaskan salt marsh. II. An experimental study of the role of edaphic conditions. *Journal of Ecology,* **72**: 669–684.

Walsh, M.E., C.M. Collins and C.H. Racine (1995) Persistence of white phosphorus particles in sediment. USA Cold Regions Research and Engineering Laboratory, CRREL Report 95-23.

REPORT DOCUMENTATION PAGE

Form Approved
OMB No. 0704-0188

1. AGENCY USE ONLY (Leave blank)	2. REPORT DATE	3. REPORT TYPE AND DATES COVERED
	December 1996	

4. TITLE AND SUBTITLE

Physical Processes and Natural Attenuation Alternatives for Remediation of White Phosphorus Contamination, Eagle River Flats, Fort Richardson, Alaska

5. FUNDING NUMBERS

6. AUTHORS

Daniel E. Lawson, Lewis E. Hunter and Susan R. Bigl

7. PERFORMING ORGANIZATION NAME(S) AND ADDRESS(ES)

U.S. Army Cold Regions Research and Engineering Laboratory
72 Lyme Road
Hanover, New Hampshire 03755-1290

8. PERFORMING ORGANIZATION REPORT NUMBER

CRREL Report 96-13

9. SPONSORING/MONITORING AGENCY NAME(S) AND ADDRESS(ES)

U.S. Army Alaska
Environmental Resources Department
Directorate of Public Works
Fort Richardson, Alaska

10. SPONSORING/MONITORING AGENCY REPORT NUMBER

11. SUPPLEMENTARY NOTES

For conversion of SI units to non-SI units of measurement consult ASTM Standard E380-93, *Standard Practice for Use of the International System of Units*, published by the American Society for Testing and Materials, 1916 Race St., Philadelphia, Pa. 19103.

12a. DISTRIBUTION/AVAILABILITY STATEMENT

Approved for public release; distribution is unlimited.

Available from NTIS, Springfield, Virginia 22161

12b. DISTRIBUTION CODE

13. ABSTRACT (*Maximum 200 words*)

This report describes the results of investigations into the role of tidal flat physical systems in the natural attenuation of white phosphorus (WP) contamination in Eagle River Flats (ERF) on Fort Richardson, Alaska. Waterfowl feeding in ponds and marshes here ingest the WP and die. These investigations found that natural attenuation and in-situ degradation of the WP could result from certain physical phenomena operating within the ERF ecosystem. Specifically, the on-going erosion and headward recession in the gullies will drain large areas of contaminated ponds in an estimated 1 to 10 years. Lowering of water levels should lead to in-situ WP degradation and natural attenuation as pond sediments dry. Annual sedimentation rates in some ponds and marshes are sufficient to bury WP in several years or more and thereby reduce the exposure to feeding waterfowl. Ice and water are also effective transporters of WP, moving it about ERF and into Eagle River and eventually into Knik Arm where its fate is unknown. Certain areas of ERF will require artificial drainage, but natural conditions can be restored following treatment. Recommendations are made for the use of natural attenuation and additional studies that are required to ensure the successful clean-up of ERF.

14. SUBJECT TERMS

Erosion
Natural attenuation
Pond drainage
Sedimentation
Tidal flat processes
White phosphorous

15. NUMBER OF PAGES 77

16. PRICE CODE

17. SECURITY CLASSIFICATION OF REPORT	18. SECURITY CLASSIFICATION OF THIS PAGE	19. SECURITY CLASSIFICATION OF ABSTRACT	20. LIMITATION OF ABSTRACT
UNCLASSIFIED	UNCLASSIFIED	UNCLASSIFIED	UL